TAMPEREEN TEKNILLINEN YLIOPISTO
TAMPERE UNIVERSITY OF TECHNOLOGY

Minna Poikelispää

Improvements of Nanofiller-Elastomer Systems by Filler Modification and Tailored Mixing Techniques

Julkaisu 1492 • Publication 1492

Tampere 2017

Tampereen teknillinen yliopisto. Julkaisu 1492
Tampere University of Technology. Publication 1492

Minna Poikelispää

Improvements of Nanofiller-Elastomer Systems by Filler Modification and Tailored Mixing Techniques

Thesis for the degree of Doctor of Science in Technology to be presented with due permission for public examination and criticism in Konetalo Building, Auditorium K1702, at Tampere University of Technology, on the 13th of October 2017, at 12 noon.

Tampereen teknillinen yliopisto - Tampere University of Technology
Tampere 2017

Doctoral candidate: Minna Poikelispää
Laboratory of Materials Science
Faculty of Engineering Sciences
Tampere University of Technology
Finland

Supervisor: Jyrki Vuorinen, Professor
Laboratory of Materials Science
Faculty of Engineering Sciences
Tampere University of Technology
Finland

Instructor: Wilma Dierkes, Associate Professor
Elastomer Technology and Engineering
Faculty of Engineering Technology
University of Twente
The Netherlands

Pre-examiners: Norbert Vennemann, Professor
Faculty of Engineering and Computer Science
Osnabrück University of Applied Sciences
Germany

Mária Omastová, D.Sc (Tech.)
Ústav polymérov SAV
Slovakia

Opponents: Norbert Vennemann, Professor
Faculty of Engineering and Computer Science
Osnabrück University of Applied Sciences
Germany

Marke Kallio, D.Sc (Tech.)
Metso
Finland

ISBN 978-952-15-3999-2 (printed)
ISBN 978-952-15-4018-9 (PDF)
ISSN 1459-2045

ABSTRACT

Elastomers are a unique material group due to their ability of high reversible deformation under stress. In actual practice, the mechanical properties of pure rubbers are not sufficient for everyday applications and their performance is typically improved by reinforcing fillers such as carbon black and silica. Nevertheless, these conventional fillers have some drawbacks, which can be overcome by developing new filler systems. Nano-size fillers result in high reinforcing potential for different polymers. The improvements in properties are mainly due to the large surface areas of tiny particles. Due to difficulties in mixing them into an elastomeric matrix, full reinforcing potential cannot be utilized yet. Therefore, research on nanofiller systems and related mixing techniques is required.

The objective of this thesis was to study the ability of the new filler systems to tailor the properties of elastomeric materials for applications requiring good mechanical and dynamic properties, in this case tyre tread. The experiments were performed by replacing the small amounts of carbon black by layered silicates, halloysite nanotubes and carbon nanotubes. The effect of replacement on the dispersion of the filler system and on the vulcanization, mechanical and dynamic properties of rubber was analysed. The approach was to improve the compatibility of filler and polymer by the surface modification of nanofillers.

It was observed that the partial replacement of very reinforcing carbon black by the nanofillers using traditional mixing techniques has only minor effect on the mechanical properties of rubber. Therefore, nanoclays and carbon nanotubes have a comparable reinforcing effect to carbon black, but additionally the partial replacement of carbon black by those reduces stiffness and improves dynamic properties such as the loss factor of rubber. Moreover, it was found that a blend of two fillers improves the dispersion and distribution of fillers, and that, with these hybrid fillers, sufficient dispersion of nanofiller loadings up to 5 phr can be achieved by traditional mixing methods. Masterbatch mixing is a way to facilitate the dispersion of carbon nanotubes and to prevent health and environmental risks possible during the mixing of nanoparticles.

PREFACE

The work was carried out in the Department of Materials Science at Tampere University of Technology. It was performed as a part of WILMIX project funded by Tekes. Nokian Tyres plc, Teknikum Oy, and Rubber Manufacturers' Association of Finland are thanked for their cooperation.

I am grateful to my supervisor Prof. Jyrki Vuorinen for his guidance and for giving an opportunity for this research. I express my sincerest gratitude to my instructor Associate Professor Wilma Dierkes for her support and tireless advice during the whole process and to Assistant Professor Essi Sarlin for pushing me to finalize this dissertation. I am thankful for Dr. Amit Das for his support and advice. Special thanks go to all of my co-authors. Their contribution was essential for this work.

I thank all my former and present colleges at TUT for nice and collaborative working atmosphere. Special thanks to Tommi Lehtinen for his invaluable help in the rubber compounding and to Assistant Professor Mikko Kanerva for commenting on the work.

Tampere, September 2017

Minna Poikelispää

LIST OF PUBLICATIONS

This thesis is based on the following publications:

I. Poikelispää, M., Dierkes, W., Das, A., Vuorinen, J., The effect of coupling agents on silicate based nanofillers / carbon black dual filler systems on the properties of a NR/BR compound. *Journal of elastomers and plastics,* 47 (2014) 738-752.

II. Sapkota, J., Poikelispää, M., Das, A., Dierkes, W., Vuorinen, J., Influence of nanoclay – carbon black as hybrid filler on mechanical and vulcanization behavior of natural rubber compounds, *Polymer Engineering and Science*, 53 (2013) 615-622.

III. Poikelispää, M., Das, A., Dierkes, W., Vuorinen, J., Synergistic effect of plasma modified halloysite nanotubes and carbon black in natural rubber - butadiene rubber blend, *Journal of Applied Polymer Science*, 127 (2013) 4688-4696.

IV. Poikelispää, M., Das, A., Dierkes, W., Vuorinen, J., The effect of partial replacement of carbon black by carbon nanotubes on the properties of natural rubber/ butadiene rubber compound. *Journal of Applied Polymer Science,* 130 (2013), 3153-3160.

V. Hoikkanen, M., Poikelispää, M., Das, A., Reuter, U., Dierkes, W., Vuorinen, J., Evaluation of mechanical and dynamic mechanical properties of multiwalled carbon nanotube-based ethylene-propylene copolymer composites mixed by masterbatch dilution. *Journal of Composite Materials* 50 (2016) 4093-4101.

VI. Hoikkanen, M., Poikelispää, M., Das, A., Honkanen, M., Dierkes, W., Vuorinen, J., Effect of multiwalled carbon nanotubes on the properties of EPDM/NBR dissimilar elastomer blends. *Polymer-Plastics Technology and Engineering* 54 (2015) 402-410.

AUTHOR'S CONTRIBUTION

I. The author is responsible for the experimental work and interpretation of the results. She wrote the paper together with Wilma Dierkes. All the authors commented on the experimental work, and read and approved the manuscript.

II. The author participated in planning and performing of the experiments, and commenting on the paper. Janak Sapkota is responsible for the experiments, the interpretation of the results, and writing of the manuscript with Amit Das. All the authors read, commented, and approved the manuscript.

III. The author is responsible for the experimental work and interpretation of the results. She wrote the paper together with Wilma Dierkes and Amit Das. All the authors commented on the experimental work, and approved the manuscript.

IV. The author is responsible for the experimental work and interpretation of the results. She wrote the paper together with Wilma Dierkes and Amit Das. All the authors commented on the experimental work, and approved the manuscript.

V. The author shared the experimental work, the analysis of the results and the writing of the manuscript with the first author. Uta Reuter is responsible for the TEM images. All the authors read, commented and approved the manuscript.

VI. The author shared the experimental work, the analysis of the results and the writing of the manuscript with the first author. Mari Honkanen is responsible for the TEM images. All the authors read, commented and approved the manuscript.

SYMBOLS AND ABBREVIATIONS

Symbols

γ_0	Strain amplitude
γ_c	Critical strain at which the loss modulus reached its maximum
η_f	Viscosity of filled polymer
η_0	Viscosity of pure polymer
θ	Angle between the incident rays and the surface of the crystal
λ	Wavelength
ρ	Density
δ	Solubility parameter
ψ	Interfacial area of fillers
φ	Volume fraction of filler
φ'	Combined volume fraction of filler and occluded rubber
d	The distance between atomic layers in a crystal
f_s	Shape factor
G	Shear modulus
G'	Storage modulus
G'_0	Storage modulus at small strain amplitude
G'_∞	Storage modulus at large strain amplitude
m	Parameter describing the strain dependency
n	Integer
Q	Swelling degree
S	Specific surface area of the filler
t	Time
T_g	Glass transition temperature

w_0	Initial weight of sample
w_t	Weight at time (t)

Abbreviations

BR	Polybutadiene rubber
CB	Carbon black
CBS	N-cyclohexyl-2-benzothiazolesulfenamide
CEC	Cation exchange capacity
CNT	Carbon nanotube
DBPA	Dibutyl phthalate absorption number
EPDM	Ethylene-propylene-diene rubber
FESEM	Field emission scanning electron microscope
HNT	Halloysite nanotube
LS	Layered silicate
MWCNT	Multi-walled carbon nanotube
NBR	Acrylonitrile butadiene rubber
NR	Natural rubber
PA	Octadecylamine
phr	Parts per hundred rubber
Py	Pyrrole
QUAT	Dimethyl-di(hydrogenated tallow) alkyl ammonium salt
rpm	Rotation per minute
SEM	Scanning electron microscopy
SBR	Styrene-butadiene rubber
SWCNT	Single-wall carbon nanotube

TDAE-oil	Treated distillate aromatic extract oil
TEM	Transmission electron microscopy
TESPT	Bis(3-triethoxysilylpropyl)tetrasulfide
Thi	Thiophene
TMQ	2,2,4-trimethyl-1,2-dihydroquinoline
XRD	X-ray diffraction
ZDBC	Zinc dibutyl dithiocarbamate
ZnO	Zinc Oxide
6PPD	N-(1,3-dimethylbutyl)-N´-phenyl-1,4-benzenediamine

TABLE OF CONTENTS

1. INTRODUCTION

Elastomers are the only material group that has high elastic deformation combined with moderate strength and very low elastic modulus. The term 'elastomer' is often used as a synonym for rubber, but in fact, the elastomer means an amorphous polymer having very flexible polymer chains whereas the word 'rubber' means a crosslinked elastomer. Elastomers are crosslinked in a chemical reaction called vulcanization, where strong covalent bonds, typically caused by sulphur or peroxides, are formed between the polymer chains and a three-dimensional network is created. The crosslinked structure accomplishes the final properties, such as strength and high elastic deformation. [1][2]

Rubber has a long history and it has been used for centuries. Christopher Columbus learned from the natives of Haiti a game played with an elastic ball in 1493. In the 17th century, the natives of South America are said to use the latex of the *Hevea Brasiliensis* rubber tree in waterproof footwear. The waterproof clothing was also the first rubber application in Europe where the rubber was imported in the 18th century. The real breakthrough of rubber occurred in 1839 when Charles Goodyear invented the vulcanization of rubber. Around 1900, the need of the rubber materials increased due to the development of pneumatic tyres and the development of synthetic rubbers started. [1][3]

Nowadays, elastomers are divided into two groups: rubbers and thermoplastic elastomers. Rubbers can further be divided into natural rubber (NR) and synthetic rubbers. NR collected from the rubber tree is still the most commonly used rubber representing nearly 50% of the total rubber consumption. Among synthetic rubbers, styrene-butadiene rubber (SBR) and polybutadiene rubber (BR) are the most widely used ones as they are generally used in tyres. In 2015, the total rubber consumption was almost 30 million metric tons and its use is growing continuously [4]. Thermoplastic elastomers are a relative new material group and their annual consumption is still rather low (4.2 million tons in 2015 [5]). They have high elastic elongation but not the chemically crosslinked structure

The special properties of rubbers are their incompressible nature and their ability to high reversible deformations under stress. In addition, they have good abrasion and corrosion resistance and a high friction coefficient. These properties are utilized in applications requiring good damping and/or sealing properties and high elastic elongation. Such applications include, e.g., tyres, seals, and conveyor belts. Some examples of the applications are presented in Figure 1.1.

Figure 1.1. Typical rubber applications.

In actual practice, elastomers are barely used as such: Different kinds of ingredients including e.g., vulcanization chemicals, fillers, plasticizers, and antidegradative agents are added to give the typical rubber properties. Fillers are used to improve the properties of rubber, such as strength and abrasion resistance, or to reduce costs. Carbon black (CB) is the most widely used reinforcing filler in rubber compounds. It is produced by thermal decomposition method or by incomplete combustion method from petroleum oil or coil. The type and properties of carbon black vary according to the processing method but typically, it is classified according to three characteristics: particle size, structure and surface chemistry. CB having small particle size and high structure has outstanding reinforcing properties in rubbers, but compared to the other generally used reinforcing filler, silica, the CB-filled rubber lacks good dynamic properties which are important, e.g., in tyre applications. Traditionally, silica is used to improve the dynamic properties of rubbers but the affinity and interaction between it and the general-purpose rubbers are poor. Therefore, a surface modification is required to achieve the full advantages of silica, but this prolongs the processing times and increases processing costs. [6][7]

The drawbacks of CB and silica mentioned above might be overcome with new filler systems guaranteeing the good mechanical and dynamic properties of rubbers. During the last decades, the polymer science has concentrated on nanofillers as they have the high aspect ratio and large surface area and therefore high reinforcing potential [8]. Nanofillers, such as carbon nanotubes (CNTs) and layered silicates (LS), are found to have many benefits. They have been reported to, e.g., increase tensile strength, hardness, modulus, abrasion resistance, electrical conductivity, and chemical resistance of rubbers at small filler concentrations. [9]

However, the surface energy of the nanofillers is high and thus they tend to form rather stable agglomerates making the dispersion of these fillers difficult. The most commonly used elastomers are hydrophobic materials, whereas many nanofiller types are hydrophilic and consequently, the interaction between these two components is weak. Therefore, the surface treatment is required to reduce the hydrophilicity of fillers and to enhance filler-polymer interaction. [10]

In literature, several studies are published in which different types of nanofillers are used in rubbers, but filler combinations are rarely applied although from a practical point of view it might be more interesting. This thesis focuses on the improvements of the polymer-nanofiller interactions and thus on the mechanical and dynamic properties of rubber compounds by the partial replacement of CB by nanofillers in a model tyre tread rubber compound. Therefore, high tensile strength and low loss factor at 60°C are desired properties, which require good polymer-filler interaction. This is tried to be improved by the surface treatments of the nanofillers. The loss angle values (tan delta) are important for tyre tread compounds as it is utilized to predict the abrasion, wet grip and rolling resistance of tyres [11].

The most appropriate mixing method for these materials is studied. Traditionally, elastomers and ingredients are blended by direct mixing, but according to numerous studies, good dispersion of nanofillers is achieved only by solution mixing. [12][13] Nevertheless, the solution mixing method in large-scale production poses practically and economically a problem in rubber factories, and the further development of the mixing technologies is required.

2. OVERVIEW OF RUBBER REINFORCEMENT

Many elastomers, especially synthetic elastomers, have naturally poor mechanical properties, but they can be improved by incorporating reinforcing fillers into the rubber. [6][7] Fillers are classified to be reinforcing if their particle size is less than 0.1 μm due to a high relative surface area, which is characteristic for small particles. The large surface area enables an efficient load transfer from the matrix to the filler. [2] Nevertheless, a small particle size does necessarily not mean a high reinforcing effect; the other characteristics such as the aspect ratio, structure and surface chemistry of fillers also have a major influence. [14][15][16]

2.1 Reinforcing effects of fillers

A lot of research work has been performed to understand the reinforcing effect of fillers. The main factors having an influence on the reinforcing potential of fillers are the formation of filler network and polymer-filler interaction. [15]

Polymer-filler interaction
The crucial factor in the reinforcement of elastomers is interaction between fillers and polymers. The polymer-filler interaction can be achieved by strong covalent bonds or weak physical forces. The formation of the covalent bonds depends on the compatibility of functional groups on the surfaces of filler and polymer. The bonds between fillers and polymers decrease the mobility of polymer chains, making them insoluble to solvents. This part of the elastomer, the bound rubber, has its own particular properties and is reinforcing the rubber. [17][18]

The amount of the bound rubber is affected not only by compatibility but also by the area of interphase. The total interfacial area of fillers (ψ) in a rubber compound depends on the specific surface area of the filler (S), the volume fraction of the filler (φ) and the density (ρ) of the filler: [19]

$$\psi = \varphi \rho S, \quad (1)$$

Polymer and filler can interact also by physical forces when polymer chains are mechanically trapped into the voids of filler aggregates and their deformation is impeded. Therefore, the polymer chains behave like rigid fillers and this increases the effective filler fraction. [13] This part of the polymer is called occluded rubber. The combined volume fraction of filler aggregate and occluded rubber (φ') can be calculated by

$$\varphi' = \varphi\left(\frac{1+0.02139DBPA}{1.46}\right), \quad (2)$$

where φ is the volume fraction of the filler and *DBPA* describes the dibutyl phthalate absorption number. [19]

Filler-filler interaction

Besides the polymer-filler interaction, the interaction between the filler particles affects the properties of a rubber. The filler-filler interaction and the formation of a filler-filler network increases the modulus of rubber. This behaviour is strain dependent: With increasing strain amplitude, the filler network breaks down due to the separation of filler particles, and the shear modulus decreases as seen in Figure. 2.1. This is called the Payne effect, and it is used to determine the dispersion of the compound: Better dispersion leads to less filler-filler interactions and thus less decrease in the storage modulus at higher strain amplitudes. [2][6][7][20] [21][22][23]

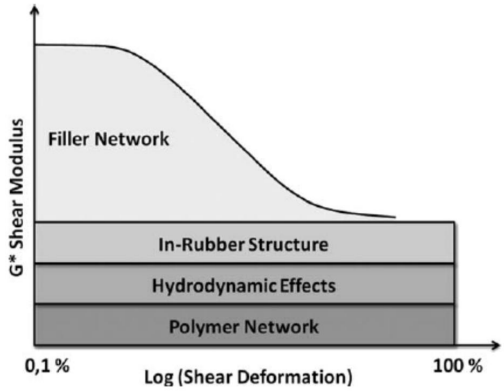

Figure 2.1. The Payne effect. [24]

The Krauss model is used to describe the Payne effect:

$$G'(\gamma_0) = G'_\infty + \frac{G'_0 - G'_\infty}{1+\left(\frac{\gamma_0}{\gamma_c}\right)^{2m}}, \quad (3)$$

where G' is the storage modulus, γ_0 is the strain amplitude, and γ_c describes the critical strain at which the loss modulus reached its maximum. $G'_0$and G'_∞ are storage modulus at small and large strain amplitudes, respectively. The parameter m describes the strain dependency. [25] [26]

Hydrodynamic effect

The hydrodynamic effect is a well-known phenomenon modelled by Einstein. According to it, the addition of solid particles to a viscous fluid increases the viscosity of the fluid. The same is valid for elastomers filled with spherical particles as described by Guth and Gold:

$$\eta_f = \eta_0(1 + 2.5\varphi + 14.1\varphi^2), \quad (4)$$

where η_f is the viscosity of the filled polymer, η_0 is the viscosity of the pure polymer and φ is the volume fraction of the fillers. The effect is also valid for the shear modulus of filled rubber (G_f): [18]

$$G_f = G_0(1 + 2.5\varphi + 14.1\varphi^2), \quad (5)$$

As the shape of the filler affects their reinforcing effect, Guth added a shape factor (f_s) describing the ratio of the length and width of the particles to the equation:

$$G_f = G_0(1 + 0.67f_s\varphi + 1.62f_s^2\varphi^2) \quad (6)$$

This equation is thus valid for all filler-polymer systems. [15]

2.2 Nanofiller reinforcement in rubbers

Nanofillers, such as nanoclays and CNTs, are a relative new filler group becoming an alternative to the conventional fillers. Although, rubber technology has utilized nanotechnology for a century already, as CB and silica are characterized by nanodimensions.

Fillers are classified to be nanofillers if at least one of their dimension is less than 100 nm. Thus, all nanofillers should by definition be reinforcing materials. The surface area of nanofillers is about 1000 times larger than the surface area of the same volume of micrometer size filler. Therefore, they have a very high surface-to-volume ratio, enabling more interfacial interaction with polymer. [2]

Nanofillers are known for the fact that high reinforcing effect can be achieved already at low loadings. However, the mixing and homogenous dispersion of nanofillers in an elastomer matrix and thus achieving the maximal efficiency of nanofillers is a challenge, as the nanofillers tend to form stable agglomerates due to their high surface energy. [9]

2.2.1 Layered silicates

Nanoclay is a widely used nanofiller appearing in various forms, but generally, the word 'nanoclay' is used for layered silicates (LSs). The most commonly used LS in polymer nanocomposites is montmorillonite (MMT) with the molecular formula of $(Na,Ca)_{0.3}(Al,Mg)_2Si_4O_{10}(OH)_2 \cdot nH_2O$. It belongs to the smectite family, where the ratio of SiO_4 and AlO_6 is 2:1. The structure of MMT is presented in Figure 2.2. MMT is composed of 1 nm wide silicate layers with a diameter from 100 to 1000 nm. [27][28][29][30][31]

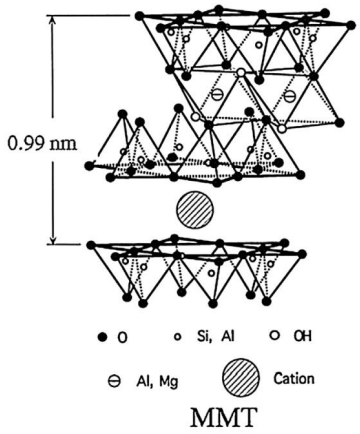

Figure 2.2. The structure of montmorillonite. [32]

The silicate layers are bonded to each other by weak van der Waals forces, which leave gaps between the layers. To form nanocomposites, polymers need to penetrate between the silicate layers during compounding. Therefore, the interlayer spacing needs to be higher than the size of the polymer chain. Otherwise, the layers remain stacked and form traditional fillers with microscale dimensions and the advantages of nanofillers are lost (Figure 2.3). [28][30][31]

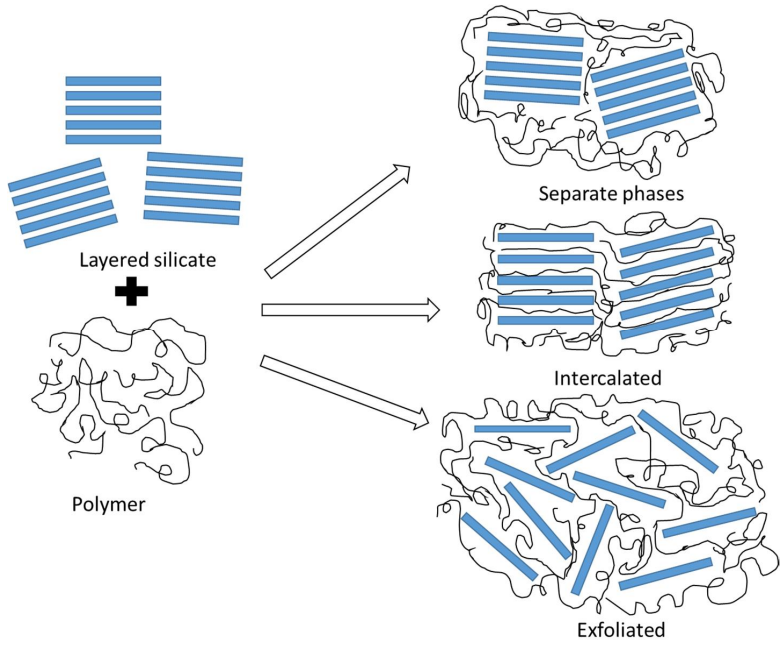

Figure 2.3. Schematic illustration of different types of polymer-clay nanocomposites.

The structure of nanocomposites formed by LSs can be intercalated or exfoliated, as illustrated in Figure. 2.3. In the intercalated structure, the polymer chains have penetrated between the silicate layers, but the layers still have an ordered structure resulting in a smaller aspect ratio and thus poorer performance. In exfoliated nanocomposites, the silicate layers are totally delaminated and disordered and they act like individual particles with a high aspect ratio. The degree of exfoliation is often increased by chemical modification. [10][30][31][33][34][35]

To increase the interlayer spacing and hydrophobicity of fillers, some cations such as Na^+, K^+, Ca^{2+}, Mg^{2+}, Al^{3+}, H^+, Li^+, Cs^+, Rb^+ and NH^{4+} can be exchanged by alkyl ammonium or phosponium ions with long hydrocarbon chains as presented in Figure 2.4. The cation exchange capacity (CEC) ratios of LSs range from 0.8 to 1.2 meq/g illustrating the average amount of cations on the individual particle. [28][34][36]

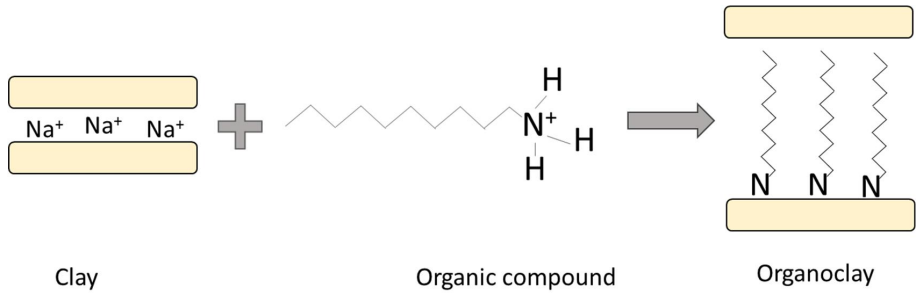

Figure 2.4. The principle of the ion-exchange reaction.

The replacement of the original cations by alkylated ions makes the surface of the filler more compatible with the hydrophobic polymer by decreasing hydophilicity of the fillers, by lowering the surface energy of the fillers and producing functional groups on the filler surface. The surface modification of the exfoliated fillers can further stabilize the structure and activate the surface of the filler for better compatibility with polymer. [10][37][38][39]

Thermoplastics filled with natural MMT have attracted a lot of attention due to the improvements in the mechanical, thermal, and the gas barrier properties of the resulting composites. Currently, such nanocomposites are used, e.g., in packaging, fire retardant coatings, and in aerospace, automobile, and medical applications. [10][40][41] [42]

Also, a number of different rubbers have been modified with LSs [37][43][44][45][46] [47][48][49][50]. The changes in the properties of rubbers depend on the LS type and its compatibility with the rubber as well as the dispersion of the fillers. The studies have shown that the modification of the LS surface increases the exfoliation degree, which leads to the significantly increased tensile modulus and tensile strength of NR. [45] Moreover, improvements in hardness and thermal stability have been achieved. In addition, organo modified LSs have been reported decreasing the scorch time of rubbers and accelerating the curing process due to the

presence of organic quaternary ammonium salts. [51] The amines are known to accelerate the sulphur curing process. The best improvement in the mechanical properties of NR is said to be achieved with 4 phr (parts per hundred rubber) LS [52].

The synergistic effect of CB and LSs has been studied by Das et al., [53] Praveen et al., [54] and Liu et al. [55]. They used a constant amount of CB and varied the amount of LSs. The addition of nanoclay improved tensile strength and tensile modulus. In addition, Das et al. [53] reported that the combination of 20 phr CB and 5 phr LSs leads to similar mechanical properties as with 30 phr CB, but has a lower loss factor, which is a desired property for tyre tread applications. In addition, Liu et al. [55] observed a decrease in the loss factor after the addition of LS into CB-filled NR.

2.2.2 Halloysite nanotubes

Halloysite nanotubes (HNTs) are naturally occurring aluminosilicates having a similar composition as kaolinite: $Al_2Si_2O_5(OH)_4 \cdot nH_2O$ [56][57][58]. HNTs consist of a two-layered tubular structure (Figure 2.5). There are siloxane groups on the surface of the outer layer, and aluminol groups on the inner layer and the edges of the tubes making the dispersion of this filler very difficult due to their inter-particle affinity. [59][60]

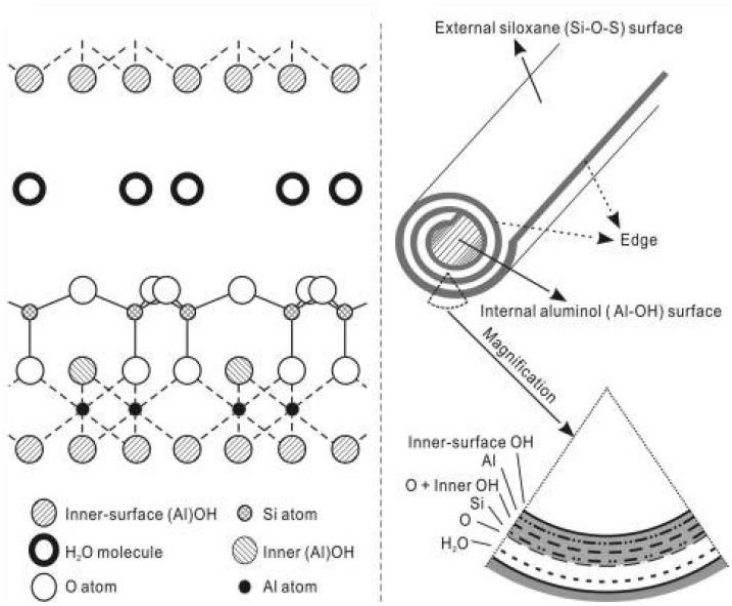

Figure 2.5. The structure of HNTs. [61]

Studies have shown that HNTs are promising reinforcing nanofillers for elastomers. The addition of HNTs has been reported to improve the mechanical properties (tensile strength) and thermal stability of rubbers [58][59][62][63][64][65][66][67][68][69]. Moreover, HNTs have been mentioned to increase the crosslink density of many studied rubbers and to increase scorch time due to the adsorption of curatives onto HNT surface [59][64][66][70], but also shorter

scorch time after addition of HNTs have been reported [67]. Moreover, HNTs have been mentioned having a negative effect on the fatigue life of NR [71]. The partial replacement of CB by considerable amount (10-40 phr) of HNTs was reported to decrease the moduli and strength of rubber due to the incompatibility with NR [72].

HNTs have been reported having better interaction with NR than silica [59] and to increase polymer-filler interaction and the dispersion of silica. [73] However, the silanol groups on the surface of HNTs still create unsatisfactory interfacial interaction with rubbers due to differences in hydrophobicity: Hydrophilic HNT is not naturally compatible with hydrophobic rubbers. Therefore, a surface modification of HNTs is required for forming strong bonds. Some modification methods including chemical modification with organosilanes, [59][61][66] methacrylic acids, [74] [63] sorbic acids, [62][64] or modification by the adsorption of ionic liquids [75][59][63] have been studied. They have been reported improving the dispersion of fillers and increase polymer-filler interaction inducing improvements in the mechanical properties of rubbers. Moreover, increments in maximum torque values and the shortening of curing time have been noticed.

2.2.3 Carbon nanotubes

Carbon nanotubes (CNTs) can be considered as graphene sheets forming a tube with capped ends. [13] The surface of CNTs consists of the regular hexagons of carbon atoms. CNTs are either single-walled nanotubes (SWCNTs) consisting of one graphene layer or multi-walled (MWCNTs) consisting of at least two nanotube layers (Figure 2.6). The length of CNTs typically varies from several micrometers to, in some cases, centimeters, while the diameter of the tubes is in nanoscale: The outer diameter of a MWCNT can vary from 2 to 50 nm. [76][77]

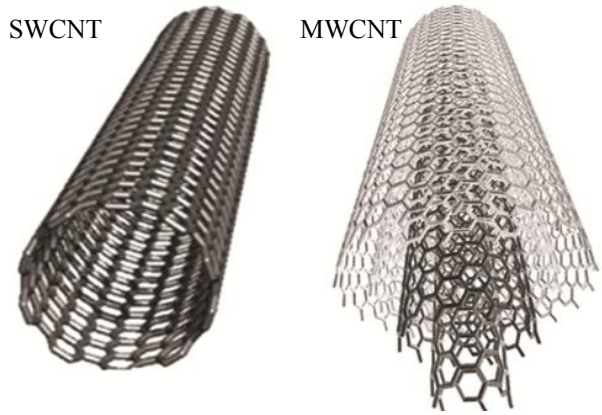

Figure 2.6. Different CNT structures. [78]

The special properties of CNTs compared to other common nanofillers are high electrical conductivity up to $2x10^7$ S/m [79], and the formation of conductive filler networks in an elastomeric matrix at 2-6 phr loadings [80][81][77]. Due to the very stable structure, the Young's modulus of SWCNTs can be even 5 TPa [82] and tensile strength from 50 to 200 GPa [76].

Most of the CNT-polymer nanocomposite studies have been made with plastics but the reinforcing effect of CNTs has also been studied for elastomers [77][83][84][85][86]. In these studies, improvements in mechanical properties have been reported already at small filler concentrations [76][77][85] due to the high aspect ratio and surface area of CNTs enabling the formation of a continuous filler network [87][88]. CNTs have also been reported to decrease the elongation at break due to the increased stiffness [80][83] and to decrease the loss factor peak and thus the abrasion resistance of rubber due to the decreased mobility of polymer chains [86] [81][85]. In addition, increase in crosslink density has been reported [89].

However, it has also been pointed out that the reinforcement effect could still be greatly improved with the better dispersion of CNTs. The solution mixing has been said to improve the dispersion and distribution of CNTs. During the mixing, weak interactions and the formation of a filler network take place. This increases the stiffness and strength of the composite due to more efficient load transfer. [84][88]

The combinations of CB and CNTs have been utilized in a few studies [83][86][90], mostly by adding different concentrations of CNTs to a constant amount of CB. This results in an increase in tensile strength and elastic modulus. Ismail et al. have studied the properties of NR when CB is partially replaced by CNTs: A synergistic effect of fillers was observed and improvements in tensile properties were achieved at low CNT concentrations. In addition, the curing process is more efficient when the amount of CNTs increases. [91]

2.3 Surface modification of fillers

The low reactivity of nanofillers makes the surface modification of these fillers necessary in order to improve the compatibility of fillers and polymers and create functional groups on the surface of fillers. This enables the filler to react with the polymer, on the surface of the filler, to lower the surface energy of the filler and thus to reduce filler-filler interactions and improve the dispersion of fillers. The improved dispersion and polymer-filler interaction lead to the improved mechanical, dynamic and thermal properties of polymer.

There are several chemical and physical methods to modify the surface of fillers. Amongst these methods, coupling agents, especially silanes, are the most commonly used modifiers in rubber technology.

2.3.1 Coupling agents

A chemical additive being able to provide a covalent bond between two dissimilar materials (polar filler and non-polar polymer) is called a coupling agent. In rubber technology, organosilanes are commonly used coupling agents with silica. They are found to improve the bonding between silica and polymer matrix, but they also affect the processing of the material. The general structure of organosilanes is $(RO)_3Si–(CH_2)_n–X$, where R is an alkane and X is a functional group (e.g., sulphur, epoxy, amino, ester or vinyl). The functional group is chosen so that it is compatible with the used polymer. [92][93]

The reaction between the silane and the silica occurs in two steps: [92]

1. Hydrolysis or direct reaction between the alkoxy groups of the silane and silanol groups on the surface of the filler resulting in formation of silanols (Figure 2.7).
2. Condensation reactions between silanols, resulting in formation of siloxane (-Si-O-Si-) bonds.

Later on, the sulphide moiety reacts with the unsaturated polymer in a vulcanization process. [94]

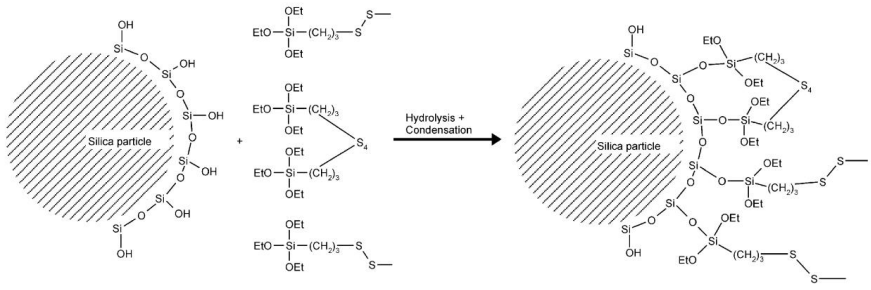

Figure 2.7. Reaction of silica with a coupling agent. [94]

2.3.2 Modification of filler surface by plasma polymerization

Plasma polymerization is a relatively new method of modifying filler surfaces. The modification is done by coating the filler with a very thin polymer film that is able to react with the polymer of the matrix. The main reasons for the plasma polymerization of fillers are the reduced polarity of filler and the modification or creation of functional groups on the surface of the filler so that the compatibility with the polymer improves.

The principle of the plasma polymerization of fillers is presented in Figure 2.8. The plasma film is formed on the outer surface of the filler by polymerizing monomer gases with the help of plasma energy. With this method, it is possible to achieve very good adhesion between the film and the substrate and still preserve the structural characteristics of the substrate. The

plasma polymerization of fillers is a challenging process compared to the modification of a planar surface due to the high surface area of particles. In the plasma polymerization of fillers, the complete surface of the filler aggregates should have a deposit by plasma. For this, the filler agglomerates need to be broken by moving the powder during the plasma polymerization. [95][96]

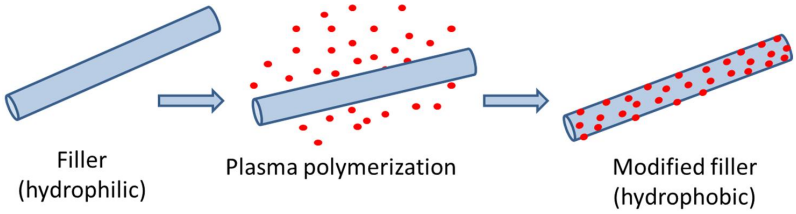

Figure 2.8. The principle of the plasma polymerization of fillers.

The plasma polymerization has been utilized in surface modifications of fillers in rubber compounds in a few cases earlier. The fillers treated by plasma include CB [96][97][98], silica [95][99][100][101] and clay [97][99][100]. The plasma treatment has been reported affecting the dispersion of fillers and the mechanical properties of rubber. However, the final properties of rubber are greatly affected by an elastomer type and by the polymer used in the plasma polymerization. [94] The plasma treatment of CB has been reported increasing the tensile strength of SBR slightly [97] but decrease that of ethylene-propylene-diene rubber (EPDM) [96]. The plasma polymerization of silica has given more promising results than the plasma treatment of CB. Especially, the plasma polymerization of silica by acetylene has improved the dispersion of silica compared to the untreated fillers as well as the mechanical properties of EPDM and acrylonitrile butadiene rubber (NBR). In the case of SBR, the plasma polymerization by polythiophene improved mechanical properties more than acetylene. [95][99][100]

3. MIXING

A rubber compound contains typically 10 to 20 different components. Therefore, the mixing of an elastomer and its ingredients plays an important role in the processing of a rubber. The aim of the mixing is to produce a homogenous rubber compound where fillers and other ingredients are evenly dispersed and distributed, and to achieve the required properties for the rubber. [102]

Rubber compounds are often mixed in multiple stages. Commonly, the curatives are added in separate stages to the prevent pre-vulcanization of the rubber compound due to increasing temperature during the mixing process. The quality of mixing is mainly dependent on the shear forces and temperature during mixing. These parameters are affected by many operating variables, such as temperature control unit setting, ram pressure, rotor speed, fill factor, and cooling. [102][103]

The mixing process can be divided into four stages: masticaton/plastication, incorporation, dispersive mixing, and distributive mixing. In practice, all these stages occur simultaneously. The mastication of a polymer is the first step in the mixing process. The aim of mastication is to reduce the molecular mass and the viscosity of the polymer or in some cases to reduce the crystallization of polymer as NR is able to crystallize when storing at cold temperatures. The mastication is done by degrading the long polymer chains by high shearing forces and/or with the help of peptizing agents.

The incorporation stage (Figure 3.1a) is divided in three overlapping steps: encapsulation, subdivision and immobilization. At first, the rubber and the ingredients form a heterogeneous mass. Then the filler is isolated by the polymer chains and the separate materials are combined into one homogeneous mass on macroscopic scale but still heterogeneous on micrometer scale. [6][102] During the subdivision, the filler agglomerates are broken into approximately 0.5 μm units. The size reduction is caused by the shearing and elongational flow of the elastomer. In the immobilization step, some polymer chains penetrate into the voids of the filler aggregates preventing the movement of this occluded rubber. [6][102] [104]

In the dispersive mixing (Figure 3.1b), the filler aggregates are broken down by high shear forces. Due to the size reduction of the aggregates and partly due to the degradation of polymer chains, the viscosity of rubber is decreased. This lowers shear forces and stresses making the dispersion of fillers more difficult and finally stopping it. When the particles have reached their final size, they are distributed homogenously throughout the rubber matrix. During this distributive mixing (Figure 3.1c), the size of the particles does not change. [6][102][103] [104]

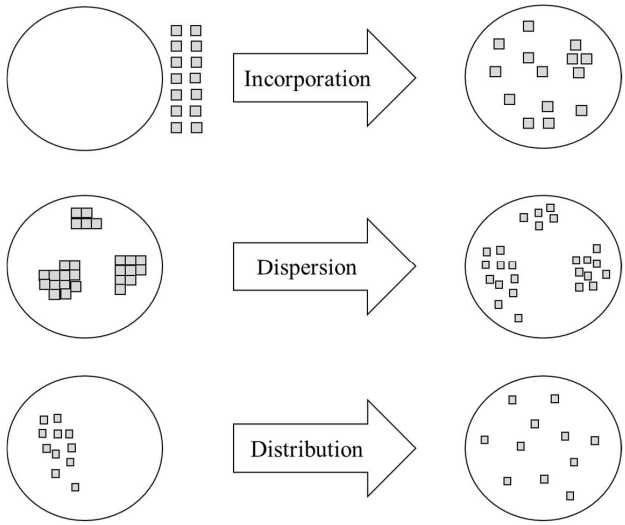

Figure 3.1. The stages of the rubber mixing.

Rubbers are typically mixed by direct mixing, in which the materials are added into an internal mixer equipped with two rotors turning in opposite directions. The internal mixers are divided into tangential mixers and intermeshing mixers according to their rotor geometry. In intermeshing mixers, the dispersive mixing of additives occurs mainly between the rotors whereas in tangential mixers the dispersive mixing occurs between the rotor and the wall of the chamber. The shearing occurring between the rotors increases the axial and radial movement of polymer making the distributive mixing process in intermeshing mixers more efficient than in tangential mixers [6][102][103]

The direct mixing in an internal mixer is the preferred method for mixing rubber compounds containing the traditional fillers. The shear forces in this process are high enough to break filler agglomerates into smaller aggregates being able to act as the reinforcing units. However, the traditional mixing method has limitations in mixing nanofillers, as they are difficult to disperse properly due to their tendency to agglomerate. Instead, a solution method has been reported to be an effective mixing method for nanofillers, especially for CNTs, and good dispersion in a rubber matrix has been achieved. [13][16][102]

In the solution mixing, the polymer is dissolved in a suitable solvent. The nanofillers and other ingredients are added to the solution and dispersed with a high shear mixer. After the mixing process, the solvent is evaporated and the rubber is vulcanized. This method is rather time-consuming and expensive compared to direct mixing and therefore not viable industrially.

For large-scale use, the masterbatch mixing of nanofillers could be more effective than the solution mixing. In this technique, a high loading of nanofillers is mixed with a polymer by

direct mixing. In the second step, this masterbatch is diluted with a matrix material. Among nanofiller-rubber composites, the masterbatch technique has been used for nanoclay. It has been reported that the rubber compound mixed by the masterbatch method has better mechanical properties than the compounds mixed by solution mixing. [105][106]

4. AIMS OF THIS STUDY

The hypotheses behind this work were:

- Nanofillers have a high reinforcing potential.
- The combination of CB and nanofillers can improve the dispersion of fillers and thus improve the polymer-filler interaction.
- Polymer-nanofiller interaction can be improved by surface modification.
- Plasma modification can be utilized to increase the polymer-filler interaction of silicate nanofillers with non-polar rubbers.
- The dispersion of fillers can be affected by mixing technologies.

The objective of the work was to study the ability of new filler systems to tailor the properties of elastomeric materials for applications requiring good mechanical and dynamic properties. Therefore, the study was conducted for elastomer blend used in tire tread. Furthermore, the aim of the work was to find out a good way to mix nanofillers with rubbers in order to achieve a good dispersion and distribution of fillers. The research questions are:

1. How does a combination of carbon black with nanofillers influence the dispersibility of fillers and the properties of an elastomeric blend?
2. Does the surface modification of nanofillers enhance the compatibility of filler and rubber and thus improve the properties of the rubber?
3. What is the potential of masterbatch mixing to improve the dispersion of nanofillers and the properties of the rubber when compared to direct mixing for the filler-polymer systems used in this study?

Dual filler systems were investigated by replacing a small amount of CB by the different types of nanofillers and by studying selected properties such as filler dispersion, vulcanization, strength, and dynamic properties (*Publications I-IV*). The nanofillers included layered silicates (*Publicatios I* and *II*), halloysite nanotubes (*Publications I* and *III*), and carbon nanotubes (*Publication IV*). The influence of surface treatment of nanofillers on polymer-filler interaction was studied in different ways: silane treated LSs and HNTs (*Publication I*), organomodified LSs (*Publication II*) and plasma treated HNTs (*Publication III*). *Publications V* and *VI* report the effect of the masterbatch mixing method of CNTs on filler dispersion. The research steps are summarized in Figure 4.1.

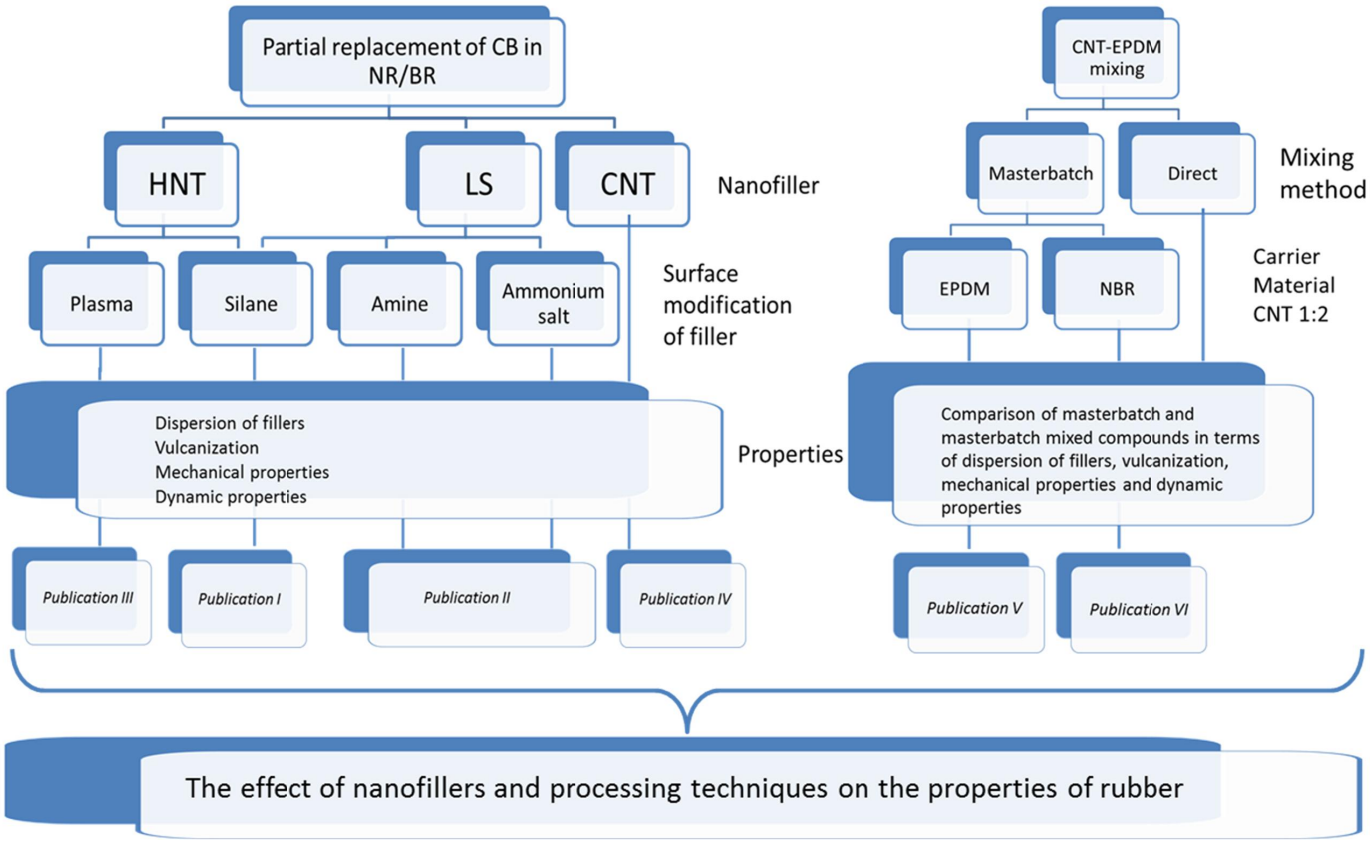

Figure 4.1. The summary of the study

5. EXPERIMENTAL

The materials and the methods used in the study are presented in the following subchapters. First, the studied nanofillers are introduced followed by a description of the manufacturing processes. Subsequently, the characterization methods are presented.

5.1 Nanofillers

The effect of a partial replacement of carbon black (CB) by nanofillers was studied with different nanofillers: 3 different types of layered silicates (LSs), carbon nanotubes (CNTs), and halloysite nanotubes (HNTs). The properties of the nanofillers are presented in Table 5.1. The masterbatch mixing studies were carried out with CNTs from Nanocyl (NC700).

Table 5.1. The nanofillers used in the study.

	Description	Shape & dimensions	Surface area, m^2/g	Specific gravity	Modification
Halloysite nanotubes (Sigma-Aldrich)	Halloysite clay	Tube, d 30 nm L 0.5-4 µm	64	2.53	-
Nanofil 116 (Rockwood Clay Additives)	Montmorillonite clay	Platelet, d <20 µm	-	2.6	Na^+ activated
Nanofil 5 (Rockwood Clay Additives)	Montmorillonite clay	Platelet, d <10 µm	-	1.4-1.8	QUAT
Nanoclay (Sigma-Aldrich)	Montmorillonite clay	Platelet, d <20 µm	-	-	PA
Baytubes C 150P (Bayer)	CNT	Tube, d 13-16 nm L 1-10 µm	-	-	-
NC700 (Nanocyl)	CNT	Tube, d 9.5 nm L 1.5 µm	250-300	-	-

QUAT: Dimethyl-di(hydrogenated tallow) alkyl ammonium salt
PA: Octadecylamine

5.2 Preparation of nanocomposites

In the partial CB replacement studies, the total filler concentration was kept constant, corresponding the amount of the CB in the reference compound, while a small amount (0-12.5 phr) of CB was replaced by nanofillers. A blend of NR and BR, as used in a typical truck tyre tread, was chosen as the matrix material. The recipe given in Table 5.2 was used as a reference compound, which contained only CB N-234.

Table 5.2. The basic recipe for NR/BR compounds and the mixing sequence.

Ingredients	Type/Producer	Amount, phr	Mixing, min
NR	SMR10	80	0
BR	Buna-cis-132/Dow Chemical Company	20	
Nanofiller	varied	varied	1
CB	N-234/Evonik	25*/42.5**/50	1.5
6PPD	Lanxess	2.0	
TMQ	Lanxess	1.0	
ZnO	Grillo Zinkoxid GmbH	5.0	
TDAE-oil	Vivatec 500/Hansen&Rosenthal GmbH	8.0	2
Stearic acid	Oleon N.V	2.0	
Ceresine wax	Statoil Wax GmbH	1.5	After incorporation of all ingredients: 4
CBS	Lanxess	1.5	Mill: 5
Sulphur	Solvay Barium Strontium GmbH	1.5	

6PPD: N-(1,3-dimethylbutyl)-N´-phenyl-1,4-benzenediamine

TMQ: 2,2,4-trimethyl-1,2-dihydroquinoline

TDAE-oil: treated distillate aromatic extract oil

CBS: N-cyclohexyl-2-benzothiazolesulfenamide

* In the CNT compounds

** In the plasma treated compounds

The compounds were mixed in a Krupp Elastomertechnik GK 1.5 intermeshing mixer. The cooling system temperature was set to 50°C and the used rotor speed was 70 rpm. The mixing sequence is presented in Table 5.2. Subsequently, the curatives of all the compounds were added on an open two-roll mill. The compounds were vulcanized to 2 mm sheets at their respective curing time at 150°C.

Silane treatment

An attempt to improve the polymer-filler interaction of LS and HNT containing compounds by a coupling agent was done by a silane treatment. The silane used for this purpose was bis(3-triethoxysilylpropyl)tetrasulfide (TESPT), which is commonly used as a coupling agent in rubber applications with silica. It is a bifunctional organosilane, which contains sulphur for the chemical coupling of the filler-silane complex to the polymer. The amount of TESPT was 10% of the amount of nanofiller in the respective recipe. The silane was added into the mixer together with the nanofiller. After the incorporation of all ingredients, the temperature was raised to 140°C by increasing the rotor speed and mixing was continued for 5 minutes to complete the silanization reaction.

Plasma treatment

Pyrrole (Py) and thiophene (Thi), both from Sigma-Aldrich, were used as monomers in the plasma polymerization process as they are promising polymers with silica [95]. The reference compound contained only CB as filler in a concentration of 42.5 phr. In the other compounds, 2.5 phr of CB was replaced with the same amount of untreated or plasma treated HNTs. The other ingredients followed the recipe presented in Table 5.2.

The plasma treatment was carried out in a plasma reactor presented in Figure 5.1. It consists of a glass flask and a long tubular region. The flask is connected to the vacuum pump (Duo Seal, model number 1402 B, Welch vacuum). The tube is surrounded by a copper coil that is connected to a radio frequency generator ACG-3B-01 from MKS/ENI. At the top of the tube, there are two ports, which are the inlet for the monomers and the connection to the pressure gauge (MKS Baratron® type 627B). The stirring of the powder is done by a magnetic stirrer. About 20 g of HNTs were placed into the bottom flask where they were treated with the activated monomers for 90 minutes. The parameters of the treatment followed the study made successfully for silica [95] and are presented in Table 5.3.

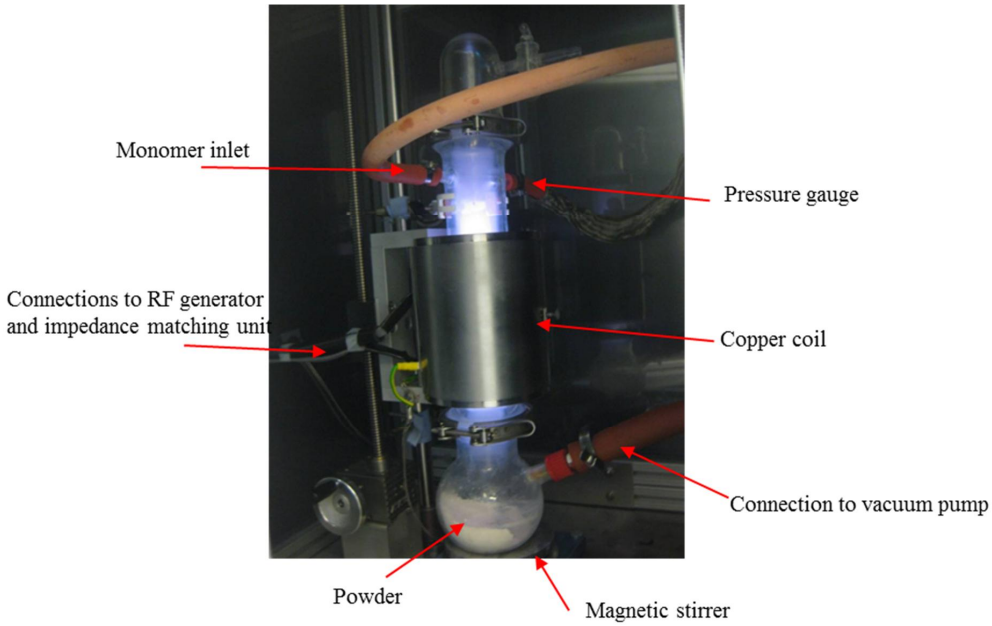

Figure 5.1. Tubular vertical plasma reactor.

Table 5.3. Parameters used in the plasma treatment.

Sample	Pressure, Pa	Monomer pressure, Pa	Power, W	Time, min
HNT-pyrrole	10	32	150	90
HNT-thiophene	10	50	150	90

Masterbatch mixing

For the masterbatch study, two masterbatches containing 50 phr CNTs were prepared with different carrier elastomers: ethylene-propylene-diene rubber (EPDM, Keltan 512) and acrylonitrile butadiene rubber (NBR, Europrene N3330).

The masterbatches were prepared in a Brabender N 350 E internal mixer. A certain amount of this masterbatch (the CNT concentrations of 6.3 phr in the final batch) was then further mixed in a separate step with EPDM, 5 phr zinc oxide (ZnO), 2 phr stearic acid, 2 phr zinc dibutyl dithiocarbamate (ZDBC) and 1 phr N-cyclohexyl-2-benzothiazolesulfenamide (CBS). The rotor speed was 70 rpm and the starting temperature was 50°C. The compound was dropped either at a temperature of 160°C or after 5 minutes mixing time. Subsequently, 1 phr sulphur was added on an open two-roll mill. The compounds were vulcanized at their respective curing time + 2 min at 160°C.

5.3 Characterization

Curing studies and Payne effect measurements were performed using an Advanced Polymer Analyzer APA 2000 (Alpha Technologies). The curing studies of the NR/BR compounds were carried out at 150°C for 25 min whereas the EPDM compounds were measured at 160°C for 20 min. The Payne effect was measured with three parallel measurements by a strain sweep from 0.28% to 100% at 100°C.

Tensile testing was performed with a Messphysik Midi 10-20 universal tester according to ISO 37 using dumbbell specimen type 1. Five parallel measurements were taken for tensile properties.

Dynamic properties were studied with a Pyris Diamond DMA from PerkinElmer Instruments, operating in tension mode. For the NR/BR nanocomposites, the measurements were done from -80°C to +80°C at a heating rate 3 K min^{-1} and the frequency of 10 Hz whereas 1 Hz frequency was used in the EPDM compounds.

The state of dispersion of the HNT particles in the NR/BR nanocomposites was investigated by a scanning electron microscope (SEM, Philips XL-30). A field emission scanning electron microscope (FESEM, Zeiss ULTRAplus) was used to analyse the fracture surfaces of the masterbatch mixed compounds. The failure surfaces were prepared by a Charpy impact hammer hit on liquid nitrogen cooled rubber strips.

The state of dispersion of selected compounds filled with both CB and nanofiller was investigated by a transmission electron microscope (TEM) using a JEM 2010 model. Ultra-thin sections, thickness 80-100 nm, were cut from the samples by an ultramicrotome (Leica Ultracut UCT) at -100°C.

Swelling behavior was studied by soaking vulcanized circular test samples in toluene until equilibrium swelling (72 hours). The diameter of the test pieces was 12 mm and thickness 2 mm. The swelling degree (Q) of the rubber was calculated by the equation:

$$Q = \frac{W_t - W_0}{W_0}, \qquad (7)$$

where W_0 is the initial weight of sample and W_t is the weight at time (t).

In the masterbatch study, the CNT content was checked by thermogravimetry (TGA). Perkin Elmer STA 6000 equipment was used for the measurements, which were conducted in air with a heating ramp from 30°C to 995°C at a rate of 10 K min^{-1}. The amount of CNTs was determined from the weight loss step measured at 550-650°C. The TEM images were taken by a Libra 120 transmission microscope at an acceleration voltage of 120 kV.

X-ray diffraction (XRD) analysis was performed in a Siemens D500 equipment to investigate the effectiveness of the clay intercalation and the change in the space gap between two clay platelets. Cu-Kα radiation (λ= 1.54056 Å) was used as source. The interlayer distance of the clay in the composites was calculated from the (001) lattice plane diffraction peak using Bragg's equation**:**

$$n\lambda = 2d\sin\theta, \quad (8)$$

where θ is the angle between the incident rays and the surface of the crystal, *d* is the the distance between atomic layers in a crystal, and *n* is an integer.

6. RESULTS AND DISCUSSION

In this chapter, the most important results of the study are presented and discussed. First, the effect of the partial replacement of CB by different types of nanofillers on the properties of NR/BR compound is presented. The properties under discussion include the dispersion of nanofillers, vulcanization properties, loss factor, and mechanical properties. The last subsection concentrates on the masterbatch mixing of CNTs.

6.1 Dispersion of nanofillers

The effect of the partial replacement of CB by nanofillers on the dispersion of particles was analysed by the Payne effect, electron microscopy and XRD. The reduction in the Payne effect is attributed to lower filler-filler interaction and therefore to the better dispersion of fillers especially in the case of silica, but the recent publications have reported the increase in the Payne effect after the addition of intercalated or exfoliated LSs or CNTs. The increase in the Payne effect has been explained by the formation of a filler network [107][108]. The Payne effect studies here showed that the partial replacement of CB by all the studied LS types as well as HNTs decreased the Payne effect whereas the CNTs increased it (Figure 6.1). Here, the total filler content was kept constant whereas in the abovementioned studies the amount of fillers increased after the incorporation of the nanofillers. Therefore, in the current study the reduction of CB loading needs to be taken into consideration. The changes in the Payne effect can partly be explained by the different total volume fraction of fillers (lower with silicate-based fillers and higher with CNTs), but clay minerals also suppress CB-CB interaction by being located in-between the CB particles and thus inducing the better dispersion and distribution of fillers as can be seen from Figure 6.2. The breakdown of the CB-CB network by the presence of LSs was also proposed by Praveen [54].

The TESPT treatment of LSs and HNTs was expected to decrease the Payne effect and to improve the polymer-filler interaction and the dispersion of nano-size silicates, as it does in the case of silica [109]. Nevertheless, the Payne effect results of the TESPT-treated LSs and HNTs did not show this effect as seen in Figure 6.1 a and b. The results can be due to the low concentrations of the nanofillers, and especially, the coupling agent, making it difficult to disperse the nanofiller system and thus limiting the effect on the properties that might be observed. This is supported by the fact that the TESPT-treatment decreased the Payne effect at 7.5 phr HNT concentration, where the silane content may be high enough to be adequately dispersed and thus to influence the properties of the rubber. Instead, the plasma treatment changed the filler-filler interaction of the rubber compound (Figure 6.1 d). The compounds containing Py-HNTs had lower filler-filler interaction, and the compounds containing Thi-HNTs had higher interaction than the compounds containing untreated HNTs. The higher Payne effect of the Thi-HNT compounds can be due to the formation of a filler network.

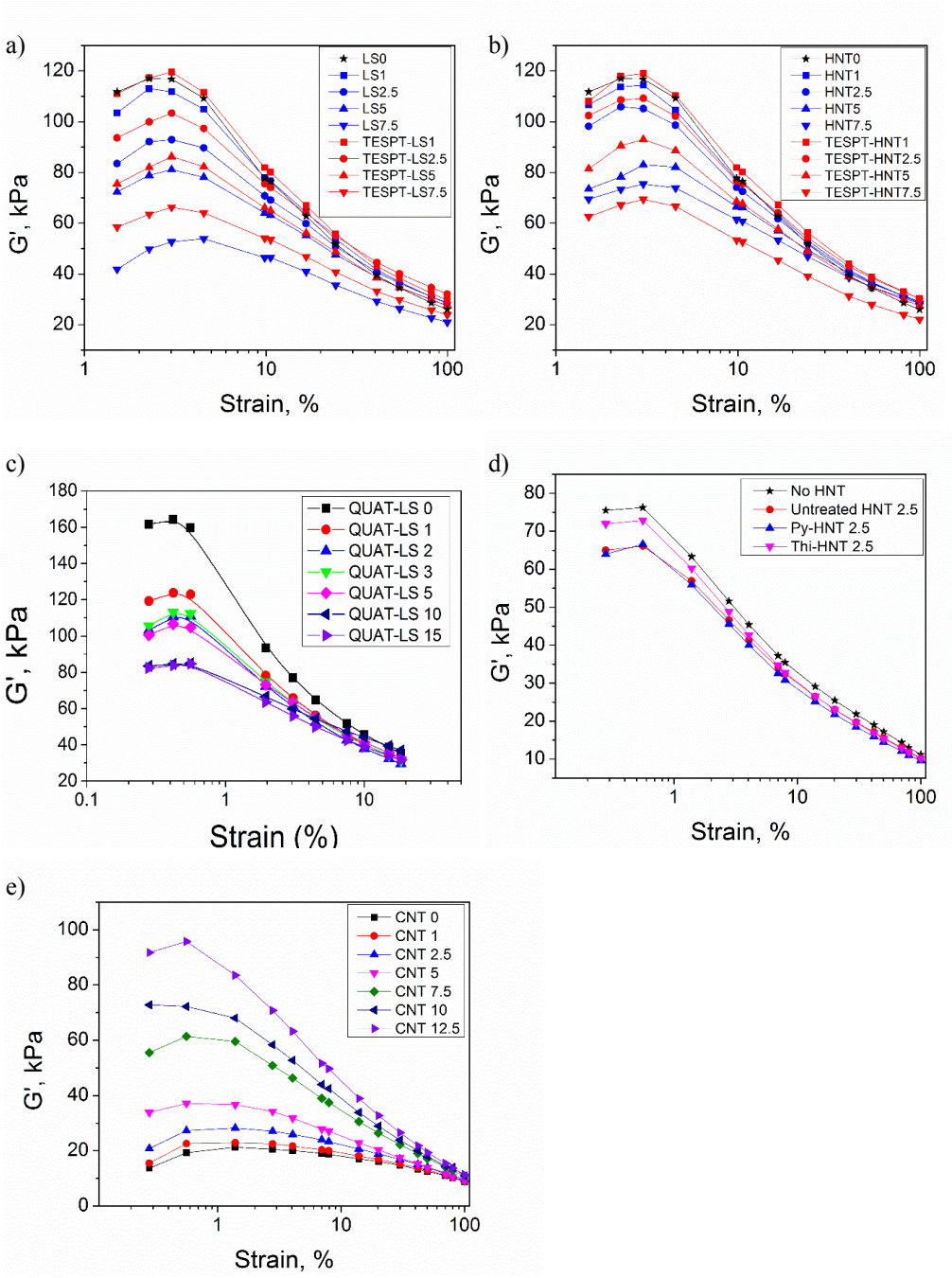

Figure 6.1. The Payne effects of NR/BR compounds with different nanofillers a) untreated and TESPT-treated LSs b) untreated and TESPT-treated HNTs, c) LS-QUAT, d) untreated and plasma treated HNTs, and e) CNTs. The numbers in the label describes the amount of the nanofiller in phr.

The improved dispersion and the compatibility of the plasma-modified fillers were proven by TEM study (Figure 6.2). It was revealed that the plasma modified HNTs were better dispersed than the unmodified HNTs, which showed a higher degree of agglomeration. In an earlier study, similar improvements were observed for silica [110]. In addition, the plasma treated HNTs improved the dispersion and distribution of CB. CB aggregates were smaller in the compounds containing the plasma treated HNTs than in the compound containing the untreated HNTs. However, Figure 6.3 shows that the HNT bundles are located between the phases making the material weaker.

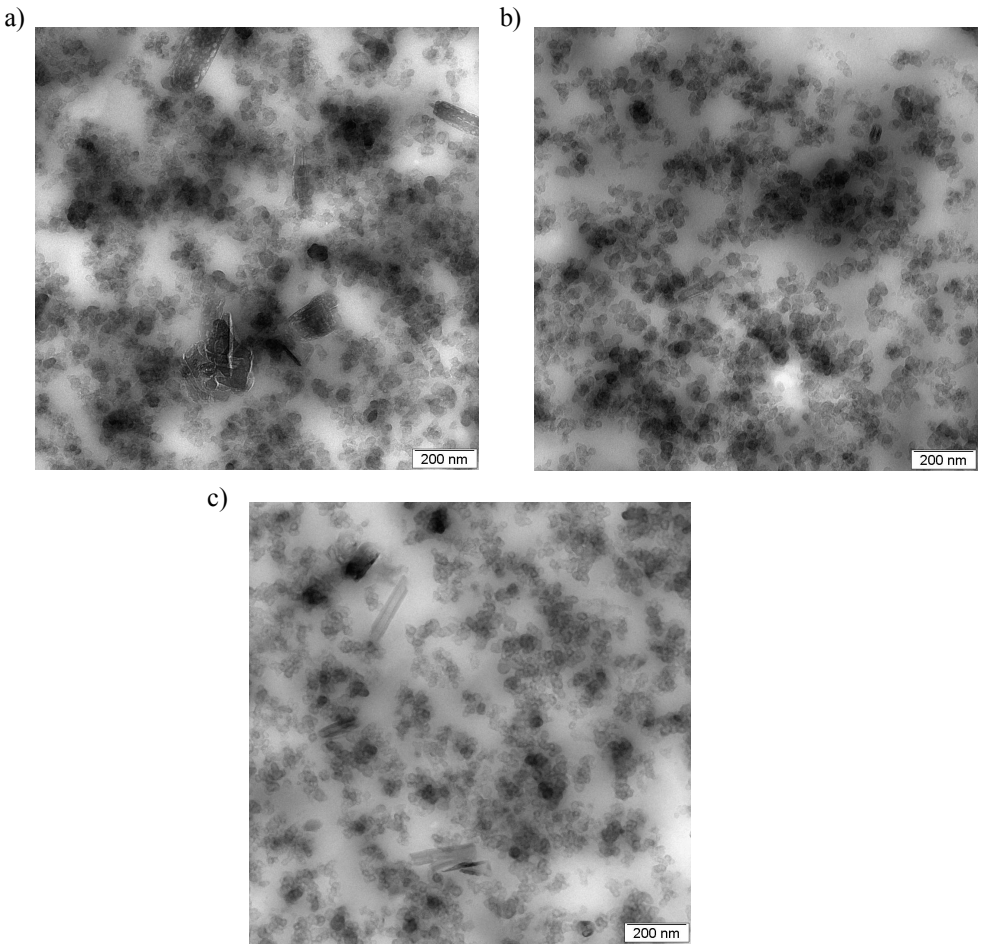

Figure 6.2. The TEM pictures of the NR/BR compounds containing a) untreated HNTs, b) pyrrole treated HNTs, and c) thiophene treated HNTs. [*Publication 1*]

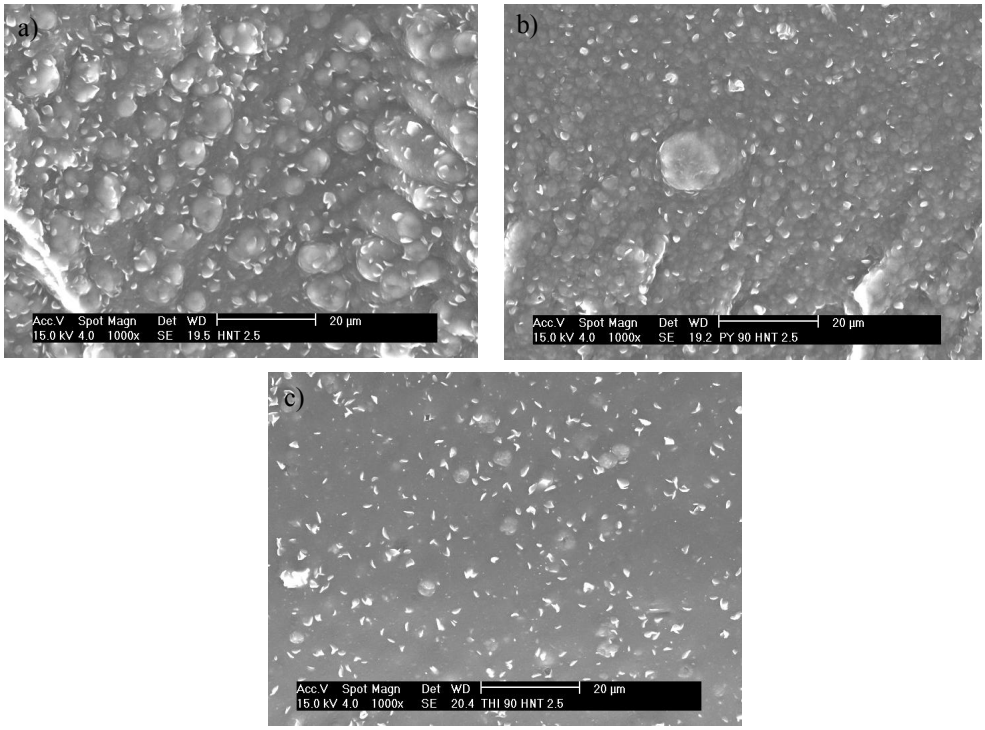

Figure 6.3. The SEM pictures of the NR/BR compounds containing a) untreated HNTs, b) pyrrole treated HNTs, c) thiophene treated HNTs. *[Publication III*]

The dispersion of organo (dimethyl-di(hydrogenated tallow) alkyl ammonium salt (QUAT) and octadecylamine (PA)) modified LSs was further studied by XRD (Figure 6.4). The XRD curves showed intercalated structures for both LSs. The clay-QUAT nanofillers had a higher intercalation level (3.81 nm) than the clay-PA filler (3.55 nm) indicating better polymer-filler interaction.

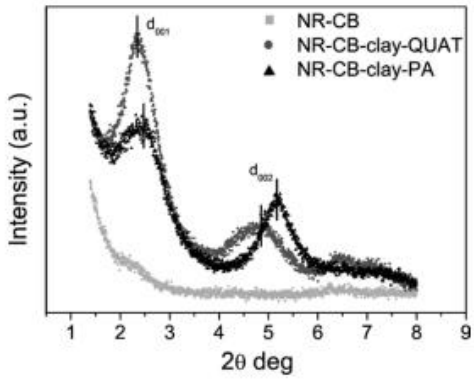

Figure 6.4. The XRD-analysis of the NR/BR compounds filled with carbon black and organoclays. *[Publication II*]

In the case of CNTs, the increase in the Payne effect was affected by the higher volume fraction of the nanofiller, but also by the formation of a filler network caused by primary CNT particles as presented also by Subramarian et al. [107]. The TEM pictures of the compounds containing both, CB and CNTs, supported the effect of the volume fraction. At CNT concentrations up to 5 phr, acceptable dispersion could be achieved with the traditional mixing technology, as seen in Figure 6.5. At 5 phr, large CNT agglomerates are not present (Figure 6.5a), whereas at higher CNT contents (10 phr), the agglomerates are clearly visible (Figure 6.5b). The dispersion of the CNTs decreased at higher CNT concentrations due to the CNT particles being closer to each other's and thus making agglomeration easier. It is also visible in the pictures that the CNTs are situated around the CB particles. Thus, the CNTs prevent the formation of CB agglomerates and improve the dispersion of this filler. The two-phase morphology of the rubber can be detected in the TEM pictures by the concentrations of fillers. Most of the fillers are located in darker elastomer phase although they can be detected in both phases.

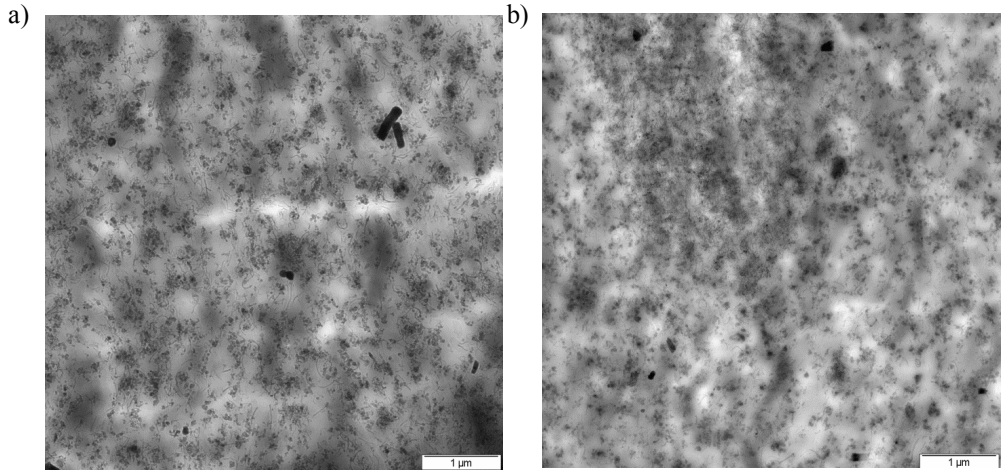

Figure 6.5. The TEM images of the NR/BR composites containing a) 5 phr CNTs and 20 phr CB, and b) 10 phr CNTs and 15 phr CB. *[Publication IV*]

6.2 Vulcanization

The rheometric curves of the NR/BR compounds are shown in Figure 6.6. The partial replacement of CB by untreated HNTs increased the difference between initial and final torque at low HNT concentration indicating more effective crosslinking reactions (Figure 6.6a). However, at higher HNT loadings the maximum torque and delta torque values decreased due to the decreased volume fraction of the fillers and the increased adsorption of curatives onto the filler, respectively. Moreover, the scorch time became longer with the addition of HNTs. This can

also be explained by the deactivation of curing additives. HNTs have silanol and aluminol groups on the surface. These groups are able to adsorb accelerators and hence interrupt the formation of crosslinks. These findings were similar to those obtained by Ismail et al. [68].

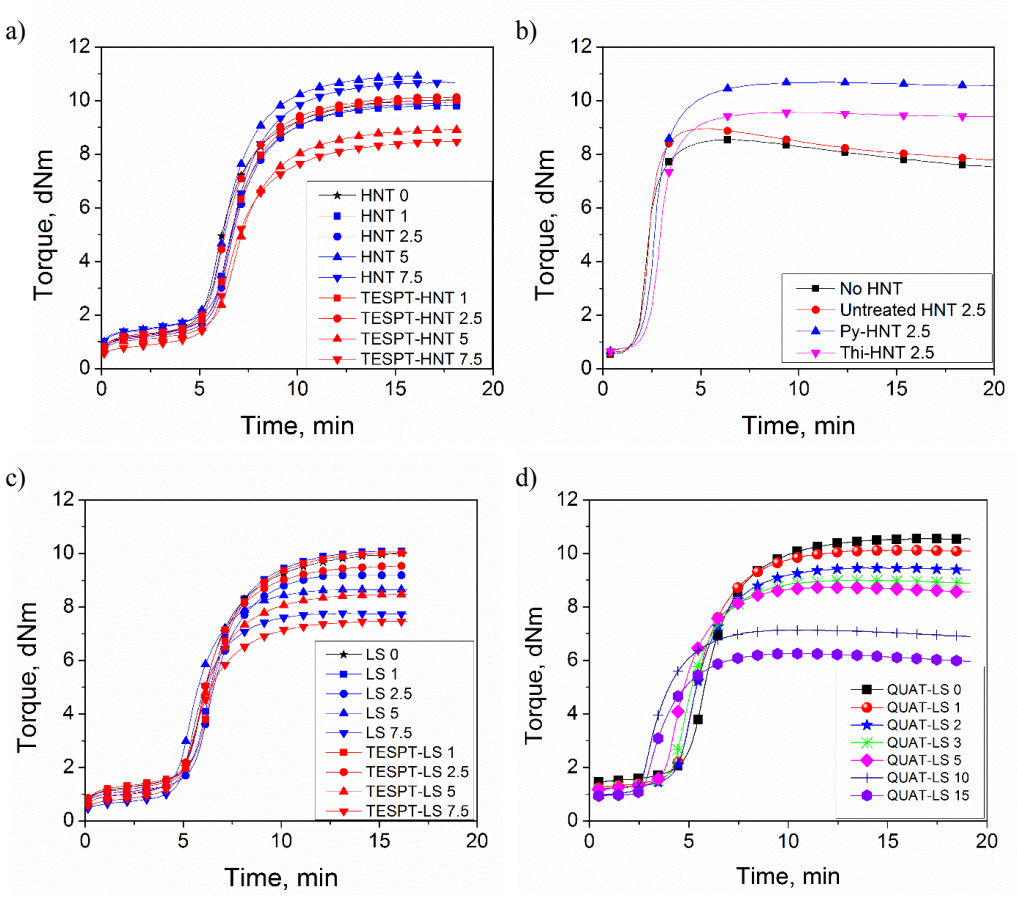

Figure 6.6. The rheograms of the NR/BR compounds containing a) HNTs without and with silane b) plasma-treated HNTs c) LSs without and with silane d) QUAT-modified LSs. The numbers in the label describes the amount of the nanofiller in phr.

The increase in the delta torque was more pronounced for the plasma treated HNTs than for the untreated HNTs indicating that the plasma coating affects to the bound rubber and network formation (Figure 6.6b). The plasma treated HNTs can affect the network formation either directly by the formation of filler-polymer bonds, or by interfering with the polymer-polymer crosslink formation. Especially in the case of pyrrole, where nitrogen-moieties are deposited on the surface in the plasma-process, these can interact with sulphur similar to the nitrogen moieties of accelerators. In addition, the plasma coating of HNTs stabilized the network and suppressed reversion.

The TESPT-treatment of HNTs led to an opposite trend compared to the plasma treatment (Figure 6.6a). The delta torque decreased when the HNT concentration increased. A similar trend was seen with the untreated LSs (Figure 6.6c). The addition of 1 phr LSs did not influence the crosslinking of the compound. At higher concentrations, the delta torque decreased when the LS concentration increased due to the adsorption of curatives on the surface of fillers. This effect was even more pronounced with the TESPT and QUAT modified LSs (Figure 6.6 c and d, respectively). In addition, the untreated LSs increased the scorch time although the change was not as evident as with HNTs indicating that LSs are less active than HNTs in this sense. Instead, the modified LSs decreased the scorch time especially at the higher LS loadings due to the increased amount of active sulphur moieties and the accelerating effect of ammonium groups in the TESPT and QUAT, respectively. During the mixing, the S-S bonds of TESPT may break down and give active sulphur for the crosslinking reaction. This effect has been reported for silica-filled rubbers [111]. The accelerating effect of ammonium groups was also observed in a study where a constant amount of LS was added to the SBR compound containing varying amounts of CB [53].

Similarly to HNTs, CNTs influenced the curing behaviour of the rubber: increasing delta torque values indicate more efficient curing compared to CB (Figure 6.7). In addition, the initiation of the vulcanization process became faster as the scorch time decreased when CNTs were incorporated, as also stated in other studies [91]. CNTs have a high thermal conductivity and thus they accelerate thermal energy transfer in a rubber matrix decreasing the onset point of vulcanization. Another reason can be metal impurities in CNTs that can be able to interfere with the vulcanization reaction.

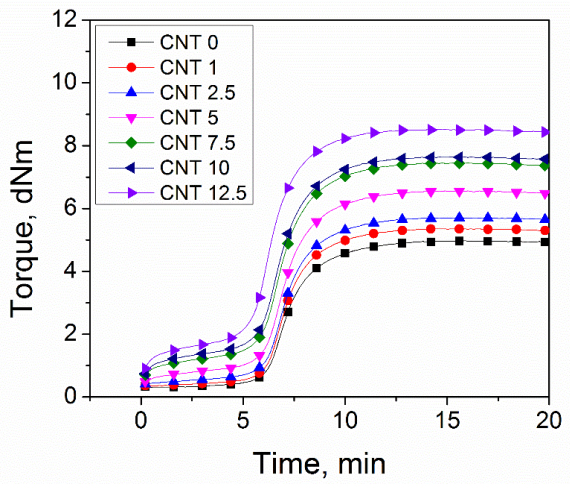

Figure 6.7. The rheograms of the NR/BR compounds filled with varying amounts of CNTs and CB.

6.3 Loss factor

The studied compound was a model tyre tread. Therefore, the effect of the partial replacement of CB by nanofillers on the loss factor of NR/BR rubber plays an important role. Figure 6.8a shows that the addition of CNTs decreased the height of the loss tangent peak due to the restricted motion of polymer chains. The lower peak for CB-CNTs filled compounds has also been observed by Cataldo [83]. In addition, the loss factor decreased at 0ºC but increased at 60ºC when the CNT content increased indicating worse wet grip and rolling resistance of tyre, respectively as seen in Figure 6.8b. Typically, the loss factor decreases or increases in both temperatures if the rubber contains only one filler. However, the synergistic effect of fillers can lead to increase in other and decrease in another temperature as has been noticed in the case of CB and silica.

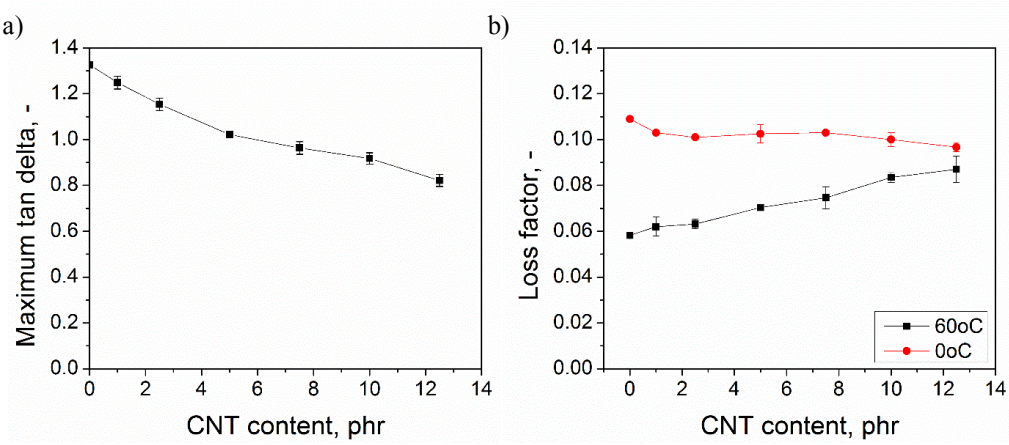

Figure 6.8. The loss angle of the NR/BR compounds containing varying amounts of CB and CNTs a) Maximum tan delta, b) Loss factor at 0˚C and at 60˚C.

Figure 6.9 shows the loss factor values as a function of the LS and HNT concentration at 0˚C and 60˚C. The loss factor at 0˚C increased when the amount of LSs increased indicating higher energy dissipation and thus better wet grip. In the case of HNTs, the trend is not so evident. The loss factor remains at constant level above 2.5 phr. Furthermore, it is clear from the figure that the loss factor values are reduced at 60˚C when the amount of untreated silicates increases indicating lower energy losses and lower rolling resistance in tyre tread applications. This is due to the better dispersion of the fillers as proven by the Payne effect (Figure 6.1). The TESPT-treatment of the fillers increases the loss factor at both temperatures, especially at higher nanofiller concentrations, which is most probably due to the worse dispersion.

The effect of the plasma treatment of HNTs on loss factor at 60ºC is presented in Figure 6.10a. In this case, the loss factor increased when nanofillers were added to the rubber indicating higher energy dissipation and rolling resistance. In addition, the use of HNTs decreased the loss factor at 0ºC indicating decreased wet grip. This is mainly due to the higher glass transition

temperature of the compound containing only CB (Figure 6.10b). In addition, the loss factor curves showed an additional broad relaxation at higher temperatures, indicating more energy loss by the movement of the polymer chains.

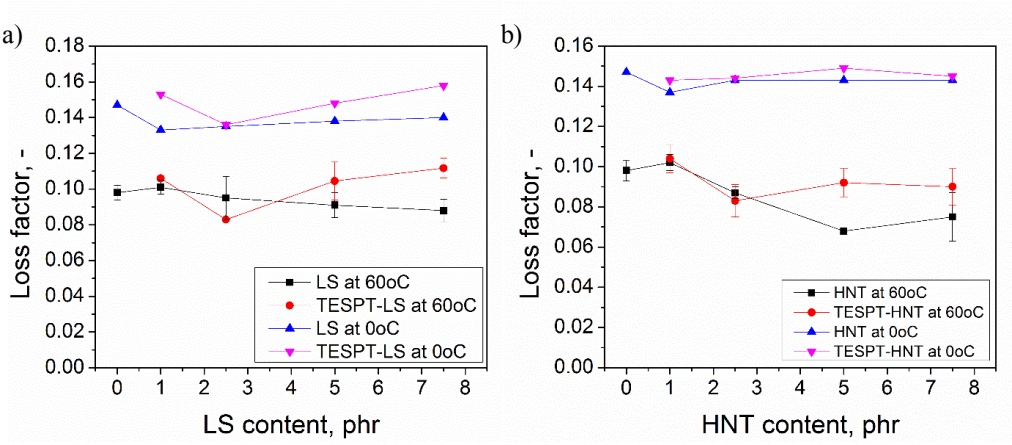

Figure 6.9. The loss factor values of the NR/BR compounds at 0°C and at 60°C with increasing amount of a) LSs and b) HNTs, without and with silane.

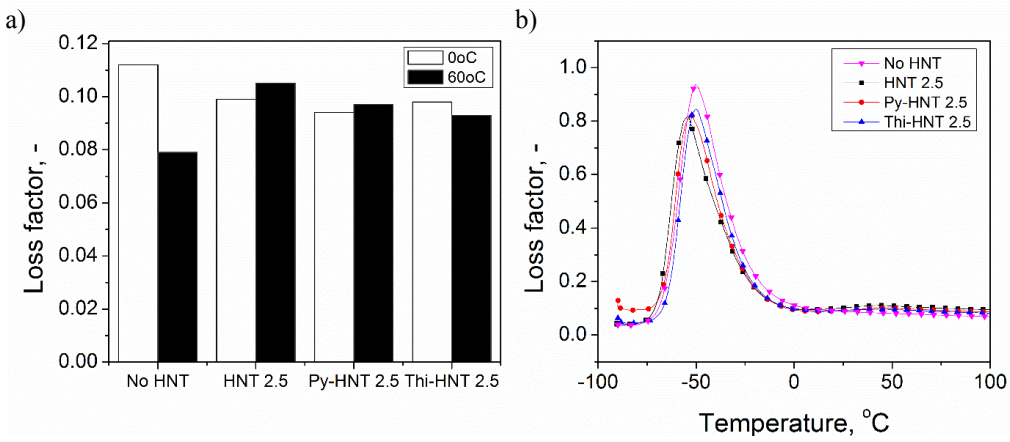

Figure 6.10. a) The loss factor values of the NR/BR compounds at 0 °C and 60°C with untreated and plasma treated HNTs. b) The temperature dependence of the loss tangent of NR/BR rubber with and without plasma treated HNTs.

The plasma treatment of HNTs had only a minor effect on the loss factor. Therefore, it seems that the plasma coating did not result in the formation of chemical links between the filler and polymer. The reason might be that no sufficient degree of modification for nanofillers with their high relative surface was achieved.

6.4 Mechanical properties

The reinforcing effect of the nanofillers compared to CB was studied by tensile tests. It was seen that the partial replacement of CB by the small loadings of nanofillers had only a minor influence on the tensile strength of the rubber (Figure 6.11). The CB used in this study is a highly reinforcing filler. As the replacement of CB by LSs did not change the strength or increased it only slightly, it must be concluded that the reinforcing effects of LS and CB are comparable, assuming that the degree of dispersion is comparable. However, the replacement of CB by LS had a clear effect on the tensile modulus: The values were lower, the more LS was added. The replacement of 7.5 phr CB by LSs decreased the volume fraction of fillers 4.6%, which explains the decrease in the tensile moduli values. The surface modified LSs did not show any significant improvements over unmodified LSs (Figure 6.11 a and b).

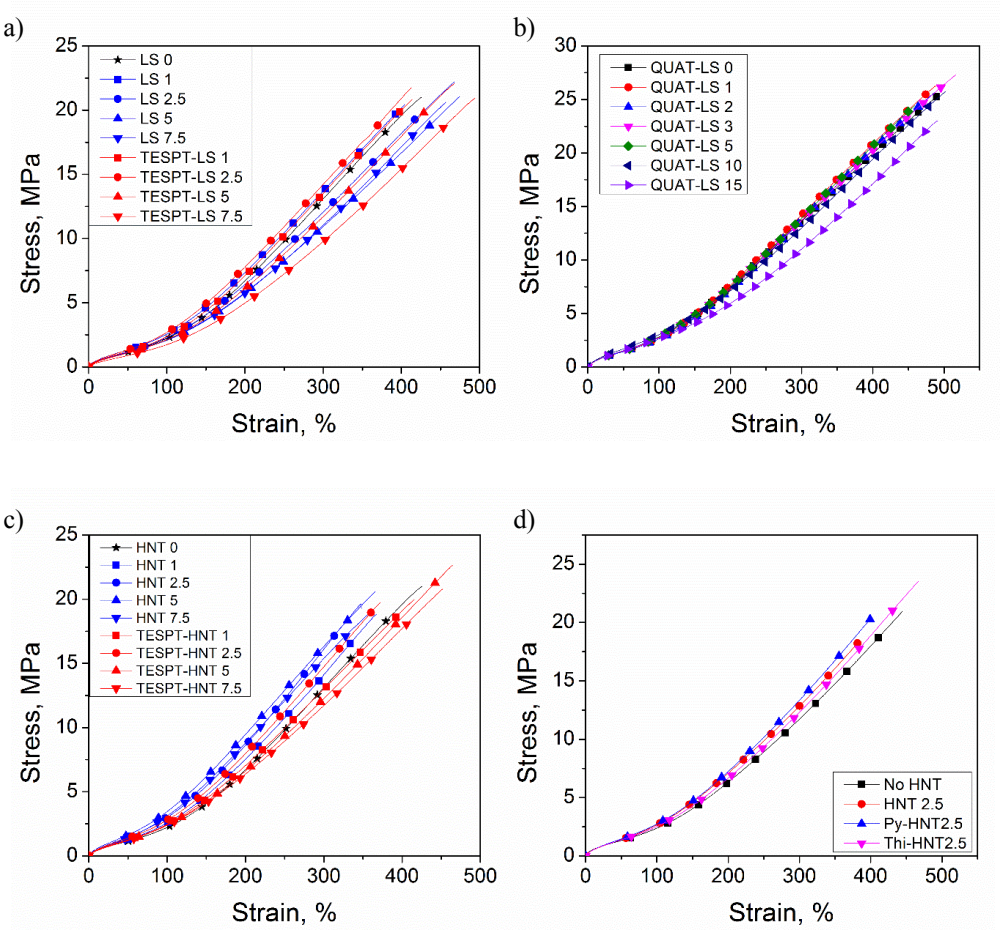

Figure 6.11. The stress-strain curves of the NR/BR compounds containing a) untreated and TESPT treated LSs, b) QUAT-modified LSs, c) untreated and TESPT treated HNTs, and d) plasma-treted HNTs.

The compounds containing HNTs show lower tensile strength and higher moduli at small HNT concentrations than the compound containing only CB. The addition of TESPT increased the tensile strength and the elongation at break, especially at higher HNT concentrations (Figure 6.11c). This is the effect that is expected from the silane: a better dispersion and a higher filler-polymer interaction.

The plasma treatment of HNTs increased the tensile strength of the rubber compound compared to the compound containing untreated HNTs (Figure 6.11d). The thiophene treated HNTs gave the highest tensile strength and elongation at break values indicating the activity of the plasma-polymerized thiophene in interacting with the fillers and enabling bound rubber formation. The sulphur moieties on the surface of HNTs enable reaction with the polymer and the formation of interpenetrating networks, as earlier postulated to explain the higher torque values.

The tensile strength of the NR/BR composites remained at the same level with the reference sample up to 5 phr CNT content (Figure 6.12). At higher CNT concentrations (>5 phr), the tensile strength decreased as polymer-filler interaction decreased due to the insufficient dispersion of CNTs. The replacement of CB by the same weight amount of CNTs increased also the tensile modulus of rubbers due to the increased volume fraction of fillers and stronger hydrodynamic effect. The volume fraction of CNTs increased 6.3% when 12.5 phr CB was replaced by the same amount of CNTs leading to almost twofold increase in stress at 100% elongation. The increased volume fraction increases the surface area of fillers and thus the interaction between the polymer and filler.

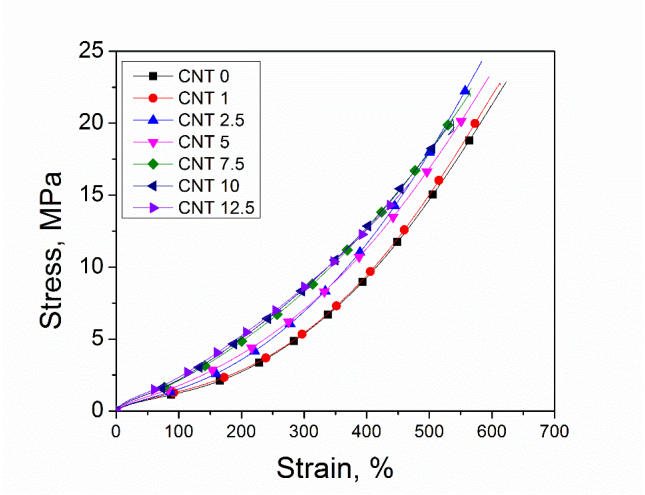

Figure 6.12. The effect of the partial replacement of CB by CNTs on the stress-strain properties of the NR/BR compound.

6.5 Masterbatch mixing of carbon nanotubes

The feasibility of the masterbatch mixing technique for the blending of EPDM with CNTs was studied by comparing the properties of the masterbatch mixed rubber composite to the directly mixed one. Non-polar EPDM and polar NBR were used as carrier materials. The aim of the masterbatch mixing was to improve the dispersion and distribution of nanofillers.

In the case of the EPDM masterbatch, the final CNT content in the rubber was analysed by TGA. The theoretical CNT content was 6.3 phr. According to the TGA measurements, the CNT contents were 6.3 phr and 5.9 phr for masterbatch mixed and directly mixed compounds, respectively. Therefore, the CNT content of the masterbatch mixed compound corresponded well with the calculated results, whereas the CNT content of the directly mixed compounds was lower indicating that some CNTs were lost during mixing.

The preparation of the EPDM-CNT masterbatch before blending it with the EPDM compound increased tensile strength and maximum torque values compared to direct mixing as seen in Figure 6.13 a and b. This is probably due to the higher CNT content, as the dispersion of the CNTs as measured by the Payne effect is comparable in both compounds (Figure 6.13c). Moreover, it is evident from Figure 6.14, that both samples had well dispersed as well as bundled CNTs present. Thus, differences in dispersion could not be proven visually this way. The use of a CNT masterbatch which is processed by direct mixing has not been studied by other researchers, but the improved mechanical properties of the rubber-CNT masterbatches manufactured by solution mixing or by mixing with NR latex have been reported [112][113]. The current results indicate that the masterbatch technique is a suitable mixing method when direct mixing is applied, but the main improvements over the traditional mixing concern processing: better controllability of the amount of the nanofiller in a rubber compound and healthier working environment due to the reduced amount of airborne CNTs.

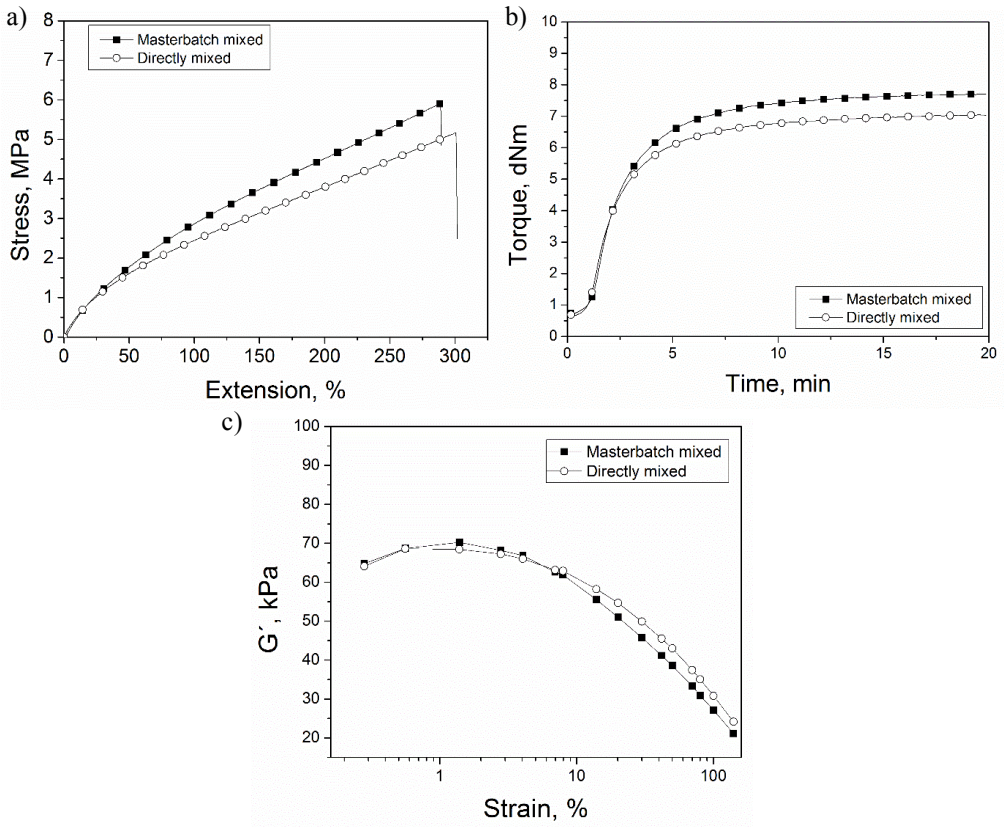

Figure 6.13. a) The effect of masterbatch mixing on a) the stress-strain behaviour, b) the vulcanization, and c) the strain sweep (Payne effect) of the EPDM/CNT compounds.

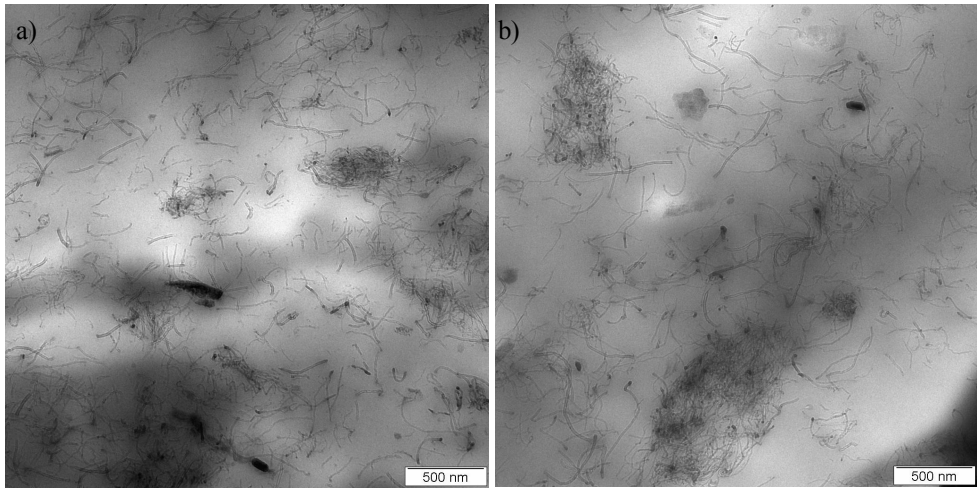

Fig. 6.14. TEM images of the compounds a) masterbatch mixing b) direct mixing. *[Publication V]*

NBR as carrier material for CNTs showed different results mainly due to the non-polar/polar nature of EPDM/NBR blends that caused the uneven distribution of fillers. As in the case where EPDM was used as a carrier material, here also the directly mixed compounds resulted in lower torque values than the masterbatch mixed compound EM-CNT 6 (Figure 6.15), but the difference was much larger here. This is due to the polar nature of the curatives that tend to migrate to the polar NBR rather than to the non-polar EPDM. When the accelerators were forced into the EPDM phase by mixing them with EPDM before the addition of the sulphur containing NBR/CNT masterbatch (EM-CNT 6 2-steps), the torque as well as the whole curing process was similar to the masterbatch mixed compound.

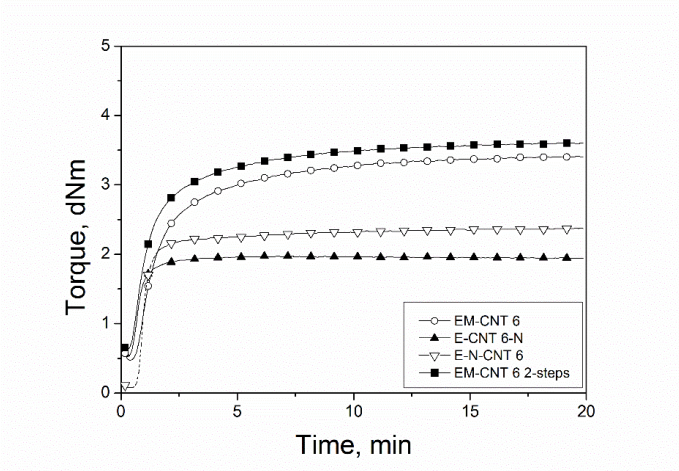

Figure 6.15. The curing curves of EPDM-NBR-CNT compounds mixed in different ways.
EM-CNT 6 = The masterbatch mixed compound having NBR as a carrier material.
E-CNT 6-N = The directly mixed compound. Mixing sequence 1. EPDM, 2. CNT, 3. NBR.
E-N-CNT 6 = The directly mixed compound. Mixing sequence 1. EPDM, 2. NBR, 3. CNT.

The directly mixed EPDM composites had a higher tensile strength and modulus then the masterbatch mixed compound, but the Payne effect was also higher (Table 6.1). In the directly mixed compounds, the tensile strength was higher when the CNTs were mixed with EPDM before blending with NBR (E-CNT 6-N) than in the compound in which the elastomers were mixed before the addition of CNTs (E-N-CNT 6). The results confirmed that the CNTs stayed in the NBR phase as also proven by TEM (Figure 6.16). The TEM images clearly showed the two-phase structure of polymers and the influence of the mixing technique. The EPDM phase forms a continuous matrix containing NBR domains. In the masterbatch mixed sample, the domain island size is much larger than in the directly mixed sample, and the NBR is heavily loaded with CNTs. A stronger interaction between CNTs and polar NBR than between CNTs and a non-polar rubber, in this case NR, has also been indicated by Le at al. [114].

Table 6.1. The properties of EPDM-NBR-CNT compounds mixed in different ways.

Mix	Tensile strength, MPa	Elongation at break, %	100% Modulus, MPa	300% Modulus, MPa	Payne effect, kPa
EM-CNT 6	2.8±0.3	780±20	0.98±0.01	1.17±0.03	28±0.6
E-CNT 6-N	4.9±0.6	540±60	1.69±0.08	3.14±0.17	44.4±0.7
E-N-CNT 6	3.6±0.2	630±80	1.61±0.12	2.53±0.26	41.5±0.7

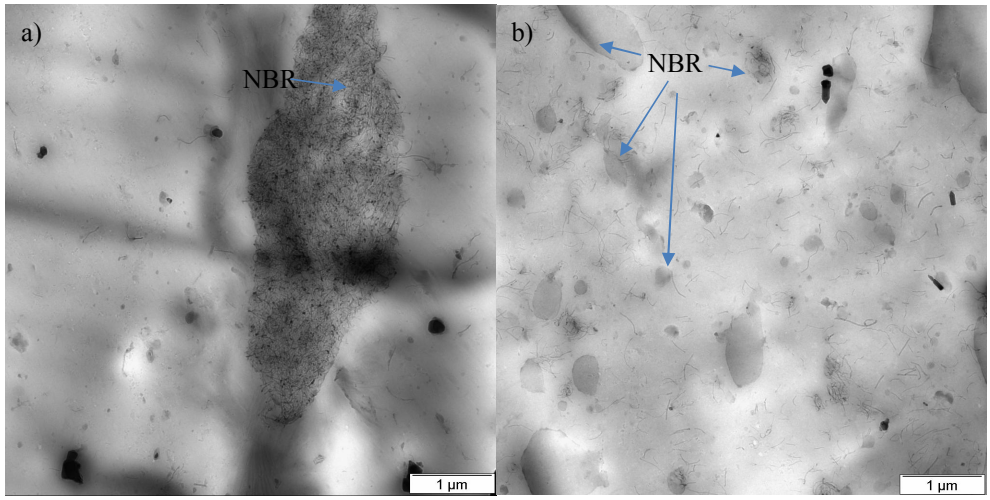

Figure 6.16. a) Masterbatch mixed EPDM/NBR with 6 phr of CNTs and b) Directly mixed reference with similar composition, mixing order 1. EPDM, 2. CNT, 3. NBR. *[Publication VI]*

7. CONCLUDING REMARKS

Reinforcing fillers play an important role in rubbers due to their ability to improve especially mechanical properties. The aim of this thesis was to study the effect of dual filler systems on the properties of a model tyre tread. This was done by partially substituting CB by the different types of nanofillers. The main target was to improve the polymer-nanofiller interaction and thus the mechanical and dynamic properties of the rubber. In addition, the influence of different mixing techniques on the dispersion of CNTs was studied.

The experimental part focused on the *research question 1*. It was observed that the partial replacement of CB by a small quantity of silicate based nanofillers results in improved dispersion of the fillers and better dynamic properties considering tyre tread applications. However, a meaningful increase in mechanical properties could not be detected. This is probably a consequence of using a high reinforcing carbon black N234 in the first place. Thus, it can be concluded that the silicate-based nanofillers have the same high reinforcing effect but they can also improve tire tread properties like rolling resistance.

The behaviour of CNTs in rubber is different compared to silicates in terms of the formation of filler network and stiffness. In earlier studies, the difficulties in the mixing of CNTs by direct mixing have been pointed out. In the present study, it was noticed that an acceptable dispersion of low CNT loadings can be achieved with the traditional mixing method. The presence of the carbon black facilitated the dispersion of the nanotubes.

Different methods of modifying the surface of nanofillers were examined with LSs and HNTs according to *research question 2*. Traditional surface treatment by silane turned out to be ineffective for the small HNT concentrations, whereas plasma treatment was found to be a potential modification method for those fillers: it reduced the hydrophilicity of the filler and thus improved its compatibility with rubber. It was also detected that the plasma treatment of HNTs increased the thermal stability of the rubber and suppressed reversion during the curing process.

The comparison of the masterbatch and direct mixing of rubber and CNTs according to *research question 3* showed that masterbatch mixing generates less airborne CNTs, and consequently reduces the health risk. The properties of the masterbatch mixed compounds were comparable to those obtained by direct mixing. Therefore, replacing directly mixed compounds with masterbatch mixed ones implies overall positive influence as long as the carrier material is compatible with the matrix material. The use of dissimilar materials as matrix and carrier leads to the unsatisfactory dispersion of nanofillers.

The main findings of this work are:

1. Nanoclays, CNTs, and highly reinforcing carbon black have comparable reinforcing effects.
2. LSs and HNTs used as fillers in rubber together with CB reduce the stiffness of rubbers.
3. LSs and HNTs decrease the loss factor of tyre tread compounds at 60°C indicating lower rolling resistance when used in tread compounds for tyres. A decrease in rolling resistance affects the fuel consumption of cars significantly and thus has a positive effect on global warming. In addition, they increase the loss factor at 0°C and thus improve the wet grip.
4. Dual filler systems facilitate the dispersion and distribution of fillers.
5. HNTs have a better reinforcing potential than layered silicates.
6. Plasma treatment is a promising surface modification method for HNTs.
7. Masterbatch mixing is an auspicious way to mix CNTs: A good dispersion of CNTs can be achieved, the CNT content in a rubber matrix is well in control, and a part of the health risks caused by airborne CNTs can be prevented.

Overall, nanofillers can be used to tailor the properties of a tyre tread compound, if good dispersion and polymer-filler interaction is achieved.

Despite the results of this study, there are still aspects that need further research. These aspects include the more efficient mixing of nanofillers in order to break filler aggregates, the uniform dispersion of nanofillers, and surface modification. With the current methods, the full reinforcing potential of nanofillers is not accomplished due to the filler aggregates remaining in the rubber compound. Moreover, the compatibility between rubber and fillers should still be improved to get strong covalent bonds between them. One important aspect in the development efforts to achieve a real breakthrough of nanofillers is that the mixing and modification methods should be suitable for the present-day rubber factories.

REFERENCES

[1] W. Hoffmann, *Rubber technology handbook*. Varl Hanser Verlag, 1989.

[2] R. N. Rothon, *Particulate-filled polymer composite, 2nd ed.* Smithers Rapra Technology, 2003.

[3] J. Loadman, *Tears of the Tree. The Story of Rubber--A Modern Marvel*. Oxford university press, New York, 2005.

[4] Http://www.statista.com/statistics/275399/world-consumption-of-natural-and-synthetic-caoutchouc/, "Visited 20.12.2016." .

[5] https://www.smithersrapra.com/market-reports/rubber-and-elastomer-industry-market-reports/the-future-of-thermoplastic-elastomers-to-2020, "Visited 4.4.2017." .

[6] J. R. White and S. K. De, *Rubber Technologist's Handbook, Volume 1*, Rapra Technology Ltd., 2001.

[7] J. E. Mark, B. Erman, and F. R. Eirich, *The science and technology of rubber (3rd edition)*. Elsevier Academic Press, 2005.

[8] M. Alexandre and P. Dubois, "Polymer-layered silicate nanocomposites: preparation, properties and uses of a new class of materials," *Mater. Sci. Eng. R Reports*, vol. 28, no. 1, pp. 1–63, 2000.

[9] S. Thomas and R. Stephen, "Nanocomposites: State of the art, new challenges and opportunities," in *Rubber Nanocomposites: Preparation, Properties, and Applications* (eds S. Thomas and R. Stephen), John Wiley & Sons (Asia) Pte Ltd, Singapore 2010, pp. 1–20.

[10] A. Das, D.-Y. Wang, K. W. Stöckelhuber, R. Jurk, J. Fritzsche, M. Klüppel, and G. Heinrich, "Rubber-Clay Nanocomposites: Some recent results," *Adv. Polym. Sci.*, vol. 239, pp. 85–166, 2011.

[11] K. H. Nordsiek, "'Integral rubber' concept - An approach to an ideal tire tread rubber," *Kautschuk Gummi Kunststoffe*, vol. 38, pp. 178–185, 1985.

[12] J. Ma, L.-Q. Zhang, and L. Geng, "Manufacturing Techniques of Rubber Nanocomposites," in *Rubber Nanocomposites: Preparation, Properties, and Applications*, (eds S. Thomas and R. Stephen), ohn Wiley & Sons (Asia) Pte Ltd, Singapore 2010 pp. 21–62,

[13] L. Bokobza, "Multiwall carbon nanotube elastomeric composites: A review," *Polymer*, vol. 48, no. 17, pp. 4907–4920, 2007.

[14] J. Fröhlich, W. Niedermeier, and H. D. Luginsland, "The effect of filler-filler and filler-elastomer interaction on rubber reinforcement," *Compos. Part A Appl. Sci. Manuf.*, vol. 36, no. 4, pp. 449–460, 2005.

[15] A. bin Samsuri, “Chapter 3. Theory and Mechanisms of Filler Reinforcement in Natural Rubber,” *Nat. Rubber Mater. Vol. 2 Compos. Nanocomposites*, vol. 2, no. 8, pp. 73–111, 2013.

[16] R. Alex, “Nanofillers in rubber-rubber blends,” in *Rubber nanocomposites, Preparation, properties and applications*, S. Thomas and R. Stephen, Eds. John Wiley & Sons (Asia) Pte Ltd, 2010, Singapore, pp. 209–237.

[17] J. L. Leblanc, “Rubber-filler interactions and rheological properties in filled compounds,” *Prog. Polym. Sci.*, vol. 27, no. 4, pp. 627–687, 2002.

[18] J. B. Donnet and E. Custodero, *Reinforcement of Elastomers by Particulate Fillers*, *4th ed* . Elsevier Inc., 2013.

[19] J. B. Donnet, R. C. Bansal, and M.-J. Wang, Eds., *Carbon black, Science and Technology*. New York: Marcel Dekker Inc., 1993.

[20] T. Sabu and S. Ranimol, *Rubber nanocomposites*. Wiley & Sons Ltd, Chichester, UK, 2010.

[21] S. Mishra, N. G. Shimpi, and U. D. Patil, “Effect of Nano CaCO3 on thermal properties of Styrene Butadiene Rubber (SBR),” *J. Polym. Res.*, vol. 14, no. 6, pp. 449–459, 2007.

[22] S. Mishra and N. G. Shimpi, “Mechanical and flame-retarding properties of styrene-butadiene rubber filled with nano-CaCO3 as a filler and linseed oil as an extender,” *J. Appl. Polym. Sci.*, vol. 98, no. 6, pp. 2563–2571, 2005.

[23] A. Payne, “Dynamic mechanical properties of fillers loaded vulcanizates,” *Rubber Plast. age*, vol. 42, pp. 963–967, 1961.

[24] M. Galimberti, V. Cipolletti, and V. Kumar, “Nanofillers in Natural Rubber,” *Nat. Rubber Mater. Vol. 2 Compos. Nanocomposites*, vol. 2, no. 8, pp. 34–72, 2013.

[25] J. L. Leblanc, *Filled Polymers: Science and Industrial Applications*. Taylor & Francis, 2009.

[26] W. Luo, X. Hu, C. Wang, and Q. Li, “Frequency- and strain-amplitude-dependent dynamical mechanical properties and hysteresis loss of CB-filled vulcanized natural rubber,” *Int. J. Mech. Sci.*, vol. 52, pp. 168–174, 2010.

[27] M. A. López-Manchado, M. Arroyo, B. Herrero, and J. Biagiotti, “Vulcanization Kinetics of Natural Rubber – Organoclay Nanocomposites,” *J. Appl. Polym. Sci.* vol. 89, pp. 1–15, 2002.

[28] S. Sinha Ray and M. Okamoto, “Polymer/layered silicate nanocomposites: A review from preparation to processing,” *Prog. Polym. Sci.*, vol. 28, no. 11, pp. 1539–1641, 2003.

[29] M. Strankowski, J. Strankowska, M. Gazda, L. Piszczyk, G. Nowaczyk, and S. Jurga, “Thermoplastic polyurethane/(organically modified montmorillonite) nanocomposites produced by in situ polymerization,” *Express Polym. Lett.*, vol. 6, no. 8, pp. 610–619, 2012.

[30] M. Alexandre and P. Dubois, “Polymer-layered silicate nanocomposites: Preparation, properties and uses of a new class of materials,” *Mater. Sci. Eng. R Reports*, vol. 28, no. 1, pp. 1–63, 2000.

[31] H. R. Dennis, D. L. Hunter, D. Chang, S. Kim, J. L. White, J. W. Cho, and D. R. Paul, “Effect of melt processing conditions on the extent of exfoliation in organoclay-based nanocomposites,” *Polymer*, vol. 42, no. 23, pp. 9513–9522, 2001.

[32] D. Basu, A. Das, K. W. Stöckelhuber, U. Wagenknecht, and G. Heinrich, “Advances in layered double hydroxide (LDH)-based elastomer composites,” *Prog. Polym. Sci.*, vol. 39, no. 3, pp. 594–626, 2014.

[33] Y. L. Lu, Z. Li, Z. Z. Yu, M. Tian, L. Q. Zhang, and Y. W. Mai, “Microstructure and properties of highly filled rubber/clay nanocomposites prepared by melt blending,” *Compos. Sci. Technol.*, vol. 67, no. 14, pp. 2903–2913, 2007.

[34] S. Sinha Ray, “1 - An Overview of Pure and Organically Modified Clays,” *Clay-containing Polym. Nanocomposites*, pp. 1–24, 2013.

[35] F. Uddin, “Clays, nanoclays, and montmorillonite minerals,” *Metall. Mater. Trans. A Phys. Metall. Mater. Sci.*, vol. 39, no. 12, pp. 2804–2814, 2008.

[36] K. S. Katti, A. H. Ambre, N. Peterka, and D. R. Katti, “Use of unnatural amino acids for design of novel organomodified clays as components of nanocomposite biomaterials.,” *Philos. Trans. A. Math. Phys. Eng. Sci.*, vol. 368, no. 1917, pp. 1963–1980, 2010.

[37] M. Ganter, W. Gronski, P. Reichert, and R. Mülhaupt, “Rubber Nanocomposites: Morphology and Mechanical Properties of BR and SBR Vulcanizates Reinforced by Organophilic Layered Silicates,” *Rubber Chem. Technol.*, vol. 74, no. 2, pp. 221–235, 2001.

[38] M. Galimberti, “Rubber Clay Nanocomposites,” *Adv. Elastomers - Technol. Prop. Appl.*, pp. 91–120, 2012.

[39] D. J. Lowe, A. V. Chapman, S. Cook, and J. J. C. Busfield, “Natural rubber nanocomposites by in situ modification of clay,” *Macromol. Mater. Eng.*, vol. 296, no. 8, pp. 693–702, 2011.

[40] G. Sui, W. H. Zhong, X. P. Yang, and Y. H. Yu, “Curing kinetics and mechanical behavior of natural rubber reinforced with pretreated carbon nanotubes,” *Mater. Sci. Eng. A*, vol. 485, no. 1–2, pp. 524–531, 2008.

[41] D. Choi, M. Abdul Kader, B. H. Cho, Y. I. Huh, and C. Nah, “Vulcanization kinetics of nitrile rubber/layered clay nanocomposites,” *J. Appl. Polym. Sci.*, vol. 98, no. 4, pp. 1688–1696, 2005.

[42] X. Fu and S. Qutubuddin, “Polymer–clay nanocomposites: exfoliation of organophilic montmorillonite nanolayers in polystyrene,” *Polymer*, vol. 42, no. 2, pp. 807–813, 2001.

[43] M. A. López-Manchado, B. Herrero, and M. Arroyo, “Preparation and characterization of organoclay nanocomposites based on natural rubber,” *Polym. Int.*, vol. 52, no. 7, pp. 1070–1077, 2003.

[44] R. Alex and C. Nah, "Preparation and characterization of organoclay-rubber nanocomposites via a new route with skim natural rubber latex," *J. Appl. Polym. Sci.*, vol. 102, no. 4, pp. 3277–3285, 2006.

[45] M. Arroyo, M. A. López-Manchado, and B. Herrero, "Organo-montmorillonite as substitute of carbon black in natural rubber compounds," *Polymer*, vol. 44, no. 8, pp. 2447–2453, 2003.

[46] F. Avalos, J. C. Ortiz, R. Zitzumbo, M. A. López-Manchado, R. Verdejo, and M. Arroyo, "Effect of montmorillonite intercalant structure on the cure parameters of natural rubber," *Eur. Polym. J.*, vol. 44, no. 10, pp. 3108–3115, 2008.

[47] Y. W. Chang, Y. Yang, S. Ryu, and C. Nah, "Preparation and properties of EPDM/organomontmorillonite hybrid nanocomposites," *Polym. Int.*, vol. 51, no. 4, pp. 319–324, 2002.

[48] B. Liu, Q. Ding, Q. He, J. Cai, B. Hu, and J. Shen, "Novel preparation and properties of EPDM/montmorillonite nanocomposites," *J. Appl. Polym. Sci.*, vol. 99, no. 5, pp. 2578–2585, 2006.

[49] K. G. Gatos and J. Karger-Kocsis, "Effects of primary and quaternary amine intercalants on the organoclay dispersion in a sulfur-cured EPDM rubber," *Polymer*, vol. 46, no. 9, pp. 3069–3076, 2005.

[50] S. J. Ahmadi, Y. Huang, and W. Li, "Fabrication and physical properties of EPDM-organoclay nanocomposites," *Compos. Sci. Technol.*, vol. 65, no. 7–8, pp. 1069–1076, 2005.

[51] J. Kim, T. Oh, and D. Lee, "Morphology and rheological properties of nanocomposites based on nitrile rubber and organophilic layered silicates," *Polym. Int.*, vol. 52, no. 7, pp. 1203–1208, 2003.

[52] C. X. Viet, H. Ismail, A. A. Rashid, T. Takeichi, and V. H. Thao, "Organoclay Filled Natural Rubber Nanocomposites: The Effects of Filler Loading," *Polym. Plast. Technol. Eng.*, vol. 47, no. 11, pp. 1090–1096, Oct. 2008.

[53] A. Das, K. W. Stöckelhuber, S. Rooj, D. Y. Wang, and G. Heinrich, "Synergistic effects of expanded nanoclay and carbon black on natural rubber compounds," *KGK Kautschuk Gummi Kunststoffe*, vol. 63, no. 7–8, pp. 296–302, 2010.

[54] S. Praveen, P. K. Chattopadhyay, P. Albert, V. G. Dalvi, B. C. Chakraborty, and S. Chattopadhyay, "Synergistic effect of carbon black and nanoclay fillers in styrene butadiene rubber matrix: Development of dual structure," *Compos. Part A Appl. Sci. Manuf.*, vol. 40, no. 3, pp. 309–316, 2009.

[55] Y. Liu, L. Li, and Q. Wang, "Effect of carbon black/nanoclay hybrid filler on the dynamic properties of natural rubber vulcanizates," *J. Appl. Polym. Sci.*, vol. 118, no. 2, pp. 1111–1120, 2010.

[56] P. Pasbakhsh, H. Ismail, M.N.A. Fauzi and A.A. Bakar, "Halloysite nanotubes as a novel nanofiller for polymer nanocomposites," *Ext. Abstr. – 21st Aust. Clay Miner. Conf. – Brisbane, August 2010*, pp. 93–96, 2010.

[57] M. Du, B. Guo, and D. Jia, "Newly emerging applications of halloysite nanotubes: A review," *Polym. Int.*, vol. 59, no. 5, pp. 574–582, 2010.

[58] J. Qiao, J. Adams, and D. Johannsmann, "Addition of halloysite nanotubes prevents cracking in drying latex films" *Langmuir*, Vol. 23, pp. 8674-8680, 2012.

[59] S. Rooj, A. Das, V. Thakur, R. N. Mahaling, A. K. Bhowmick, and G. Heinrich, "Preparation and properties of natural nanocomposites based on natural rubber and naturally occurring halloysite nanotubes," *Mater. Des.*, vol. 31, no. 4, pp. 2151–2156, 2010.

[60] P. Pasbakhsh, H. Ismail, M. N. A. Fauzi, and A. A. Bakar, "Influence of maleic anhydride grafted ethylene propylene diene monomer (MAH-g-EPDM) on the properties of EPDM nanocomposites reinforced by halloysite nanotubes," *Polym. Test.*, vol. 28, no. 5, pp. 548–559, 2009.

[61] P. Yuan, P. D. Southon, Z. Liu, M. E. R. Green, J. M. Hook, S. J. Antill, and C. J. Kepert, "Functionalization of halloysite clay nanotubes by grafting with aminopropyltriethoxysilane," *J. Phys. Chem. C*, vol. 112, no. 40, pp. 15742–15751, 2008.

[62] B. Guo, F. Chen, Y. Lei, X. Liu, J. Wan, and D. Jia, "Styrene-butadiene rubber/halloysite nanotubes nanocomposites modified by sorbic acid," *Appl. Surf. Sci.*, vol. 255, no. 16, pp. 7329–7336, 2009.

[63] Y. Lei, Z. Tang, L. Zhu, B. Guo, and D. Jia, "Functional thiol ionic liquids as novel interfacial modifiers in SBR/HNTs composites," *Polymer*, vol. 52, no. 5, pp. 1337–1344, 2011.

[64] H. Ismail, S. Z. Salleh, and Z. Ahmad, "Curing Characteristics, Mechanical, Thermal, and Morphological Properties of Halloysite Nanotubes (HNTs)-Filled Natural Rubber Nanocomposites," *Polym. Plast. Technol. Eng.*, vol. 50, no. March 2012, pp. 681–688, 2011.

[65] S. Rooj, A. Das, and G. Heinrich, "Tube-like natural halloysite/fluoroelastomer nanocomposites with simultaneous enhanced mechanical, dynamic mechanical and thermal properties," *Eur. Polym. J.*, vol. 47, no. 9, pp. 1746–1755, 2011.

[66] P. Pasbakhsh, H. Ismail, M. N. A. Fauzi, and A. A. Bakar, "EPDM/modified halloysite nanocomposites," *Appl. Clay Sci.*, vol. 48, no. 3, pp. 405–413, 2010.

[67] H. Ismail, P. Pasbakhsh, M. N. Ahmad Fauzi, and A. Abu Bakar, "The Effect of Halloysite Nanotubes as a Novel Nanofiller on Curing Behaviour, Mechanical and Microstructural Properties of Ethylene Propylene Diene Monomer (EPDM) Nanocomposites," *Polym. Plast. Technol. Eng.*, vol. 48, no. 3, pp. 313–323, 2009.

[68] H. Ismail, P. Pasbakhsh, M. N. A. Fauzi, and A. Abu Bakar, "Morphological, thermal and tensile properties of halloysite nanotubes filled ethylene propylene diene monomer (EPDM) nanocomposites," *Polym. Test.*, vol. 27, no. 7, pp. 841–850, 2008.

[69] H. Ismail and S. M. Shaari, "Curing characteristics, tensile properties and morphology of palm ash/halloysite nanotubes/ethylene-propylene-diene monomer (EPDM) hybrid composites," *Polym. Test.*, vol. 29, no. 7, pp. 872–878, 2010.

[70] K. Senthivel, K. Manikandan, and B. Prabu, "Studies on the Mechanical Properties of Carbon Black/Halloysite Nanotube Hybrid Fillers in Nitrile Rubber Nanocomposites," *Mater. Today Proc.*, vol. 2, no. 4, pp. 3627–3637, 2015.

[71] H. Ismail, S. Z. Salleh, and Z. Ahmad, "Fatigue and hysteresis behavior of halloysite nanotubes-filled natural rubber (SMR L and ENR 50) nanocomposites," *J. Appl. Polym. Sci.*, vol. 127, no. 4, pp. 3047–3052, 2013.

[72] H. Ismail, S. Z. Salleh, and Z. Ahmad, "The effect of partial replacement of carbon black (CB) with halloysite nanotubes (HNTs) on the properties of CB/HNT-filled natural rubber nanocomposites," *J. Elastomers Plast.*, vol. 45, no. 5, pp. 445–455, 2012.

[73] P. Pasbakhsh, H. Ismail, M. N. A. Fauzi, and A. A. Bakar, "The partial replacement of silica or calcium carbonate by halloysite nanotubes as fillers in ethylene propylene diene monomer composites," *J. Appl. Polym. Sci.*, vol. 113, no. 6, pp. 3910–3919, 2009.

[74] B. Guo, Y. Lei, F. Chen, X. Liu, M. Du, and D. Jia, "Styrene–butadiene rubber/halloysite nanotubes nanocomposites modified by methacrylic acid," *Appl. Surf. Sci.*, vol. 255, no. 5, pp. 2715–2722, 2008.

[75] B. Guo, X. Liu, W. Y. Zhou, Y. Lei, and D. Jia, "Adsorption of Ionic Liquid onto Halloysite Nanotubes: Mechanism and Reinforcement of the Modified Clay to Rubber," *J. Macromol. Sci. Part B*, vol. 49, no. 5, pp. 1029–1043, Aug. 2010.

[76] A. Fakhru'l-Razi, M. A. Atieh, N. Girun, T. G. Chuah, M. El-Sadig, and D. R. A. Biak, "Effect of multi-wall carbon nanotubes on the mechanical properties of natural rubber," *Compos. Struct.*, vol. 75, no. 1–4, pp. 496–500, 2006.

[77] A. Das, K. W. Stöckelhuber, R. Jurk, M. Saphiannikova, J. Fritzsche, H. Lorenz, M. Klüppel, and G. Heinrich, "Modified and unmodified multiwalled carbon nanotubes in high performance solution-styrene-butadiene and butadiene rubber blends," *Polymer*, vol. 49, pp. 5276–5283, 2008.

[78] V. Choudhary and A. Gupta, "Polymer/Carbon Nanotube Nanocomposites", *Carbon nanotubes - Polymer nanocomposites,* InTech, 2011, DOI: 10.5772/18423.

[79] T. W. Ebbesen, H. J. Lezec, H. Hiura, J. W. Bennett, H. F. Ghaemi, and T. Thio, "Electrical conductivity of individual carbon nanotubes," *Nature*, vol. 382, no. 6586, pp. 54–56, Jul. 1996.

[80] L. Bokobza and M. Kolodziej, "On the use of carbon nanotubes as reinforcing fillers for elastomeric materials," *Polym. Int.*, vol. 55, no. 9, pp. 1090–1098, Sep. 2006.

[81] L. D. Perez, M. A. Zuluaga, T. Kyu, J. E. Mark, and B. L. Lopez, "Preparation, characterization, and physical properties of multiwall carbon nanotube/elastomer composites," *Polym. Eng. Sci.*, vol. 49, no. 5, pp. 866–874, 2009.

[82] M. S. P. Shaffer and J. K. W. Sandler, "Carbon Nanotube/Nanofibre Polymer Composites," *Process. Prop. Nanocomposites*, pp. 1–59, 2006.

[83] F. Cataldo, "Reinforcing effect of multiwall carbon nanotubes in carbon black filled NR compounds," *Rubber Fibres Plast. Int.*, vol. 4, pp. 78–83, 2009.

[84] A. M. Shanmugharaj, J. H. Bae, K. Y. Lee, W. H. Noh, S. H. Lee, and S. H. Ryu, "Physical and chemical characteristics of multiwalled carbon nanotubes functionalized with aminosilane and its influence on the properties of natural rubber composites," *Compos. Sci. Technol.*, vol. 67, no. 9, pp. 1813–1822, 2007.

[85] A. De Falco, S. Goyanes, G. H. Rubiolo, I. Mondragon, and A. Marzocca, "Carbon nanotubes as reinforcement of styrene-butadiene rubber," *Appl. Surf. Sci.*, vol. 254, no. 1 SPEC. ISS., pp. 262–265, 2007.

[86] N. Yan, J. K. Wu, Y. H. Zhan, and H. S. Xia, "Carbon nanotubes/carbon black synergistic reinforced natural rubber composites," *Plast. Rubber Compos.*, vol. 38, no. 7, pp. 290–296, 2009.

[87] A. Das, G. R. Kasaliwal, R. Jurk, R. Boldt, D. Fischer, K. W. Stöckelhuber, and G. Heinrich, "Rubber composites based on graphene nanoplatelets, expanded graphite, carbon nanotubes and their combination: A comparative study," *Compos. Sci. Technol.*, vol. 72, no. 16, pp. 1961–1967, 2012.

[88] L. Bokobza, "Mechanical, electrical and spectroscopic investigations of carbon nanotube-reinforced elastomers," *Vib. Spectrosc.*, vol. 51, no. 1, pp. 52–59, 2009.

[89] R. M. Cadambi and E. Ghassemieh, "Optimized Process for the Inclus ion of Carbon Nanotubes in Elastomers with Improved Thermal and Mechanical Properties," *J. Appl. Polym. Sci.*, vol. 124, no. 7, pp. 4993–5001, 2012.

[90] S.-R. Ryu, J.-W. Sung, and D.-J. Lee, "Strain-Induced Crystallization and Mechanical Properties of NBR Composites With Carbon Nanotube and Carbon Black," *Rubber Chem. Technol.*, vol. 85, no. 2, pp. 207–218, 2012.

[91] H. Ismail, A. F. Ramly, and N. Othman, "The effect of carbon black/multiwall carbon nanotube hybrid fillers on the properties of natural rubber nanocomposites," *Polym. - Plast. Technol. Eng.*, vol. 50, pp. 660–666, 2011.

[92] P. Walker, "Silane and Other Adhesion Promoters in Adhesive Technology," in *Handbook of Adhesive Technology, Revised and Expanded*, CRC Press, 2003.

[93] M. J. Owen, "Chapter 9 – Coupling agents: chemical bonding at interfaces," in *Adhesion Science and Engineering*, *The Mechacnis of adhesion,* D.A Dillard and A.V. Pocius Eds, 2002, pp. 403–431.

[94] J.W. ten Brinke, S.C. Debnath, L.A.E.M. Reuvekamp, and J.W.M. Noordermeer, "Mechanistic aspects of the role of coupling agents in silica-rubber composites, " *Compos. Sci. Technol*., vol 63, pp. 1165-1174, 2003.

[95] M. Tiwari, *Plasma coating of silica, a key to improved dispersion and properties of reinforced elastomer blends*. Ph.D Thesis, University of Twente, Enschede, the Netherlands, 2010.

[96] T. Mathew, *Surface modification of carbon black by plasma*. Ph.D. thesis, University of Twente, Enschede, The Netherlands, 2008.

[97] G. Akovali and I. Ulkem, "Some Performance Characteristics of Plasma Surface Modified Carbon Black in the (SBR) Matrix," *Polymer*, vol. 40, no. 26, pp. 7417–7422, 1999.

[98] T. Mathew, R. N. Datta, W. K. Dierkes, A. G. Talma, W. J. Van Ooij, and J. W. M. Noordermeer, "Plasma polymerization surface modification of carbon black and its effect in elastomers," *Macromol. Mater. Eng.*, vol. 296, no. 1, pp. 42–52, 2011.

[99] C. Nah, M. Y. Huh, J. M. Rhee, and T. H. Yoon, "Plasma surface modification of silica and its effect on properties of styrene-butadiene rubber compound," *Polym. Int.*, vol. 51, no. 6, pp. 510–518, 2002.

[100] G. Mathew, M. Y. Huh, J. M. Rhee, M. H. Lee, and C. Nah, "Improvement of properties of silica-filled styrene-butadiene rubber composites through plasma surface modification of silica," *Polym. Adv. Technol.*, vol. 15, no. 7, pp. 400–408, 2004.

[101] J. H. Roh, J. H. Lee, and T. H. Yoon, "Enhanced adhesion of silica for epoxy molding compounds (EMCs) by plasma polymer coatings," *J. Adhes. Sci. Technol.*, vol. 16, no. 11, pp. 1529–1543, Jan. 2002.

[102] J. F. Funt, *Mixing of rubber*. Smithers Rapra Technology Ltd, 2009.

[103] R. F. Grossman, Ed., *The mixing of rubber*. London, UK: Chapman & Hall, 1997.

[104] W. Dierkes, *Economic mixing of silica compounds, Interaction between the chemistry of the silica-silane reaction and the physics of mixing*. Ph.D Thesis, University of Twente, Enschede, the Netherlands, 2005.

[105] A. Das, R. Jurk, K. Werner Stöckelhuber, T. Engelhardt, J. Fritzsche, M. Klüppel, and G. Heinrich, "Nanoalloy Based on Clays: Intercalated-Exfoliated Layered Silicate in High Performance Elastomer," *J. Macromol. Sci. Part A*, vol. 45, no. 2, pp. 144–150, Jan. 2008.

[106] S. Ghosh, R. A. Sengupta, and G. Heinrich, "High Performance Nanocomposite based on Organoclay and Blends of Different Types of SBR with BR," *Kautschuk Gummi Kunststoffe*, vol. 1–2, pp. 48–54, 2011.

[107] K. Subramaniam, A. Das, D. Steinhauser, M. Klüppel, and G. Heinrich, "Effect of ionic liquid on dielectric, mechanical and dynamic mechanical properties of multi-walled carbon nanotubes/polychloroprene rubber composites," *Eur. Polym. J.*, vol. 47, no. 12, pp. 2234–2243, 2011.

[108] A. Das, K. W. Stöckelhuber, S. Rooj, D.-Y. Wang, and G. Heinrich, "Synergistic effects of expanded nanoclay and carbon black on natural rubber compounds," *Kautschuk Gummi Kunststoffe*, vol. 63, pp. 296–302, 2010.

[109] L. A. E. M. Reuvekamp, J. W. ten Brinke, P. J. van Swaaij, and J. W. M. Noordermeer, “Effects of Time and Temperature on the Reaction of TESPT Silane Coupling Agent During Mixing with Silica Filler and Tire Rubber,” *Rubber Chem. Technol.*, vol. 75, pp. 187–198, 2002.

[110] M. Tiwari, J. W. M. Noordermeer, W. J. van Ooij, and W. K. Dierkes, “Plasma polymerization of acetylene onto silica: an approach to control the distribution of silica in single elastomers and immiscible blends,” *Polym. Adv. Technol.*, vol. 19, pp. 1672–1683, 2008.

[111] B. T. Poh and C. C. Ng, “Effect of silane coupling agents on the mooney scorch time of silica-filled natural rubber compound,” *Eur. Polym. J.*, vol. 34, no. 7, pp. 975–979, Jul. 1998.

[112] C. Kummerlöwe, N. Vennemann, E. Yankova, M. Wanitschek, C. Grös, T. Heider, F. Haberkorn, and A. Siebert, “Preparation and properties of carbon nanotube composites with nitrile- and styrene-botadiene rubebrs,” *Polym. Eng. Sci.*, vol. 53, pp. 849–856, 2013.

[113] J. Xu, S. Li, Y. Li, and X. Ta, “Preparation, morphology and properties of natural rubber/carbon black/multi-walled carbon nanotubes conductive composites,” *J. Mater. Sci. Mater. Electron.*, vol. 27, no. 9, pp. 9531–9540, 2016.

[114] H. H. Le, M. Parsaker, M. N. Sriharish, S. Henning, M. Menzel, S. Wießner, A. Das, Q. K. Do, G. Heinrich, and H. J. Radusch, “Effect of rubber polarity on selective wetting of carbon nanotubes in ternary blends,” *Express Polym. Lett.*, vol. 9, no. 11, pp. 960–971, 2015.

Publication I

Minna Poikelispää, Amit Das, Wilma Dierkes, Jyrki Vuorinen

The effect of coupling agents on silicate based nanofillers / carbon black dual filler systems on the properties of a NR/BR compound

Journal of elastomers and plastics 47 (2015) 738-752

Article

JOURNAL OF ELASTOMERS & PLASTICS

Journal of Elastomers & Plastics
1–15

DOI: 10.1177/0095244314538436
jep.sagepub.com
SAGE

The effect of coupling agents on silicate-based nanofillers/carbon black dual filler systems on the properties of a natural rubber/butadiene rubber compound

Minna Poikelispää[1], Amit Das[1,2], Wilma Dierkes[1,3] and Jyrki Vuorinen[1]

Abstract

Nanofillers have been introduced a few years ago, but their application in elastomers is still a challenge. With the existing rubber processing equipment and constraints of rubber mixing, dispersion of nanofillers is difficult. The processability and performance of compounds containing plate- or tube-like silicates in a blend with conventional fillers, such as carbon black (CB), are investigated, and the effect of surface modification of the nanofillers is studied.

Processing is facilitated by the replacement of CB by the nanofillers, but curing efficiency is reduced. The dispersion of the fillers is improved with the addition of nanofillers. The dynamic properties of the cured composite material are affected, giving the composite material lower hysteresis, while the mechanical properties are merely affected by the addition of nanofillers. Additionally, the filler–polymer interaction is increased. The addition of a compatibilizing and coupling agent, a silane, has only a minor effect and does not improve processing and properties significantly for these combined filler systems.

[1] Department of Materials Science, Tampere University of Technology, Tampere, Finland
[2] Leibniz Institute of Polymer Research Dresden, Germany
[3] Department of Elastomer Technology and Engineering, Faculty of Engineering Technology, University of Twente, Enschede, The Netherlands

Corresponding author:
Minna Poikelispää, Department of Materials Science, Tampere University of Technology, P.O. Box 589, Tampere 33101, Finland.
Email: minna.poikelispaa@tut.fi

Keywords
Elastomer, nanofiller, layered silicate, halloysite nanotubes, silane coupling agent

Introduction

Carbon black (CB) is widely used as a filler for elastomers due to its reinforcing properties. However, the production of CB causes pollution as it is prepared from petroleum feedstock. The replacement of CB with naturally occurring minerals is one way to reduce this environmental burden, and an alternative are mineral nanofillers, as they show an outstanding reinforcing potential due to their small particle size and high aspect ratio. This allows using a lower filler loading, which also has a positive effect on certain material characteristics, especially dynamic mechanical properties.

Nanoclays are layered silicates (LSs) such as montmorillonite, which is the most intensively studied silicate mineral. They are 2:1 phyllosilicates and consist of octahedral and tetrahedral sheets; octahedral layers of alumina or magnesia are placed between the tetrahedral sheets and they share oxygen atoms.[1] In order to achieve nanosized fillers, these layers need to be intercalated and exfoliated. The thickness of one single layer is approximately 1 nm. LSs are reported to have many benefits over conventional fillers, such as CB and silica; they reduce viscosity and gas permeability and increase strength, hardness, and moduli of the material at small concentrations.[2–6]

Recent studies[7–19] were also focused on halloysite nanotubes (HNTs), which are naturally occurring 1:1 alumosilicates with tubular form. HNTs have silanol groups on the edges of the tubes which make the dispersion more difficult due to their interparticle affinity. Thus, the main challenges with both, LSs and HNTs, is to have good dispersion and polymer–filler interaction.

The most crucial aspect of getting a good property profile of an elastomeric material is interaction and adhesion between the polymer and the filler, especially in the case of nanofillers, with appropriate dispersion. In the special case of silicates, the chemical structure of the filler surface results in high interparticular forces, resulting in aggregation of the filler. This is the case for compounds with only nanofillers but also for filled compounds that contain a blend of conventional fillers and nanofillers, in which the latter in general is the minority component. The small particle size, that is large surface area, and high van der Waals forces between two particles make it difficult to properly disperse and distribute it in the matrix material.

A proven way to overcome the interparticular forces in rubber mixing is the treatment of the filler with a coupling agent such as silane. These coupling agents not only form a bond between the filler and the polymer during vulcanization, but also act as a covering agent. During mixing, they chemically react with the polar groups on the filler surface, resulting in reduced polarity and lower concentration of surface active groups responsible for the filler–filler interaction. This technology was successfully introduced for silica as filler and silane as coupling agent.[20] However, in the case of dual filler systems with the silicate as the minor component, dispersion and effective reaction of the compatibilization and coupling agent with the nanofiller is problematic due to its very low concentrations.

Bis(3-triethoxysilylpropyl)tetrasulfide (TESPT) is commonly used as a coupling agent in rubber applications with silica. TESPT is a bifunctional organosilane, which contains sulfur for chemically coupling the filler–silane complex to the polymer. As LSs and HNTs have partly the same chemical moieties on their surface as silica, silanol groups, it can be assumed that TESPT could be used as a coupling agent for these fillers as well. However, the concentration of OH groups on the HNT and silicate surface is lower than the concentration on the surface of silica, which is reported to be four to five silanol groups per square nanometer for precipitated silica.[21] From these three silicate-based fillers, HNTs have the lowest silanol group density.[22] This will result in a lower reaction rate and yield for the surface modification, and it has to be investigated if it still gives sufficient surface modification for improved dispersion and filler–polymer interaction and adhesion. The LS used in this study was activated by sodium (Na^+) ions, which increase the cation-exchange capacity and intergallery distances. The surface modification of these silica layers with silane is expected to improve dispersion, to stabilize the dispersed filler in the rubber matrix, and to provide a coupling between the silicate and the polymer. This should finally result in improved properties of the material. The HNTs are also expected to react with the coupling agent, and thus, to disperse easier and show a better filler–polymer interaction.

In this study, HNTs and LSs were treated with a silane. The effect of a partial replacement of CB by silane-treated nanoclays on the properties of rubber was investigated.

Experimental

Materials

LS used in this study was Nanofill 116 (Rockwood Clay Additives, Germany). This is a Na-modified silicate, which is expected to be easily dispersible compared with untreated LSs. It has a density of 2.6 g/cm^3 and a median particle size of smaller than 20 μm in the nonexfoliated state. The HNTs were delivered by Sigma-Aldrich (St Louis, Missouri, USA). The diameter of the nanotubes was 30–70 nm and the length varied between 1 and 4 μm. The specific surface area of these tubes was 65 m^2/g. Other compounding ingredients are specified in Table 1.

Test methods

The Mooney viscosity of the compounded material was measured using an MV 2000 Mooney Viscometer from Alpha Technologies (Washington, USA). The measurement included 1 min heating time and 4 min measuring time at 100°C. Curing studies were performed by using an Advanced Polymer Analyzer 2000 from Alpha Technologies (Akron, Ohio, USA). They were carried out at 150°C for 20 min, and the compounds were vulcanized at their respective curing times t_{90} at 150°C.

Tensile tests of the samples were carried out with a midi 10-20 universal tester (Messphysik Materials Testing, Austria) according to ISO 37 standard. Dynamic properties were studied with an Advanced Polymer Analyzer 2000 from Alpha Technologies at 60°C. A frequency of 10 Hz and 3.5% strain were used.

Table 1. Formulation of NR/BR compounds.

Ingredients	Type/producer	Amount of rubber(phr)
NR	SMR10	80
BR	Buna-*cis*-132/Dow Chemical Company	20
Nanofiller		0/1/2.5/5/7.5
N-234	Evonik	50/49/47.5/45/42.5
6PPD	Lanxess	2.0
TMQ	Lanxess	1.0
ZnO	Grillo Zinkoxid, GmbH	5.0
TDAE oil	Vivatec 500/Hansen & Rosenthal, GmbH	8.0
Stearic acid	Oleon N.V	2.0
Ceresine wax	Statoil wax, GmbH	1.5
CBS	Lanxess	1.5
Sulfur	Solvay Barium Strontium, GmbH	1.5

N-234: carbon black; 6PPD: *N*-(1,3-dimethylbutyl)-*N*′-phenyl-1,4-benzenediamine; TMQ: 2,2,4-trimethyl-1,2-dihydroquinoline; TDAE oil: treated distillate aromatic extract oil; CBS: *N*-cyclohexyl-2-benzothiazolesulfenamide; NR: natural rubber; BR: butadiene rubber; ZnO: zinc oxide.

Bound rubber (BDR) measurements were carried out by dissolving 0.2 g of uncured rubber in toluene for 96 h. Toluene was exchanged every 24 h. After 96 h, the samples were dried and weighed. The BDR content was calculated by the formula:

$$\mathrm{BDR}\ (\%) = \frac{m_0 - (m_1 - m_2)}{m_0} \times 100,$$

$$m_0 = m_s \times \frac{100}{\mathrm{cpd}}$$

where m_0 is the rubber content in the sample, m_1 is the combined weight of bag and sample, m_2 is the weight of the dried bag and sample, m_s is the weight of the dry sample, and cpd is the total amount of rubber and filler in the compound in parts per hundred.[23]

The state of dispersion of the HNT particles in the natural rubber (NR)/butadiene rubber (BR) nanocomposites was investigated by scanning electron microscopy (SEM) using a Philips XL-30 model (Philips, Amsterdam, The Netherlands).

Material preparation

NR, BR, fillers, and other ingredients except curatives were mixed in a Krupp Elastomertechnik GK 1.5 E intermeshing mixer (Germany; mixing chamber temperature 50°C and rotor speed 70 rpm. After addition of the ingredients, the temperature was raised to 140°C and mixing was continued for 5 min at constant temperature to complete the silanization reaction. The accelerator and sulfur were added on an open two-roll mill. In the reference compound, only CB was used as filler with a concentration of 50 phr using the same mixing protocol. In the compounds with HNTs and LSs, a certain amount of CB was substituted by the same amount of silicates/HNTs up to 7.5 phr.

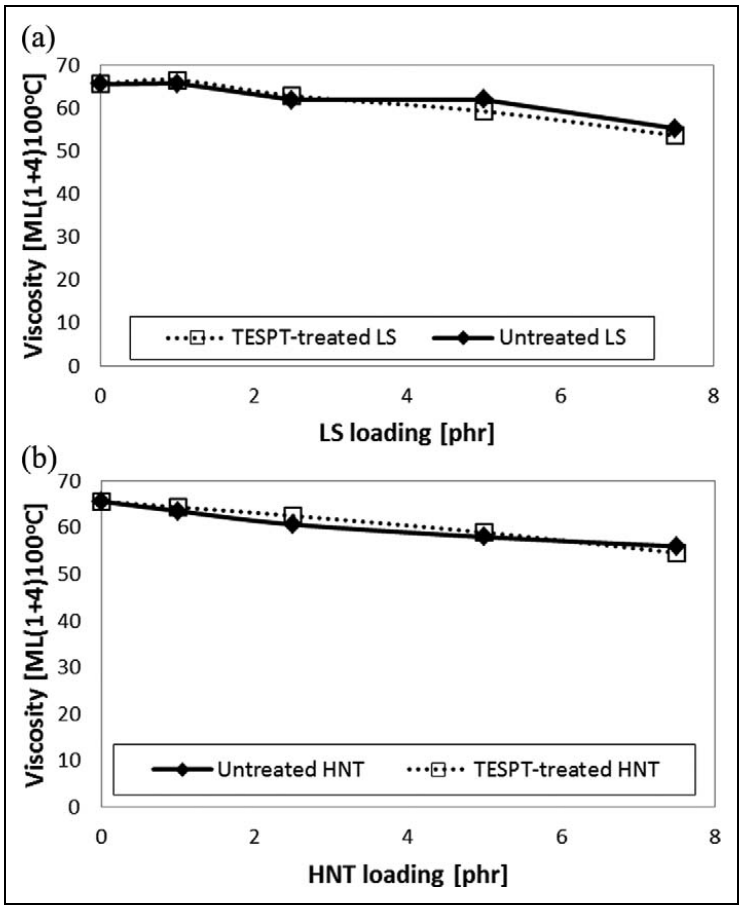

Figure 1. Mooney viscosity of the compounds with increasing amount of nanofillers, without and with silane, for (a) LSs and (b) HNTs. LS: layered silicate; HNT: halloysite nanotube.

Results and discussion

Figure 1(a) and (b) show the Mooney viscosity of the final compounds after the productive mixing step. The viscosity decreases proportionally with the amount of nanofiller added to the compound for both filler types. This might be due to better dispersion of the CB particles.

The curing behavior of the compounds is shown in Figure 2. The final torque of the compounds with just 1 phr of LS is similar to the final torque of the reference compound. Low quantities of LS do not influence cross-linking of the compound nor the final torque by a viscosity effect. For higher quantities, the final torque is lower, the higher the LS concentration, probably due to the viscosity reduction seen earlier.

Again, no difference in final torque is found between compounds with silane-modified and -unmodified LSs. No clear trend can be seen for the scorch time. Ismail and Mathialagan reported the decrease in scorch time when silica and calcium carbonate

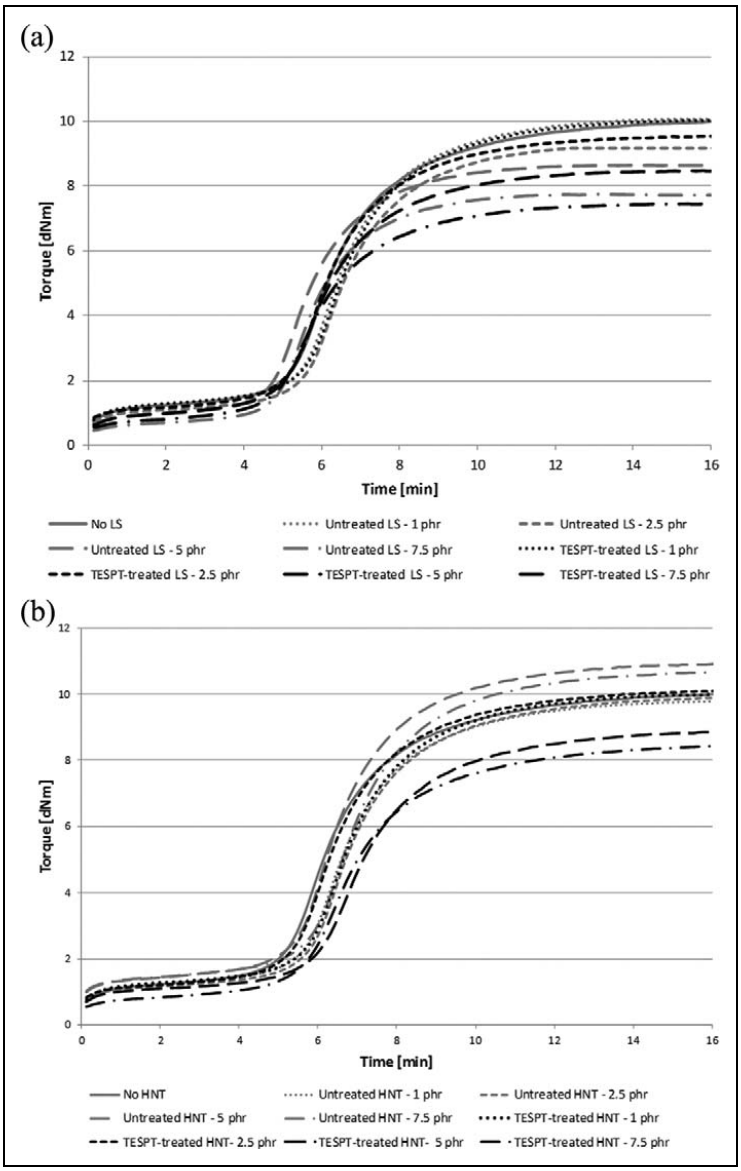

Figure 2. Rheograms of the compounds without and with silane with varying amount of (a) LSs and (b) HNTs. LS: layered silicate; HNT: halloysite nanotube.

were replaced by bentonite as it reduces their tendency to react with accelerators.[6] Here, CB, which does not absorb accelerators, was used, and the differences in scorch time could not be observed. Kim et al. reported that a compound containing 10 phr organoclays shows reversion, while the compound containing 1 phr silane shows this phenomenon to a lesser extent. This was explained by an antireversion effect of the coupling

agent.[4] As the curing time and temperature were lower in the present study, the possible antireversion effect could not be seen in this case.

For the compounds with untreated HNTs, the trend is different. An increasing final torque with increasing HNT concentration is observed. For TESPT-treated HNTs, the torque decreases with increasing HNT concentration indicating better filler dispersion. Rooj et al. observed opposite behavior in HNT-filled NR compounds. The torque was higher with TESPT-treated HNTs than with untreated HNTs.[8] However, they used HNTs as the only filler. In this study, CB was used as primary filler, and addition of HNTs also improved the dispersion of CB which causes the reduction in maximum torque. The scorch time becomes longer with addition of HNTs, which can be explained by inactivation of curing additives due to adsorption. The same effect was observed when HNT-filled NR was studied.[9] The HNTs appear to be more active than the LS in this sense. However, the influence of HNTs on the final torque was lower than the influence of the LSs; the efficiency of cross-linking is reduced by HNT but to a lesser extent than by LS.

The storage modulus G' as a measurement of the Payne effect, which gives an indication of filler–filler interaction, is shown in Figure 3. A reduced Payne effect expresses a lower degree of filler–filler interaction, which implies better dispersion of the filler. For the compounds with unmodified LS, the Payne effect is reduced. There is a gradual reduction up to 5 phr of LS, and between 5 phr and 7.5 phr of LS an overproportional reduction occurs. The presence of LS suppresses filler–filler interaction, even of the CB, in the compound. This might be explained by the low interaction between CB and silicates, and the fact that a higher concentration of LS increases the probability that LS particles arrange themselves between the CB particles. Another explanation of the reduction of the moduli can also be the decrease in filler volume fraction when CB is replaced by silicates. Replacing 7.5 phr of CB by LSs or HNTs decreases the total volume fraction of fillers by 4%. The loss modulus G'' is slightly reduced with increasing nanofiller content. In the case of HNTs, both moduli decrease proportionally with increasing concentration of the nanofiller. For both filler systems, the addition of the silane seems not to be effective, as it does not result in significant differences of the moduli. Rooj et al. reported an increase in Payne effect with increased concentration of HNTs in a fluoroelastomer composite.[7] In this case, the increase can be explained by higher filler concentrations, whereas in the present article the filler concentration was equal and the ratio of CB to nanofiller varied.

As one of the envisaged applications of this material is tire treads, the dynamic properties of the cured material are important. This is in particular true for tan δ value, that is, the ratio of the loss modulus to the storage modulus. Responsible for the energy loss expressed in the tan δ value is a slippage of the polymer chains over the surface of the filler, which is stronger for higher values of the loss angle, and the interactions and bonds between the polymer chains and the filler surface are weaker. Figure 4 shows the values of the loss angle as a function of the nanofiller concentration at 60°C, the temperature of a tire on the road and thus the temperature for measuring rolling resistance. An increasing amount of nanofillers reduces tan δ values, and this indicates that less energy is lost by dissipation. For the application in tire treads, this means that the rolling resistance will be reduced by the addition of these fillers. These results are in line with

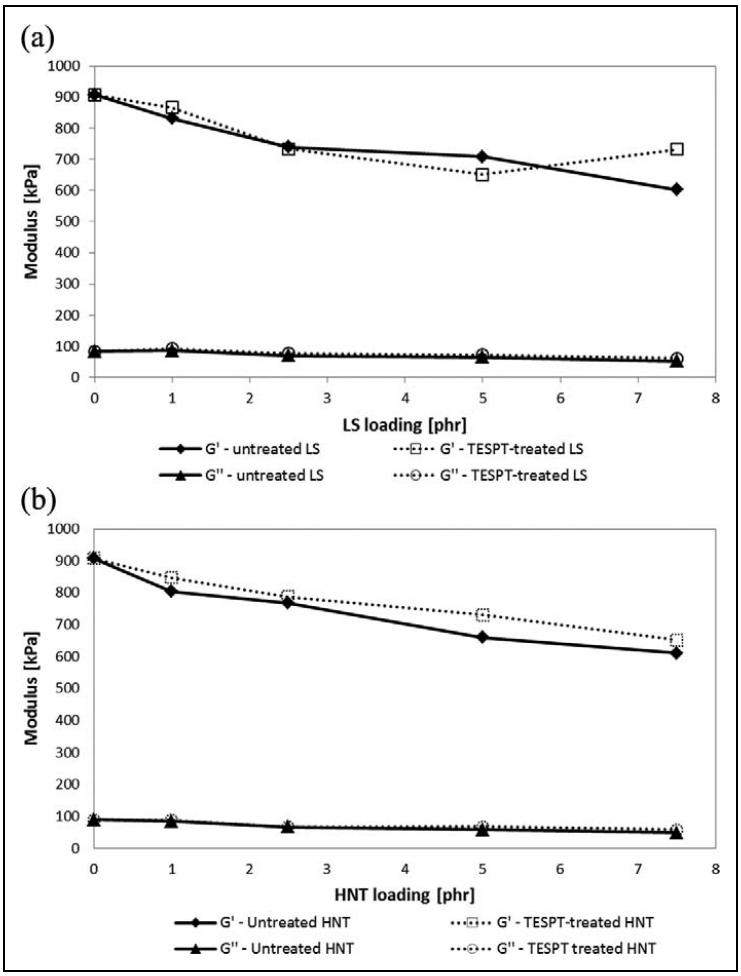

Figure 3. Storage and loss moduli of the compounds without and with silane with increasing amount of (a) LSs or (b) HNTs. LS: layered silicate; HNT: halloysite nanotube.

the results reported by Pasbakhsh et al. for ethylene propylene diene monomer (EPDM)/HNT nanocomposites.[11] The influence of the silane is not very conclusive, but it is obvious that the addition of higher concentrations of nanofillers together with silane leads to higher tan δ values than the material without silane. A strong coupling between the filler and the polymer in general gives lower tan δ values; in this case, this coupling seems not to be effective in that sense. It might very well be that the silane covers the filler by physical adsorption, either the nanofillers or the CB, resulting in more physical interaction between the fillers and the polymer and thus more energy dissipation due to slippage. There is no indication of strong chemical bonds between the polymer and the filler in this system.

Figure 5 shows the results of the stress–strain measurements. The strength of the materials does not change with the replacement of CB by the LS; the reinforcing effect of both nanofillers is comparable with the reinforcing effect of CB, as seen in Figure 5.

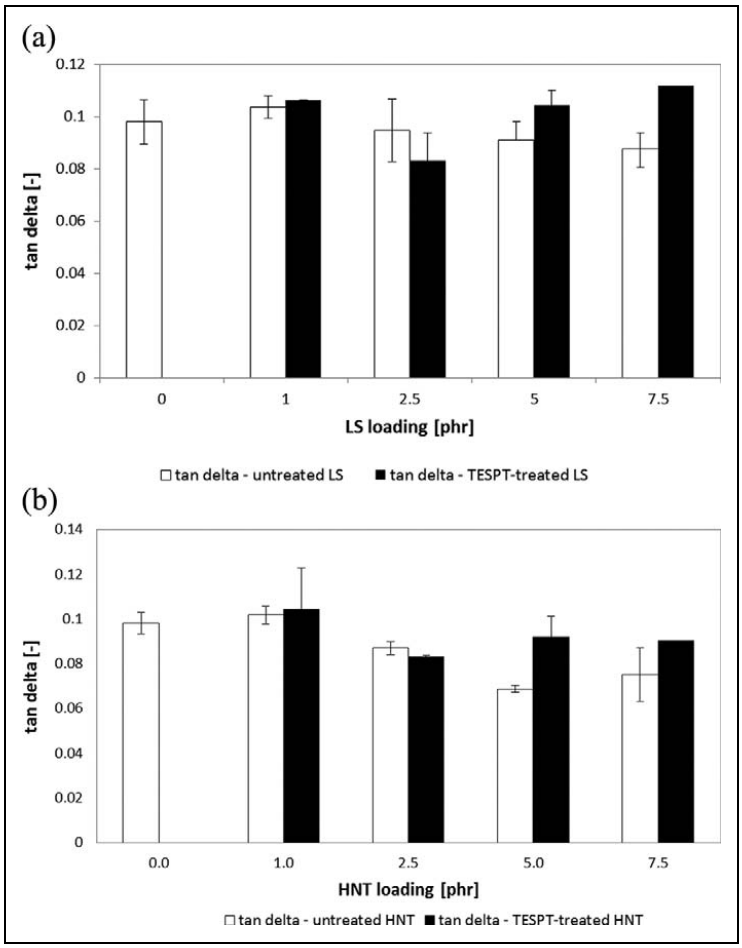

Figure 4. Tan δ values of the compounds with increasing amount of nanofillers, without and with silane at 60°C, for (a) LSs and (b) HNTs. LS: layered silicate; HNT: halloysite nanotube.

Only for HNTs at higher concentrations, a slight additional reinforcing effect is observed. There is no influence on material strength when silane is added. Elongation at break values show shows an increasing trend for higher quantities of nanofillers, though the variation is rather high, especially in the case of HNTs.

Ismail et al. observed that tensile strength increases up to 20 phr of HNTs in HNT/NR nanocomposites and a reduction in elongation at break.[9] When silica and calcium carbonate were partially replaced by bentonite, the tensile strength of the EPDM compounds containing calcium carbonate and bentonite increased generally with increasing bentonite loading, indicating that this filler has a higher reinforcing effect than calcium carbonate. The tensile strength of the compounds containing silica and bentonite increased with the increased bentonite loading up to 15/15 phr loading, respectively, showing a synergistic effect and improved dispersion due to the presence of both fillers.[6]

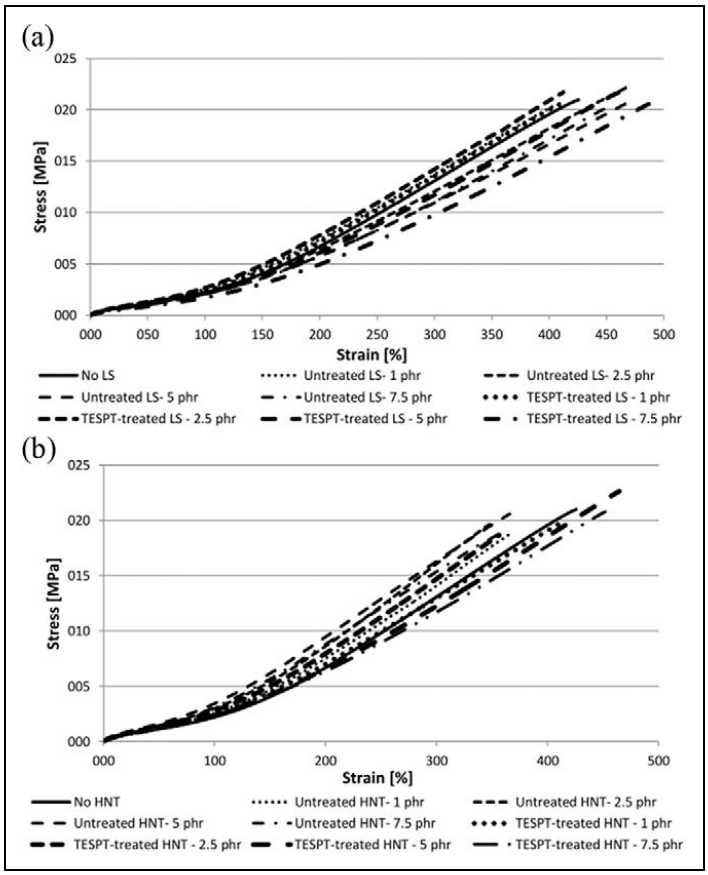

Figure 5. Stress–strain curves of the cured materials without and with silane with increasing amount of (a) LSs and (b) HNTs. LS: layered silicate; HNT: halloysite nanotube.

As in our study, Kim et al. reported that TESPT did not improve the tensile strength and elongation at break of organoclay-filled NR/BR compounds but rather decreased the stress–strain properties.[4]

In terms of moduli, the replacement of CB by LS has a clear effect; when more LS is added, the values are lower. Again, the presence of silane does not make a difference, as seen in Figure 6. Other studies reported that TESPT increased the tensile moduli of organoclay-filled NR/BR compounds,[4] and an increase in tensile modulus in HNT-filled NR nanocomposites.[9] According to Rooj et al., the TESPT treatment increased the M300 modulus but decreased tensile strength and elongation at break in HNT-filled NR nanocomposites.[8] In Figure 6, it is also obvious that the HNT-filled materials do not show a clear trend as the LS-filled compounds do. This might be explained by the more difficult processing behavior of the HNT-compounds, which can result in differences in dispersion of the fillers.

The measurement of the BDR content is a way to directly determine the filler–polymer interaction. In this study, no difference is made between physically and chemically BDR, as the chemical bond between the coupling agents and the nanofiller is

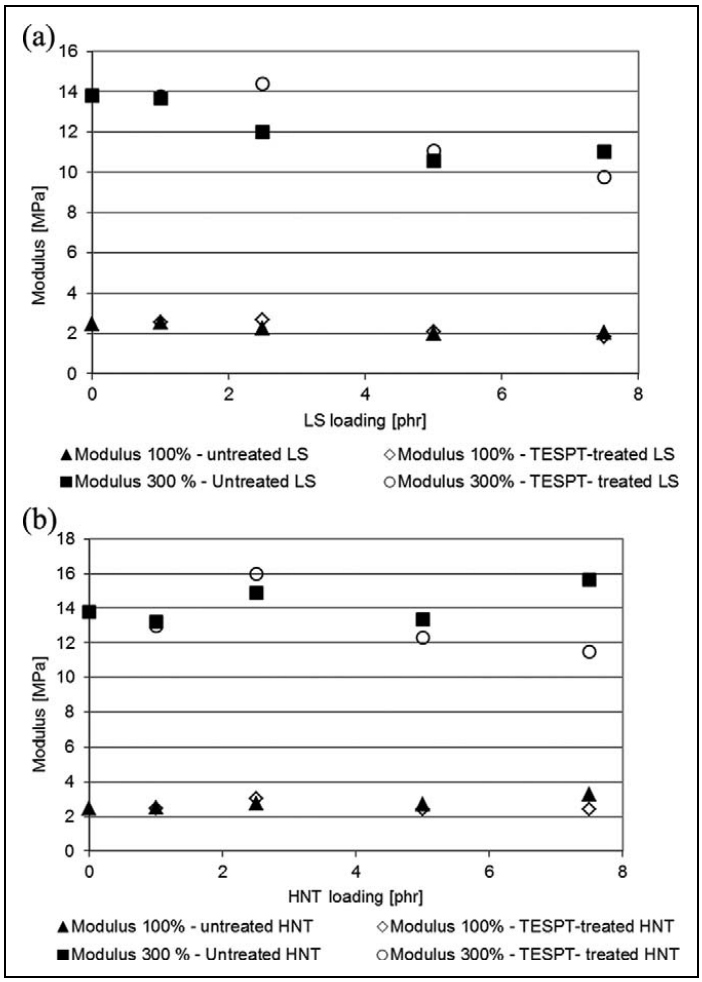

Figure 6. 100% and 300% moduli of the compounds without and with silane with increasing amount of nanofillers for (a) LSs and (b) HNTs. LS: layered silicate; HNT: halloysite nanotube.

expected to be rather low due to the low concentrations of these components. As concluded earlier, there is no structural increase in chemical filler–polymer interaction due to the silanization seen here neither, as seen in Figure 7. The addition of the silane is not effective in these systems. For the compound containing LS, the BDR content is increased when silane is added, showing an improvement of the interaction between the polymer and the filler. However, the difference is rather small. The replacement of CB by LS results in a higher amount of BDR up to a maximum. At high concentrations of LS and without silane, the LSs are less dispersed, and therefore, the polymer chains cannot attach to all the particles in an optimal way.

For HNT-filled rubber, the BDR content increases, as more amount of nanofiller is added. Due to the low compatibility of the polar HNT with the apolar polymer, it is not

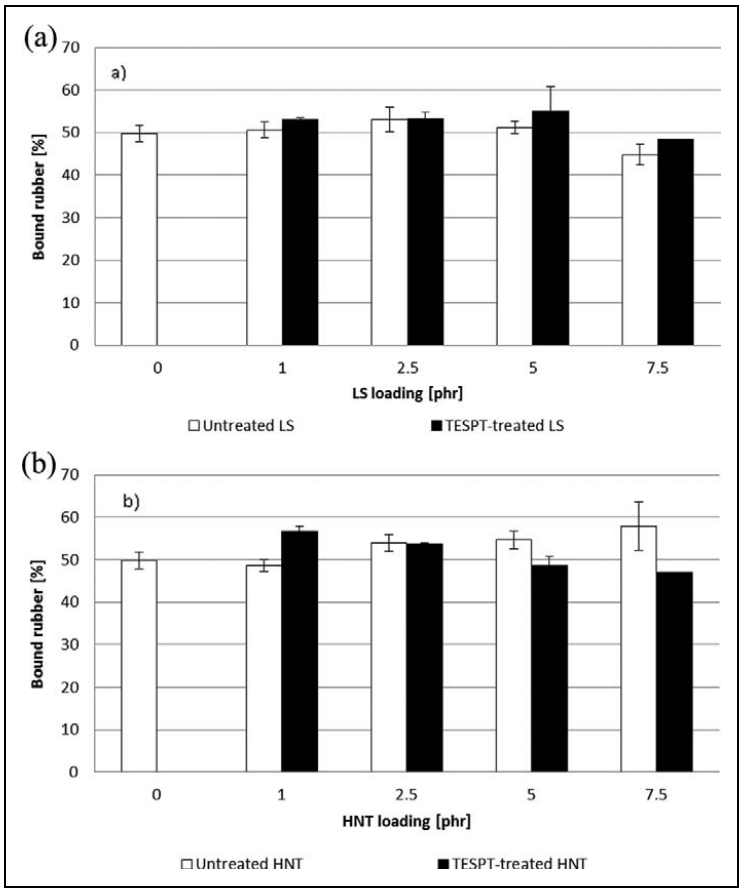

Figure 7. BDR content of the cured compounds without and with silane with increasing amount of (a) LSs and (b) HNTs. BDR: bound rubber; LS: layered silicate; HNT: halloysite nanotube.

very probable that this is the result of an interaction between the nanofiller and the polymer. It might be caused by better dispersion of the CB filler due to the presence of the HNTs, which results in better polymer–filler interaction. The results of the materials containing silanes are rather unexpected. BDR content decreases with increasing nanofiller and silane contents. This is in accordance with the higher tan δ values as seen in Figure 4(a) and indicates weaker filler–polymer interaction. An explanation for this effect might be an interaction between the CB and the silane, which reduces the interactions of this filler with the polymer.

Figure 8(a) and (b) shows SEM pictures of the compounds with untreated and TESPT-treated LS at a concentration of 5 phr. In the compound containing untreated LSs, clusters of nanoparticles are visible, and failure of the material took place from the interfaces between rubber and nanofiller. When using TESPT-treated LSs, clusters are not visible, indicating that the dispersion is better. Furthermore, the particles seem to be covered with a rubber layer due to the better bonding of the polymer to the filler. The

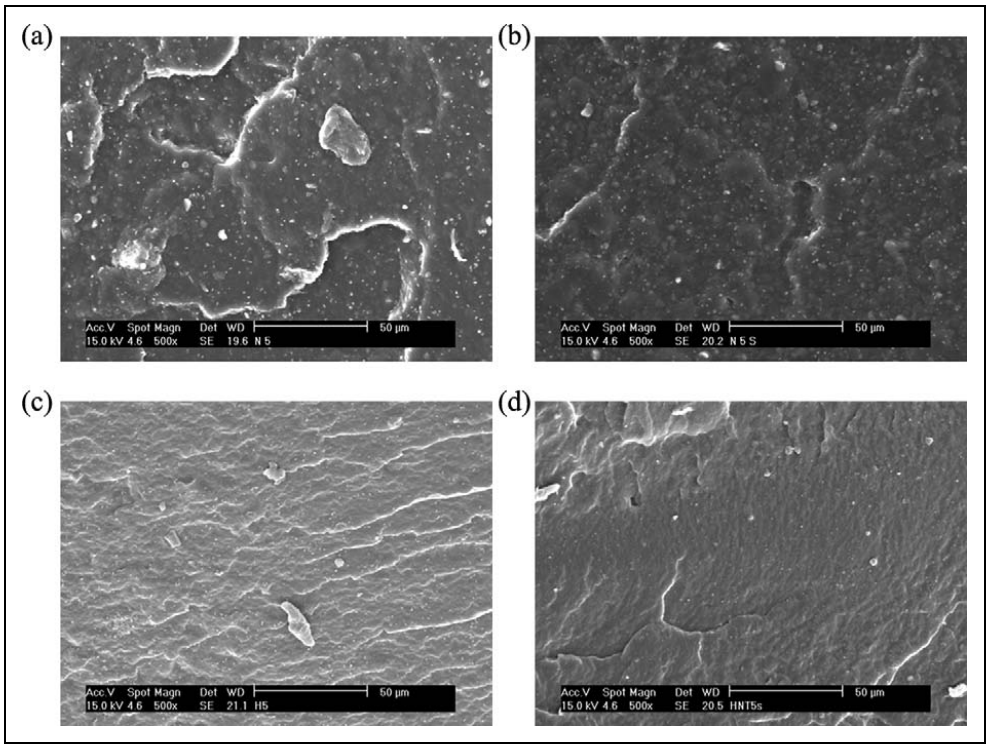

Figure 8. SEM pictures of NR/BR compounds containing 5 phr of nanofiller. (a) Untreated LS, (b) TESPT-treated LS, (c) untreated HNTs, and (d) TESPT-treated HNTs. SEM: scanning electron microscopy; NR: natural rubber; BR: butadiene rubber; LS: layered silicate; TESPT: bis(3-triethoxysilylpropyl)tetrasulfide; HNT: halloysite nanotube.

same effects can be seen in Figure 8(c) and (d), which illustrate untreated and TESPT-treated HNTs, respectively. The compound containing untreated HNTs shows some agglomerates, but in the case of TESPT-treated HNTs, this kind of clusters is not visible. In the compound containing TESPT-treated HNTs, the particles seem to be smaller than in the compound containing untreated HNTs. This may be due to either better coverage of the particles with rubber or smaller aggregates and thus better dispersion.

Conclusions

The replacement of CB by LSs as well as HNTs facilitates processing, as it reduces the viscosity of the compound. The addition of both nanofillers reduces the efficiency of the curing process resulting in lower final torque values. The dynamic properties are affected by the blend of fillers. The storage and loss modulus are reduced when the amount of HNTs is increased, as is the loss angle. This makes the dual filler systems attractive for tire applications, as lower tan δ values result in lower rolling resistance. The strength of the material is merely affected, and the moduli are reduced by the addition of LSs. The

effect of HNTs is not very explicit, which can be explained by the more difficult processing of this material. The BDR values are increased, indicating an effect of the nanofillers on filler–polymer interaction.

The addition of silane does not improve the properties as it does in neat silica-filled compounds. This is probably a consequence of the very low amount of silane that was added, in accordance with the low loading of the silicate filler.

Overall, it can be concluded that the replacement of a small quantity of CB with a silicate results in improved dispersion of the fillers and better dynamic properties. However, a significant increase in mechanical properties could not be observed.

Funding

The technical and financial support for this project from Nokian Tyres and Teknikum is acknowledged as well as the funding for the WILMIX project (Grant no. 40352/08) from Tekes, Finland.

References

1. Alexandre M and Dubois P. Polymer-layered silicate nanocomposites: preparation, properties and uses of a new class of materials. *Mater Sci Eng* 2000; 28: 1–63.
2. Arroyo M, López-Manchado MA, and Herrero B. Organo-motmorillonite as substitute of carbon black in natural rubber compounds. *Polymer* 2003; 44: 2447–2453.
3. Ghassemieh E. Enhancement of the properties of EPDM/NBR elastomers using nanoclay for seal applications. *Polym Compos* 2009; 30: 1658–1667.
4. Kim W, Kim SK, Kang JH, et al. Structure and properties of the organoclay filled NR/BR nanocomposites. *Macromol Res* 2006; 14:187–193.
5. El-Nashar DE, Ahmed NM, and Yehia AA. The role of ion-exchange bentonites in changing the properties of styrene-butadiene rubber composites. *Mater Des* 2012; 34: 137–142.
6. Ismail H and Mathialagan M. Comparative study on the effect of partial replacement of silica or calcium carbonate by bentonite on the properties of EPDM composites. *Polym Test* 2012; 31: 189–208.
7. Rooj S, Das A, and Heinrich G. Tube-like natural halloysite/fluoroelastomer nanocomposites with simultaneous enhanced mechanical, dynamic mechanical and thermal properties. *Eur Polym J* 2011; 47: 1746–1755.
8. Rooj S, Das A, Thakur V, et al. Preparation and properties of natural nanocomposites based on natural rubber and naturally occurring halloysite nanotubes. *Mater Des* 2010; 31: 2151–2156.
9. Ismail H, Salleh SZ, and Ahmad Z. Curing characteristics, mechanical, thermal, and morphological properties of halloysite nanotubes (HNTs)-filled natural rubber nanocomposites. *Polym Plast Technol Eng* 2011; 50: 681–688.
10. Ismail H, Salleh SZ, and Ahmad Z. Fatigue and hysteresis behavior of halloysite nanotubes-filled natural rubber (SMR L and ENR 50) nanocomposites. *J Appl Polym Sci* 2012; 127: 3047–3052.
11. Pasbakhsh P, Ismail H, Ahmad Fauzi MN, et al. EPDM-modified halloysite nanocomposites. *Appl Clay Sci* 2010; 48: 405–413.
12. Ismail H, Pasbakhsh P, Ahmad Fauzi MN, et al. Morphological, thermal and tensile properties of halloysite nanotubes filled ethylene propylene diene monomer (EPDM) nanocomposites. *Polym Test* 2008; 27: 841–850.

13. Pasbakhsh P, Ismail H, Ahmad Fauzi MN, et al. Influence of maleic anhydride grafted ethylene propylene diene monomer (MAH-g-EPDM) on the properties of EPDM nanocomposites reinforced by halloysite nanotubes. *Polym Test* 2009; 28: 548–559.
14. Pasbakhsh P, Ismail H, Ahmad Fauzi MN, et al. The partial replacement of silica or calcium carbonate by halloysite nanotubes as fillers in ethylene propylene diene monomer composites. *J Appl Polym Sci* 2009; 113: 3910–3919.
15. Lei Y, Tang Z, Guo B, et al Functional thiol ionic liquids as novel interfacial modifiers in SBR/HNTs composites. *Polymer* 2011; 52: 1337–1344.
16. Du M, Guo B, Lei Y, et al. Carboxylated butadiene-styrene rubber/halloysite nanotube nanocomposites: Interfacial interaction and performance. *Polymer* 2008; 49: 4871–4876.
17. Guo B, Lei Y, Chen F, et al. Styrene-butadiene rubber/halloysite nanotubes nanocomposites modified by methacrylic acid. *Appl Surf Sci* 2008; 255: 2715–2722.
18. Guo B, Chen F, Lei Y, et al. Styrene-butadiene rubber/halloysite nanotubes nanocomposites modified by sorbic acid. *Appl Surf Sci* 2009; 255: 7329–7336.
19. Poikelispää M, Das A, Dierkes W, et al. Synergistic effect of plasma-modified halloysite nanotubes and carbon black in natural rubber-butadiene rubber blend. *J Appl Polym Sci* 2013; 127: 4688–4696.
20. Luginsland HD, Fröhlich J, and Wehmeier A. In fluence of different silanes on the reinforcement of silica-filled rubber compounds. *Rubber Chem Technol* 2002; 75: 563–579.
21. Iler RK. *Chemistry of silica: solubility, polymerization, colloid and surface properties and biochemistry*. New York: John Wiley & Sons, 1979.
22. Du M, Guo B, and Jia D. Newly emerging applications of halloysite nanotubes: a review. *Polym Int* 2010; 59: 574–582.
23. Leblanc JL and Hardy P. Evolution of bound rubber during the storage of uncured compounds. *Kautsch Gummi Kunstst* 1991; 44: 1119–1124.

Publication II

Janak Sapkota, Minna Poikelispää, Amit Das, Wilma Dierkes, Jyrki Vuorinen

Influence of nanoclay – carbon black as hybrid filler on mechanical and vulcanization behavior of natural rubber compounds

Polymer Engineering and Science, 53 (2013) 615-622

Influence of Nanoclay-Carbon Black Hybrid Fillers on Cure and Properties of Natural Rubber Compounds

Janak Sapkota,[1] Minna Poikelispää,[1] Amit Das,[1,2] Wilma Dierkes,[1,3] Jyrki Vuorinen[1]
[1] *Department of Materials Science, Tampere University of Technology, Plastics and Elastomer Technology, FI-33101 Tampere, Finland*

[2] *Leibniz Institute of Polymer Research Dresden, D-01069 Dresden, Germany*

[3] *Department of Elastomer Technology and Engineering, University of Twente, NL-7522NB Enschede, The Netherlands*

The influence of organically modified nanoclay-carbon black (CB) hybrid filler on the curing behavior of natural rubber (NR) was explored in this investigation. Here an effort was paid to understand the curing kinetics of organomodified nanoclay filled rubber compounds. On the basis of two different types of modified clay, NR nanocomposites were prepared and cured by a conventional vulcanization system. A faster curing rate and lower torque values were found when the modification was done by quaternary ammonium compounds. The activation energy of the rubber curing process decreased with the incorporation of nanoclay. In addition, it was revealed that the quaternary ammonium compounds used as modifier in the clay show a plasticization effect. Additionally, X-ray diffraction studies indicated, that the basal spacing of the clay minerals was increased in both cases after incorporation in the rubber matrix. The dynamic mechanical analysis using a strain sweep mode showed that the Payne effect decreases because of an improved dispersion of CB induced by the presence of nanoclay. POLYM. ENG. SCI., 00:000–000, 2012.

INTRODUCTION

Over the past few years, nanoengineered polymeric materials have become one of the rapidly growing new groups of materials used as alternatives to the conventionally filled polymers and polymer blends. The growing interest has mainly been triggered by the over-proportionally enhanced properties they impose on the materials, such as the significant improvement in the overall properties while allowing for reduced filler loadings [1–7].

For elastomeric materials, a good dispersion of the filler is the basic requirement to achieve optimum reinforcement and the best property profile. Carbon black (CB) has been widely used as filler in the rubber industry for many decades. However, recently major interests have shifted to use of nanofillers, which provide significant improvements in thermoplastics. This is not the case in elastomers as mixing and crosslinking processes are yet to be properly mastered. This creates problems in the controlling aggregation and agglomeration of filler particles, dispersion, and filler–matrix interactions. Various modification methods including surface modification, grafting, and use of different compatibilizing agents are currently being studied to overcome these problems.

Surface modification with surfactants is essential for nanoclays in order to achieve an optimal homogenous dispersion of the filler. For cationic surfactants such as quaternary ammonium compounds are used. Incorporation of such modified clay into rubbery materials in order to obtain favorable mechanical and physical properties has been a primary task [1–7]. Most of these researches have been focused on the effect of these particular fillers as the partial or complete replacement of conventional fillers on the performance of the nanocomposites. However, cure kinetics and processing behavior are equally important in determining the final properties of a composite material, particularly, when agents activating vulcanization, such as an ammonium compound, are involved. Most of the mechanical properties of the rubber compounds are related to the type and degree of vulcanization, besides the type and amount of filler. Multiple and complex reactions involved in the vulcanization of the rubber compounds, which might be influenced by the presence of chemicals activating vulcanization in the fillers, can lead to variations in mechanical properties. The actual mechanism of vulcanization and its effect on mechanical properties can only be revealed by a study of the curing reaction and its kinetics [8–10].

Correspondence to: Jyrki Vuorinen; e-mail: jyrki.vuorinen@tut.fi
DOI 10.1002/pen.23297
Published online in Wiley Online Library (wileyonlinelibrary.com).

The detailed understanding of the curing mechanism is essential as it gives valuable information on how the curing reactions are progressing during the vulcanization stage. There are many alternatives to do sulfur vulcanization by the selection of curatives in the rubber compounds, but the knowledge of the mechanisms makes it possible to choose reaction conditions that favor one path over others.

The mechanical properties of any rubber are dependent on the state of cure. The energy consumed during the processing and vulcanization of rubber is linked to the cost of the final end product [11].

The study of cure kinetics can, hence, give a clear insight into the actual mechanisms of curing and its effect on mechanical properties of the end products. Mainly for commercial production of the composites, it is very essential to find the best curing parameters, as it will directly influence cost and effectiveness of the final end product.

During the fabrication of the rubber compounds, the knowledge of the kinetics of crosslinking is very useful [12]. The study of cure kinetics can hence give a clear insight into the actual mechanisms of curing and its effect on the mechanical properties of the end products [13]. For instances, the curing kinetics of hydrogenated carboxylated nitrile rubber (HXNBR) with epoxycyclohexyl polyhedral oligomeric silsesquioxanes was studied by differential scanning calorimetry (DSC) and the apparent activation energy was found to be dependent on the POSS content and the heating rate [14]. As far as the recent studies with rubber–clay nanocomposites are concerned, plenty of reports can be found as the typically used clays contain vulcanization active pieces [15, 16]. The vulcanization kinetics of NBR (acrylonitrile butadiene rubber) filled with organically modified bentonite revealed that the curing rate was superior to the treated bentonite composites, while the reaction orders pointed out the dependency of the vulcanization reaction on the initial reactants if compared to the catalytic effect of the reaction products [17]. Two quaternary phosphonium salts (aromatic and aliphatic) were used as intercalants for Na-montmorillonite and the effect of intercalant structure on clay morphology and natural rubber (NR) vulcanization kinetics was investigated. The vulcanization process was sensibly accelerated by the organoclay and a higher crosslinking degree was observed in the nanocomposite, which gave rise to materials with improved processing and physical characteristics [18]. Lopez-Manchado et al. investigated the effect of the incorporation of a bentonite on the vulcanization kinetics of NR by means of both cure-meter testing and DSC under dynamic and isothermal conditions. The vulcanization curves showed that the modified clay behaved as an effective vulcanizing agent, accelerating the vulcanization reaction of the elastomer [19].

A literature survey revealed that there is no detailed study about the curing kinetics of truck tire compounds, such as NR filled with CB and organomodified clay. Thus, the aims of this investigation were to study the effects of nanoclay loading (in the presence of CB) on the properties of NR nanocomposites, as well as the curing kinetics and activation energy for different clay/NR nanocomposites. Two different organically modified montmorillonite (MMT) clays were selected as fillers in addition to CB; NR was used as a matrix material. The cure characteristics were studied and analyzed to determine the activation energy. Furthermore, various mechanical tests were performed in order to understand the synergistic reinforcement effects of this system.

TABLE 1. Details of the nanoclays.

Properties/materials	Nanofil® 5	Nanoclay®-682616
Manufacturer/supplier	Rockwood clay additives	Sigma Aldrich
Shape	Platelet	Platelet
Dimensions	<10 μm	≤ 20 μm
Specific gravity	1.4–1.8	n.n.
Modification	Dimethyl-di(hydrogenated tallow) alkyl ammonium salt, 20–30 wt% (Clay-QUAT)	Octadecylamine, 25–30 wt% (Clay-PA)
Gallery distance	2.8 nm[a]	2.2 nm[a]

[a] The data were obtained either from the product data sheet or from Ref. 8.

EXPERIMENTAL

Materials

NR (standard Malaysian type grade SMR 10) was used as base polymer, reinforced with two kinds of clays: The first clay was modified by dimethyl-di(hydrogenated tallow) alkyl ammonium salt (clay-QUAT) and the second by octadecylamine (clay-PA). Details of the clay materials are shown in Table 1. Other materials used for compounding were butadiene rubber [(Buna Cis 132) stearic acid (2 phr), zinc oxide (ZnO, 5 phr)], TDAE-oil (treated distillate aromatic extract, 8 phr), CB [(N-234, the amount varied), TMQ (2,2,4-trimethyl-1,2-dihydroquinoline, 1 phr)], CBS (*N*-cyclohexyl-2-benzothiazole sulfonamide, 2.5 phr), sulfur (1.5 phr), paraffin (1.5 phr), and 6PPD (N(1,3-Dimthylbutyl)-*N*′-phenyl-*p*-phenylenediamine, 2 phr). All materials were industrial grade.

Sample Preparation

Compounding of the rubber compound was done in a Krupp Elastomertechnik GK 1.5 laboratory mixer with 8 bar ram pressure. The chamber volume of the mixer is 1.5 l. The fill factor used was 0.75. A standard two roll mill was used for milling. In the first part of the study, the amount of CB was replaced gradually by different loadings of nanoclay, as shown in Table 2.

For the second part of the study, 10 phr of each type of nanofiller was used with 40 phr of CB. For comparison, a compound with 50 phr of CB was taken as reference.

 DOI 10.1002/pen

TABLE 2. Compounds with filler variation and their curing times.

Carbon black (phr)	Nanoclay + modifier (phr)	T_{90} at 150°C (min)
50	0	10.0
49	1	8.9
48	2	8.7
47	3	8.2
45	5	7.8
40	10	6.9
35	15	5.9

For all mixing procedures, the cooling system was set to 40°C. After the mixing of the masterbatch in the internal mixer, curatives were added on a two-roll mill for ~10 min in order to get a good dispersion.

Characterization

The Mooney viscosities of all samples were measured directly (without relaxation) after milling by using a MV 2000 from Alpha Technology, OH. A large rotor was used with a test temperature of 100°C for 1 min preheating time and a testing time of 4 min. All tests were conducted in triplicate.

An Advanced Polymer Analyzer 2000 (APA 2000, from Alpha Technologies, OH) was used to measure the viscoelastic properties of the raw, uncured, and cured elastomers and compounds.

Curing studies and Payne effect measurements were performed by using an Advanced Polymer Analyzer 2000 (Alpha Technologies, OH). Curing was separately done at temperatures at 140, 150, and 160°C for 60 min, and the compounds were vulcanized at their respective curing time at 150°C.

The Payne effect was studied in a strain sweep from 0.28 to 100% at 100°C.

The mechanical properties of the different samples were measured in a tensile test with dumbbell shaped specimens (ISO 37). Tests were done on a Messphysik Midi 10–20 universal tester at a transverse rate of 500 mm/min.

The hardness tests of the samples were done according to ASTM D 2240 by a hand held durometer AFRI Hardness Tester. X-ray diffraction (XRD) analysis was carried out by Siemens D500 to investigate the effectiveness of the clay intercalation and the change in space gap between the two clay platelets. Cu-Kα radiation ($\lambda = 1.54056$ Å) was used as a source. The interlayer distance of the clay in the composites was calculated from the (001) lattice plane diffraction peak using Bragg's equation.

RESULTS AND DISCUSSION

The XRD patterns of the compounds are represented in Fig. 1. One sharp peak was found for both clay filled compounds towards low angles, which could be because of presence of crystallites of corresponding modification

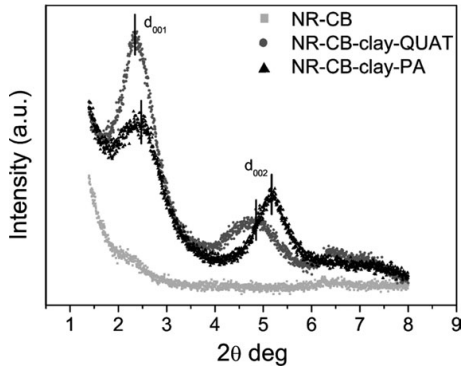

FIG. 1. XRD patterns of nanoclay and carbon black filled rubber compounds.

in the clay structure. The first maximum peak for the NR-CB-clay-QUAT sample was obtained at an angle of 2.31° while that of the NR-CB-clay-PA was obtained at 2.48 (Fig. 1). Further calculation of the plane spacing using Bragg's law results in a value for the compound with clay-QUAT of 3.81 nm, and for clay-PA a spacing of 3.55 nm was found. As expected, these spacing are higher compared to the initial planar spacing of the modified MMT clay, which is in the range of 2.2 nm for clay-PA and 2.8 nm for clay-QUAT. As the initial space gap was higher with QUAT-modified clay, more rubber chains are able to intercalate inside the gallery and the gap increases. Since the QUAT-modified clay offered higher intercalated structure than the PA-modified clay, further work was done with variation of clay-QUAT loading.

Figure 2 shows the effects of clay loading on the Mooney viscosity of rubber-clay compounds. An initial decrease in viscosity was found, followed by an increase for higher loadings. The initial decrease in viscosity might be caused by the replacement of CB by well-dispersed clay. However, at a certain concentration, the nanofiller is no longer well dispersed, leading to an increase in viscosity at higher nanofiller loadings.

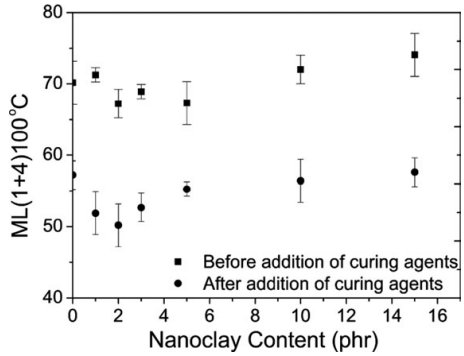

FIG. 2. Mooney viscosity of rubber compounds before and after addition of curing agents.

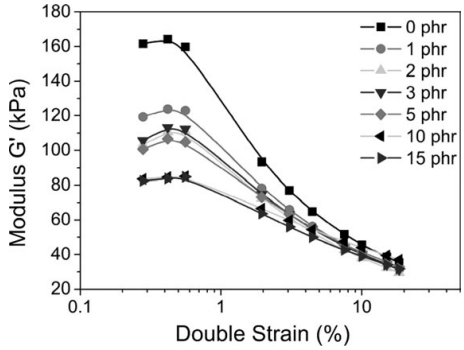

FIG. 3. Storage moduli of the rubber compounds as a function of strain amplitude.

The dependence of the dynamic properties on the strain amplitude at low deformation can give a better understanding of the filler–filler networks in a rubber matrix. This nonlinear behavior of filled rubber compounds is called Payne effect. Figure 3 shows the storage modulus G' for the samples as a function of strain. The Payne effect decreased with increasing nanoclay content. This is an indication that the CB has a higher filler–filler interaction than the modified clay; therefore the replacement of CB by clay results in a lower modulus at low strains. Additionally, the presence of the clay might induce a better dispersion of CB as well. One intercalated clay particle also can interrupt the CB–CB network by occupying a position between them; this could lead a lower overall filler–filler network. Another explanation could be given if the higher density of the clay is concerned as compared with CB. Here, we have replaced the same amount of black by clay in wt%, not vol% and as a result after substitution with clay the overall volume faction of the fillers was less and the composites showed less Payne effect. Nevertheless, the presence of only 1 phr of nanoclay reduced the Payne effect over-proportionally from 160 to 120 kPa. This is in accordance with earlier measurements [2], in which a small amount of nanofiller has a significant effect on properties. However, very recently it has been reported that exfoliated or intercalated nanoclay can show higher Payne effects because of an additional network formation by the clay platelets with the help of hydrogen bonds [2]. Silanol groups at the edge of each clay particles are interacting with each other and form an additional filler–filler network. However, in this particular case a higher amount of stearic acid was used in the formulation to assist the delamination of the clay.

To explore the curing behavior as a function of the nanoclay loading, the curing characteristics were studied. The results are given in Fig. 4. It is evident from this figure that the curing time decreased with increasing clay content, as did the scorch time. The decrease in curing and scorch time can be explained by the modification of the clay: The modification agent of the clay contains ammonium compounds, and these compounds are well known as accelerators for sulfur vulcanization. Therefore, the ammonium group of the clay modifier might take part in the amine complexation reaction and thus facilitate the curing reaction of NR. A decrease of the maximum torque is observed for increasing nanoclay concentrations: The maximum torque of the compound with 15 phr clay is roughly halfway of the maximum of the compound without clay. The clay used here contained a large amount of long chain quaternary ammonium compounds, and at curing temperature, this compound can act as a plasticizer and result in a decrease of the ultimate torque.

As far as the mechanical properties of these composites are concerned, the modulus values at 300% elongation decreased with clay loading (Fig. 5). It also shows that the final tensile strength decreased slightly with increasing clay loadings. The decrease in strength at higher concentrations is probably caused by insufficient filler dispersion, as also seen in the Mooney viscosity values. As can be observed from XRD some of the clay layers were well separated from each other to form intercalated structure but still there should be some agglomerations of the organo-modified clay. It was reported earlier that modification of clay is necessary but not a sufficient step, particularly when the host matrix is nonpolar NR [20]. The elongation at break followed the same pattern than the tensile strength, and the decrease is again due to the insufficient overall distribution of the organoclay. Looking at the stress–strain properties as a whole, it seems as if the property changes due to the reduction in CB content are partly balanced by the addition of the nanofiller. The nanoclay has a reinforcing effect, as clearly seen from the moduli values in Fig. 5, but in this case it is less than expected from a nanosized material with a high aspect ratio. The hardness of the materials with different nanoclay loadings is also presented in Fig. 5, and there is no significant variation in the hardness level as a function of the filler loading.

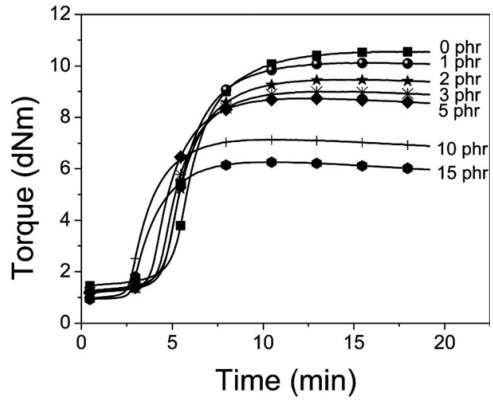

FIG. 4. Curing curves of different NR-CB-clay (QUAT) compounds.

DOI 10.1002/pen

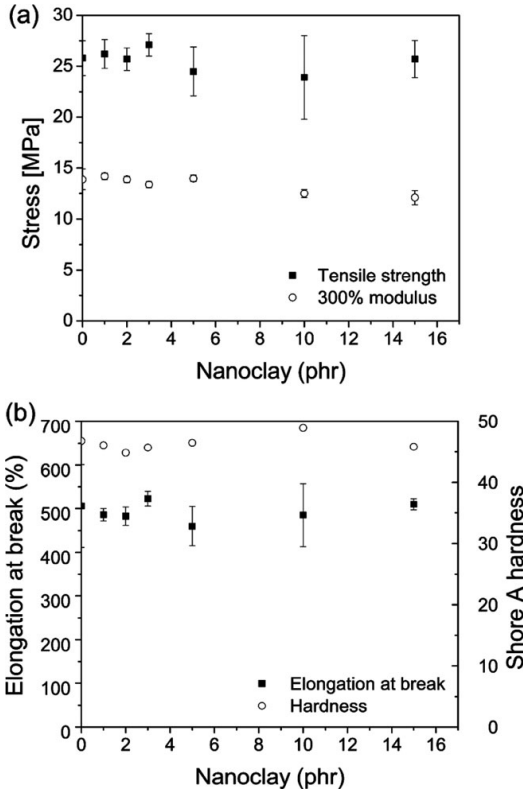

FIG. 5. Mechanical properties of the rubber clay composites obtained from stress–strain experiments (a) tensile strength and modulus at 300% elongation and (b) elongation at break and hardness.

Crosslinking Kinetics and Activation Energy

As reference material for this study, the compound with 50 phr CB was used. Both minimum and maximum torque altered significantly when 10 phr of CB was replaced by clay: Both values are reduced, resulting in a lower ultimate torque (Fig. 6). The temperature sensitivity for all three materials is comparable: at 140°C, the degree of curing is rather stable and plateau type curing curves could be found, while at 160°C, reversion occurs. The presence of clay does not make a difference for this trend. These curves also show clearly the effect of temperature on the thermal stability of the material: The higher the curing temperature, the more pronounced the reversion. Additionally, with increasing temperature, the scorch time as well as the maximum torque reduced.

The basic equation describing the kinetic parameters for rubber curing may be given as: [21]

$$\frac{d\alpha}{dt} = k(T)f(\alpha) \tag{1}$$

where $d\alpha/dt$ is the vulcanization rate, t is the time, K is the specific rate constant at temperature T, and $f(\alpha)$ is the function corresponding to the phenomenological kinetic model.

For vulcanization studies, it is defined as:

$$\propto = \frac{M_t - M_0}{M_\mathrm{h} - M_0} \tag{2}$$

where M_o, M_t, and M_h are torque values at the time zero, at a given time of curing and at the end of crosslinking.

The function $K(T)$ in *Eq. 1* is related to the activation energy by the Arrhenius equation,

$$K(T) = K_0\, \mathrm{e}^{-E_a/RT} \tag{3}$$

$$\ln\, K(T) = \ln\, K_0 + \frac{E_\mathrm{a}}{RT} \tag{4}$$

where K_0 is the pre-exponential factor, E_a is the activation energy, and R is the universal gas constant. By plotting the values of ln $K(T)$ versus $1/T$, the activation energy E_a can be calculated. Combining *Eq. 1* and *Eq. 3*, the following relationship can be obtained:

$$\frac{d\alpha}{dt} = K_0\, \mathrm{e}^{-E_\mathrm{a}/RT} f(\alpha) \tag{5}$$

In curing reactions, the function $f(\alpha)$may get different forms depending upon the reaction mechanism. For the nth order kinetics of the chemical reaction, $f(\alpha)$ is given by Borchardt and Daniels [22] as follows:

$$f(\alpha) = (1-\alpha)^n f(\alpha) = (1-\alpha)^n, \quad n \geq 1 \tag{6}$$

where n is the order of the reaction. However, for a multistep chemical reaction, a more complex reaction model should be used to describe the kinetics. For this purpose, the autocatalytic model given by Sestak–Berggren [23] can be used:

$$f(\alpha) = \alpha^m(1-\alpha)^n, \quad 0 \leq m \leq 1, \quad n \geq 1, \tag{7}$$

and by substituting *Eq. 7* into *Eq. 5*, the following kinetic model can be obtained:

$$\frac{d\alpha}{dt} = K(T)\alpha^m(1-\alpha)^n \tag{8}$$

Figure 7 exhibits the plots of the curing data and rate of conversion ($d\alpha/dt$) versus the degree of conversion (α) of the three different rubber compounds for vulcanization at different temperatures. They show that with an increase in curing temperature, the cure rate increases. The shape of the conversion curve is also dependent on the temperature: For a higher temperature, the maximum conversion rate is reached at higher degrees of conver-

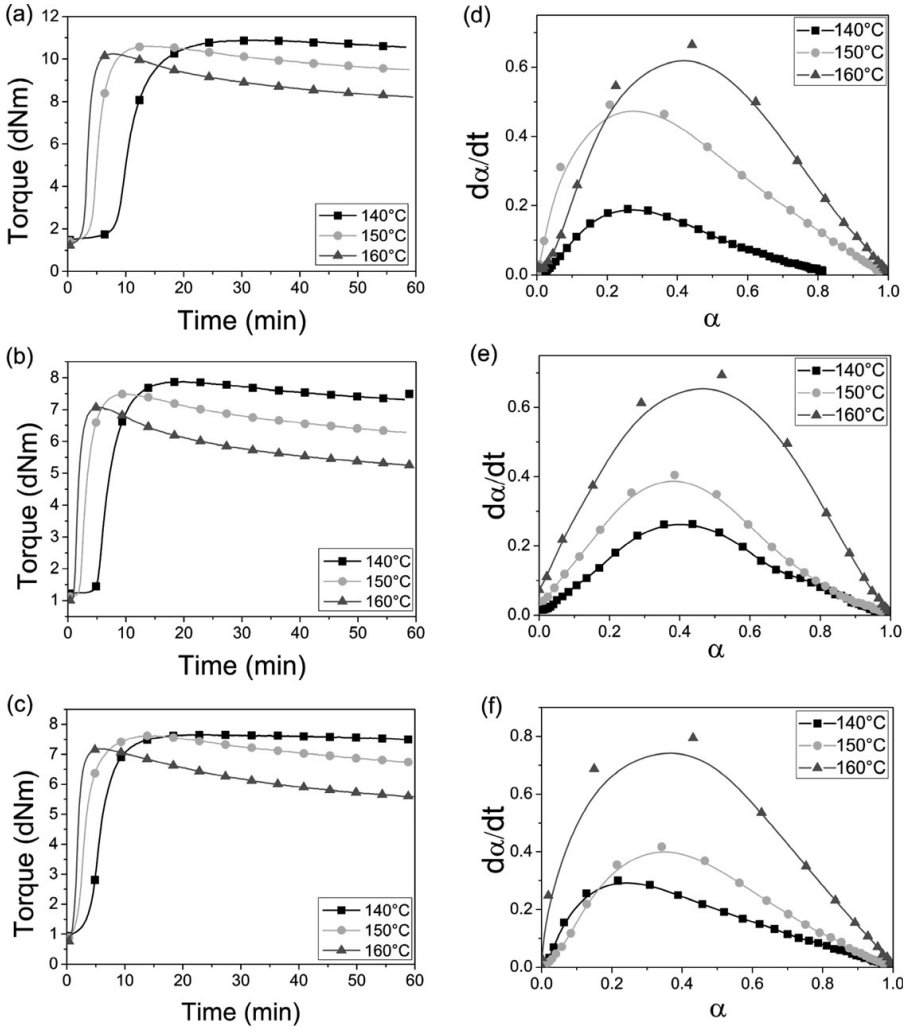

FIG. 6. Rheometric curing curves of rubber compounds at different temperatures (a) NR-CB (50 phr), (b) NR-CB (40 phr)-clay-QUAT (10 phr), and (c) NR-CB (40 phr)-clay-PA (10 phr), and (d–f) are the plots of the conversion rate vs. degree of conversion, respectively.

sion, and the peak height of the conversion rate curve is increased. One explanation for the significantly higher rate of conversion at higher temperatures is the increased mobility of the polymer chains, which makes it easier to form the network by the rather short crosslinks. The maximum conversion is obtained in a rather narrow window at degrees of conversion between 0.2 and 0.4 for all compounds and temperatures. Different kinetic parameters of the vulcanization reaction of the three different rubber compounds were determined from the data given above and are tabulated in Table 3. The values of rate constant (K), and order of reaction m and n are the fitted kinetic parameter obtained from *Eq. 8* and calculated through a nonlinear multiple regression analysis from the experimental data (Fig. 7). Furthermore, an Arrhenius type plot of ln K versus $1/T$ is drawn, from which the activation energy of vulcanization (E_a) can be calculated, as shown in Fig. 8. The lower activation energy is an indication of the ease of the crosslinking process. The slope of the straight line in the plot of ln K versus $1/T$ gives the activation energies for the different compound types.

The activation energy of the different compounds decreased considerably after incorporation of modified clay and the NR-CB-clay-QUAT as compared to that of the NR-CB-clay-PA (see Table 3). So, the quaternary

 DOI 10.1002/pen

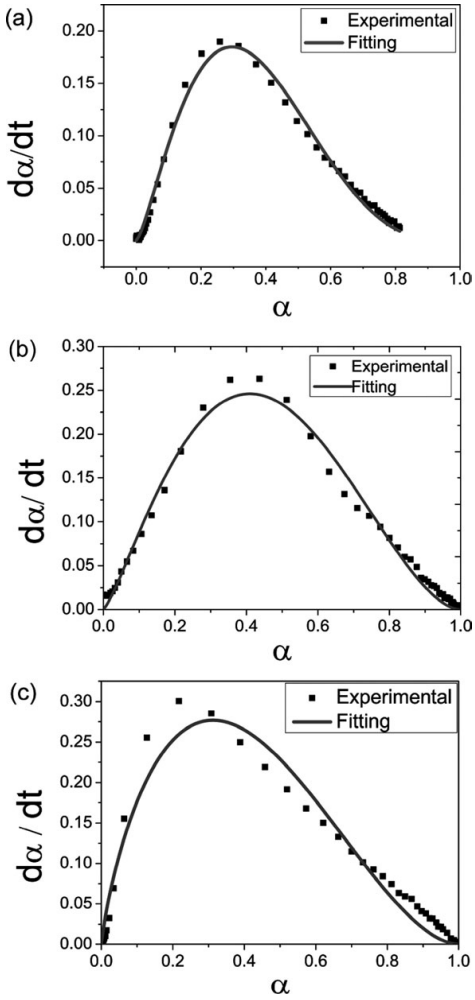

FIG. 7. Rate of conversion ($d\alpha/dt$) versus the degree of conversion (α) of three different rubber compounds at 140°C (a) NR-CB, (b) NR-CB-clay-QUAT, and (c) NR-CB-clay-PA.

ammonium compounds dimethyl-di(hydrogenated tallow) alkyl ammonium salt shows ease of crosslinking as compared to other primary amine modifier.

TABLE 3. Different kinetic parameters and activation energies of the rubber compounds.

Temperature (°C)	NR-CB			NR-CB-clay-QUAT			NR-CB-clay-PA		
	140	150	160	140	150	160	140	150	160
K (1/sec)	3.23	3.18	5.00	2.03	3.05	3.30	1.42	1.97	2.54
M	1.39	1.19	1.26	1.27	1.17	1.00	0.82	0.68	0.57
N	3.32	1.94	1.68	1.84	1.99	1.27	1.81	1.66	1.26
E_a (kJ/mol)		67			52			54	

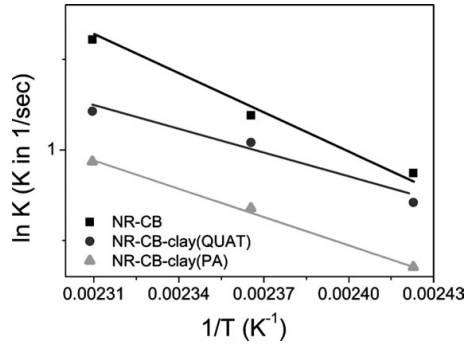

FIG. 8. Arrhenius type plot of ln K versus $1/T$ for the calculation of the activation energy.

CONCLUSIONS

The dynamic mechanical analysis in a strain sweep measurement of the rubber compounds showed that the layered clay induced dispersion of CB. Mooney viscosity results showed that the replacement of CB with modified nanoclay can help in dispersion of the fillers. Strong interactions between CB, nanoclay, and NR matrix were found. The partial replacement of CB with nanoclay influences the curing behavior substantially, and the addition of clay significantly decreases the activation energy of the networking process. This indicates that the crosslinking reaction is initiated and proceeds easier in the presence of clay as filler. Further investigation is necessary for understanding the kinetics of curing reaction in presence of organically modified clay-CB hybrid filler system in rubber compounds at a broader temperature window.

REFERENCES

1. A. Das, K.W. Stöckelhuber, D-Y Wang, R Jurk, J Fritzsche, H Lorenz, M Klüppel, and G Heinrich, *Adv. Polym. Sci*., **239**, 85 (2011).
2. A. Das, K.W. Stöckelhuber, S. Rooj, D.-Y. Wang, and G. Heinrich, *Kautsch. Gummi Kunstst*., **63**, 296 (2010).
3. A. Das, R. Jurk, K.W. Stöckelhuber, T. Engelhardt, J. Fritzsche, M. Klüppel, and G. Heinrich, *J. Macromol. Sci. A: Pure Appl. Chem*., **45**, 144 (2008).
4. A. Das, R. Jurk, K.W. Stöckelhuber, and G. Heinrich, *eXPRESS Polym. Lett*., **11**, 717 (2007).
5. A. Das, K.W. Stöckelhuber, P.S. Majumder, T. Engelhardt, J. Fritzsche, M. Klüppel, and G. Heinrich, *J. Macromol. Sci. A: Pure Appl. Chem*., **7**, 46 (2009).
6. A. Das, F.R. Costa, U. Wagenknecht, and G. Heinrich, *Eur. Polym. J*., **44** 3456 (2008).
7. A. Das, K.W. Stöckelhuber, R. Jurk, D. Jehnichen, and G. Heinrich, *Appl. Clay Sci*., **51**, 117 (2011).
8. A. El Labban, P. Mousseau, R. Deterre, and J.L. Bailleul, *Rubber Chem. Technol*., **83**, 331 (2010).
9. J.U. Iyasele and F.E. Okieimen, *J. Chem. Soc. Nigeria*, **33**, 162 (2008).

10. N. Makul and P. Rattanadecho, *Int. Commun. Heat Mass Trans.*, **37**, 914 (2010).
11. M.A. Kader and C. Nah, *Polymer*, **45**, 2237 (2004).
12. E.E. Ehabe and S.A. Farid, *Eur. Polym. J.*, **37**, 329 (2001).
13. D. Choi, M.A. Kader, B.H. Cho, Y.-I. Huh, and C. Nah, *J. Appl. Polym. Sci.*, **98**, 1688 (2005).
14. Q. Liu, W.T. Ren, Y. Zhang, Y. Zhang, *J. Appl. Polym. Sci.*, **123**, 3128 (2012).
15. A. Usuki, A. Tukigase, and M. Kato *Polymer*, **43**, 2185 (2002).
16. K.G. Gatos, N.S. Sawanis, A.A. Apostolov, R. Thomann, and J. Karger-Kocsis, *Macromol. Mater. Eng.*, **289**, 1079 (2004).
17. C. Albano, M. Hernandez, M.N. Ichazo, J. Gonzalez, and W. DeSousa, *Polym. Bull.*, **67**, 653 (2011).
18. F. Avalos, J.C. Ortiz, R. Zitzumbo, M.A. Lopez-Manchado, R. Verdejo, and M. Arroyo, *Eur. Polym. J.*, **44**, 3108 (2008).
19. M.A. Lopez-Manchado, M. Arroyo, B. Herrero, and J. Biagiotti, *J. Appl. Polym. Sci.*, **89**, 1 (2003).
20. S. Rooj, A. Das, K.W. Stöckelhuber, U. Reuter, and G. Heinrich, *Macromol. Mater. Eng.*, **297**, 369 (2012).
21. S. Montserrat and J. Málek, *Thermochim. Acta*, **47**, 228 (1993).
22. H.J. Borchardt and F.J. Daniels, *J. Am. Chem. Soc.*, **41**, 79 (1956).
23. J. Sestak and G. Berggren, *Thermochim. Acta*, **3**, 1 (1971).

 DOI 10.1002/pen

Publication III

Minna Poikelispää, Amit Das, Wilma Dierkes, Jyrki Vuorinen

Synergistic effect of plasma modified halloysite nanotubes and carbon black in natural rubber - butadiene rubber blend

Journal of Applied Polymer Science, 127 (2013) 4688-4696

Journal of Applied Polymer Science

Synergistic Effect of Plasma-Modified Halloysite Nanotubes and Carbon Black in Natural Rubber—Butadiene Rubber Blend

Minna Poikelispää,[1] Amit Das,[1,2] Wilma Dierkes,[1,3] Jyrki Vuorinen[1]

[1]Plastics and Elastomer Technology, Department of Materials Science, Tampere University of Technology, P.O. Box 589, FI-33101 Tampere, Finland

[2]Composite Materials, Leipniz Institute of Polymer Research Dresden, D-01069, Germany

[3]Elastomer Technology and Engineering, University of Twente, NL-7522 AE Enschede, The Netherlands

Correspondence to: M. Poikelispää (E-mail: minna.poikelispaa@tut.fi)

ABSTRACT: Halloysite nanotubes (HNTs) were investigated concerning their suitability for rubber reinforcement. As they have geometrical similarity with carbon nanotubes, they were expected to impart a significant reinforcement effect on the rubber compounds but the dispersion of the nanofillers is difficult. In this work, HNTs were surface-modified by plasma polymerization to change their surface polarity and chemistry and used in a natural rubber/butadiene rubber blend in the presence of carbon black. The aim of the treatment was to improve the rubber–filler interaction and the dispersion of the fillers. A thiophene modification of HNTs improved stress–strain properties more than a pyrrole treatment. The surface modification resulted in a higher bound rubber content and lower Payne effect indicating better filler–polymer interaction. Scanning electron microscopy measurements showed an increased compatibility of elastomers and fillers. As visualized by transmission electron microscopy, the thiophene-modified HNTs formed a special type of clusters with carbon black particles, which was ultimately reflected in the final mechanical properties of the nanocomposites. The addition of HNTs increased loss angle. © 2012 Wiley Periodicals, Inc. J. Appl. Polym. Sci. 000: 000–000, 2012

KEYWORDS: plasma polymerization; polymer–filler interactions; nanocomposites; halloysite

Received 11 January 2012; accepted 17 May 2012; published online
DOI: 10.1002/app.38080

INTRODUCTION

Carbon black and silica are conventionally used fillers in rubbers. Their primary particles have dimensions in the nanometer range, and structural reinforcing units have dimensions of a few hundreds of nanometers. In the last decade, in which nanotechnology has been developed and implemented, nanofillers have extensively been investigated as fillers for polymers. They have been found to carry many benefits compared to conventional fillers: They have been reported to, for example, reduce viscosity and increase tensile strength, hardness, modulus, abrasion resistance, electrical conductivity as well as chemical resistance.[1–11] Nanoclays are widely studied materials used with rubbers. Typically, they are layered silicates, and usually phyllosilicates such as montmorillonite, hectorite, and saponite are used.

Recent studies[1,2,12–14] have focused on halloysite nanotubes (HNTs), which are 1 : 1 alumosilicates, a naturally occurring clay mineral with the empirical formula $Al_2Si_2O_5(OH)_4{\cdot}2H_2O$. HNTs have a double layered crystalline structure. There are Si—O groups on the surface of the outer layer and $Al(OH)_3$-groups on the inner side and edges of the tube.[13] The OH-groups have interparticle affinity which complicates dispersion of clay materials, but the filler–filler interactions are lower with HNTs than with layered silicates.[13] Furthermore, HNTs do not require exfoliation. Because of the tubular form, HNTs have a higher aspect ratio than other clay materials. The aspect ratio of HNT can vary between 10 and 130 depending on the dimensions of the tubes. The high aspect ratio and surface area of HNTs is expected to result in a special reinforcing effect on the polymer matrix.

Conventional fillers are generally processed by direct incorporation into the rubber matrix, eventually with the help of a coupling agent. The incorporation of nanofillers is more challenging, and it is difficult to achieve a good dispersion by direct incorporation. Therefore, a successful application of nanofillers depends mainly on a good dispersion of the fillers.

Besides dispersion, the interaction between rather hydrophobic polymers and hydrophilic fillers cause a challenge. The compatibility can be improved by changing the polarity of the fillers. Different kinds of coupling agents, such as silanes, are typically used to change the surface properties of the fillers. The coupling agents

Table I. Formulation of NR/BR Compounds and Mixing Procedure

Ingredients	Type/producer	Amount (phr)	Mixing (min)
NR	SMR10	80	0
BR	Buna-cis-132/ Dow Chemical Company	20	
Nanofiller		0/2.5	1
N-234	Evonik	42.5/40.0	1.5
6PPD	Lanxess	2.0	
TMQ	Lanxess	1.0	
ZnO	Grillo Zinkoxid GmbH	5.0	
TDAE-oil	Vivatec 500/ Hansen & Rosenthal GmbH	8.0	2
Stearic acid	Oleon N.V	2.0	
Ceresine wax	Statoil Wax GmbH	1.5	Mixing: 4
CBS	Lanxess	1.5	Mill: 5
Sulfur	Solvay Barium Strontium GmbH	1.5	

N-234: Carbon black.
6PPD: N-(1,3-dimethylbutyl)-N′-phenyl-1,4-Benzenediamine.
TMQ: 2,2,4-trimethyl-1,2-dihydroquinoline.
TDAE-oil: treated distillate aromatic extract oil.
CBS: N-Cyclohexyl-2-Benzothiazolesulfenamide.

are typically added to the blend during mixing. The reaction between the coupling agent and the filler requires a certain temperature and time for the silanization reaction to be completed.

An alternative could be a pretreatment of the filler by plasma treatment. Silica has been successfully modified by plasma polymerization treatments.[15–19] HNTs have a comparable surface chemistry to silica; therefore, it is expected that the surface of HNTs can also be modified by plasma polymerization. By choosing the appropriate monomer, the following effects can be expected:

- The polarity of the HNT surface can be reduced.
- The functional groups on the surface, mainly hydroxyl groups, can be shielded.
- The chemical composition of the surface can be changed to hydrocarbons.
- Functional groups can be created in the surface.

The creation of functional groups which can react with the polymer during curing might result in interpenetrating networks: Besides the polymer–polymer network, a strong covalent filler–polymer network can be build up during vulcanization. Furthermore, the sulfur and nitrogen moieties in the plasma polymers can contribute to the crosslinking reaction. This will influence the properties of the final material.

In the plasma polymerization process, the plasma is generated by electric discharge. With the help of plasma energy, the monomer gases, which continuously float into the reactor, are activated and form electrons, ions, and radicals. They are able to polymerize and form a deposit on the surface of the filler. This surface coating consists of a two-dimensional network of the monomer in question, it is very adherent and it preserves the structural characteristics of the nanotubes.

In this work, HNTs were surface-modified by plasma polymerized pyrrole and thiophene. The effect of the surface coating on surface polarity and chemistry was investigated, as well as the effect of this filler on the rubber properties.

EXPERIMENTAL

Materials

HNTs were delivered by Sigma–Aldrich. The diameter of the nanotubes was 30–70 nm and the length varied between 1 and 4 μm. The specific surface area of these tubes was 65 m^2/g. Pyrrole (py) and thiophene (thi), both from Sigma–Aldrich, were used as monomers in the plasma polymerization process. The other materials used are presented in Table I.

Plasma Treatment

The plasma polymerization was performed in a tubular vertical reactor. It consists of a round flask made from Pyrex glass, which is connected to the vacuum pump (Duo Seal, model number 1402 B from Welch vacuum), and a long cylindrical tube which is surrounded by a copper coil. The coil is connected to a radiofrequency generator from MKS/ENI, type ACG-3B-01. At the top of the tube, there are ports for the inlet of monomers and the connection of pressure gauge (MKS Baratron® type 627B). No carrying gas was used in the modification process. Stirring of the powder was done by a magnetic stirrer. About 20 g of HNTs were placed into the flask where they were treated with the activated monomers. The parameters of the plasma treatment of the different batches are presented in Table II.

Table II. Parameters of Plasma Treatment

Monomer	Initial pressure[a] (Pa)	Monomer pressure[b] (Pa)	Power (W)	Time (min)
Pyrrole (Py90)	10	22	150	90
Thiophene (Thi90)	10	40	150	90

[a]Pressure in the reactor before monomer is applied.
[b]Monomer inlet pressure.

Characterization of the Treated Fillers

The deposition of the plasma coating was quantified by thermogravimetric analysis in a Perkin-Elmer STA 6000 thermogravimetric analysis (TGA). The heating temperature changed from 25°C to 995°C and the heating rate was 20°C/min; a nitrogen atmosphere was used. The total weight loss within this temperature window was taken into consideration.

Changes in surface polarity were studied by an immersion test. The test was done by pouring a small amount of filler onto the surface of a solvent; in this case, water was used. The original HNTs sink immediately due to their hydrophilic surface, whereas the treated fillers should float longer as they are less hydrophilic. More quantitative measurements were made by a water penetration test. In this test, 0.02 g of filler was placed into a glass column and the opening was sealed with two layers of a hydrophobic filter (pore size 0.2 μm). The column was placed in water and the change in weight due to absorption of water was measured over time.

Preparation of Nanocomposites

Natural rubber (NR), butadiene rubber (BR), nanofillers, and other ingredients presented in Table I were mixed in a Krupp Elastomertechnik GK 1.5 E intermeshing mixer (50°C, 70 rpm). Then, *N*-cyclohexyl-2-benzothiazolesulfenamide (CBS) and sulfur were added on an open two-roll mixing mill. In the reference compound, only carbon black (CB) was used as filler in a concentration of 42.5 phr. In the HNTs containing compounds, 2.5 phr of CB was replaced by the same amount of HNTs. The total mixing time was nearly 15 min.

The Mooney viscosity of the compounded material was measured in a MV 2000 Mooney Viscometer from Alpha Technologies. The measurement included 1 min heating time and 4 min measuring time at 100°C. Curing studies and Payne effect measurements were performed using an Advanced Polymer Analyzer 2000 from Alpha Technologies. Curing studies were carried out at 160°C for 60 min and 193°C for 30 min. The compounds were vulcanized at their respective curing time at 160°C. The Payne effect was studied in a strain sweep from 0.28 to 100% at 100°C.

Swelling behavior was studied by soaking vulcanized circular test pieces in toluene until equilibrium swelling (72 h). The diameter of the test pieces was 12 mm and thickness 2 mm. The swelling degree Q of the rubber was calculated by the equation:

$$Q = \frac{W_t - W_0}{W_0}$$

W_0 is the initial weight of sample and W_t is the weight at time t.

Tensile tests of the samples were performed with a Messphysik Midi 10–20 universal tester according to ISO 37. Dynamic properties were studied with a GABO Eplexor 2000N, operating in tension mode. The vulcanized sheet with a thickness of 2 mm was cut into rectangles of 35 × 10 mm^2. Storage modulus (E'), loss modulus (E''), and loss tangent (tan δ) were recorded at a heating rate 10°C/min from −80 to +80°C. The frequency used in these measurements was 10 Hz with a dynamic load at 0.5% strain and static load at 1% strain, which was kept constant through the measurement.

Bound rubber (BDR) measurements were performed by dissolving 0.2 g of uncured rubber in toluene for 96 h. Toluene was exchanged every 24 h. After 96 h, the samples were dried and weighed. The BDR content was calculated by the formula:

$$\mathrm{BDR}\% = \frac{m_0 - (m_2 - m_3)}{m_0} \times 100$$

with

$$m_0 = m_s \times \frac{100}{\mathrm{cpd}}$$

where m_0 is the weight of the rubber content in the sample, m_2 is the combined weight of the bag and sample, m_3 is the weight of the dried bag and sample, m_s is the weight of the dry sample and cpd is the total amount of rubber and filler in the compound in phr.[20]

The state of dispersion of the HNT particles in the NR/BR nanocomposites was investigated by scanning electron microscopy (SEM) using a Philips XL-30, and by transmission electron microscopy (TEM) using a JEM 2010 model. Cross-section samples were used for the SEM measurements. For TEM samples, the ultrathin section of the samples was cut by an ultramicrotome (Leica Ultracut UCT) at −100°C with a thickness of ~ 80–100 nm. Because of the very low amount of halloysites compared to CB, it was very difficult to locate the halloysite particles. Both fillers showed the same contrast in bright field images, only the shape of the two fillers was different. Hence, for detection of the HNTs, TEM investigations were performed at an energy loss of 0 eV (= bright field image) and 180 eV for each region. By comparing the two images, it was possible to distinguish between CB and HNT.

RESULTS AND DISCUSSION

Filler Characterization

To check the changes in hydrophobicity, the water immersion test was performed: As expected, the untreated HNT powder sank in water immediately; after treatment, a part of the material floated on water for a certain period. This proves the reduction in polarity of the HNTs after plasma treatment, although it also indicates an inhomogeneous coating, which could be caused by filler aggregates in the reactor during the plasma treatment. The water absorption results are presented in Figure 1. Pure HNTs as well as pyrrole- and thiophene-coated HNTs absorbed water over time and after a certain period an equilibrium level was attained. However, pure HNTs absorbed more water than plasma-treated HNTs, indicating a more hydrophobic nature of plasma-treated HNTs. In earlier studies with plasma-treated silica, such a reduction in water absorption was also observed, but the effect was a lot stronger.[15] This preliminary investigation indicated that pyrrole- and thiophene-coated HNTs are more hydrophobic and less polar than the untreated

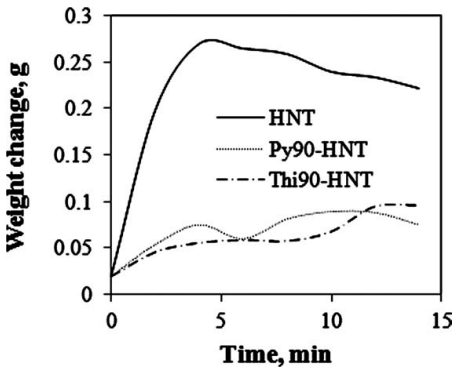

Figure 1. Water absorption of the plasma-coated HNTs.

filler, and they could be more compatible with a nonpolar rubber matrix.

The TGA curves of untreated, pyrrole and thiophene polymerized HNTs are shown in Figure 2. The difference in weight loss between treated and untreated fillers at the final temperature of 995°C is the amount of the plasma-polymerized film on the surface of the filler. The decomposition of the pyrrole and thiophene start around 200°C. In this area, the difference in the TGA curves can be observed. According to repeated measurements, HNTs treated with pyrrole had 0.7 wt % coating on average, whereas HNTs treated with thiophene had 1.0 wt % coating on average.

Mooney Viscosity and Curing Studies

The Mooney viscosities of the composites with the different types of fillers were determined. The composites showed a substantial increase in viscosity for the composite containing pyrrole-coated HNTs (Figure 3). The viscosity of the compound with the thiophene-treated HNTs was slightly lower, but still higher than the viscosity of the compound with untreated HNTs and without any HNTs. Untreated HNTs did not affect the viscosity at all. The increase in viscosity is due to enhanced

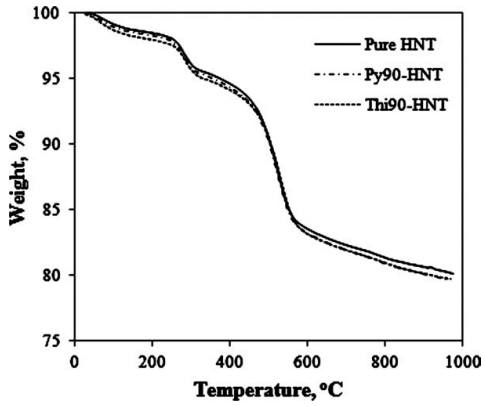

Figure 2. Thermogravimetric analysis of the plasma-coated HNTs.

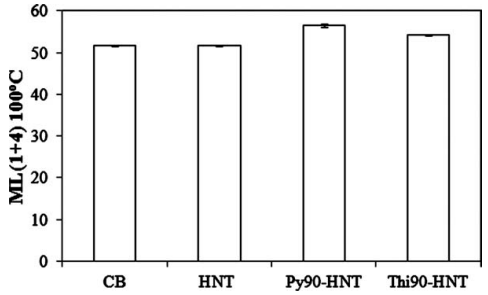

Figure 3. Mooney viscosity of the NR/BR compounds.

polymer–filler interactions, as plasma-modified HNTs interact with the elastomer chains more firmly and increase the reinforcement.

The rheograms taken at 160°C are presented in Figure 4(a). It is interesting to note that both, compounds with plasma-treated HNTs, showed a plateau in the cure curve, whereas carbon black and pure HNT-filled compounds showed a decrease in the torque values after the optimum curing time. Reversion is a well-known phenomenon for sulfur-cured diene rubbers, especially when cured at higher temperatures, and this ultimately affects properties and performance of the material. Here, the plasma-coated HNTs seem to stabilize the network and suppress the reversion; they act as antireversion agents in the rubber compound. At the same time, the maximum rheometric torque increases with the addition of both types of plasma-coated HNTs, and it is higher for the compound containing plasma-pyrrole-treated HNTs than for the compound containing thiophene-treated HNTs. The increase in torque may be due to crosslinking density. To see if the extent of curing or the degree of crosslinking were influenced by the modifier of the HNTs swelling degree was calculated. The swelling data (Table III) indicates that the extent of overall crosslinking was marginally higher for all HNT-filled samples compared with carbon black sample. Thus, HNTs are giving more rubber–filler interactions as a result of improvement of total crosslinking density coming from chemical and physical crosslinking of the rubber chains. A minor effect can be found if the HNTs are modified by plasma coating.

As can be seen from Figure 4(b), at high temperature (193°C), the reversion can be observed for all compounds in this case, but the extent to which it occurs is much lower for compounds with plasma-treated HNTs than for compounds with untreated HNTs or CB. The plasma polymers seem to either result in a more stable network or it prevents rearrangement of the crosslinks at higher temperatures.

At both temperatures, the cure curves for the CB and CB/HNT-filled compounds are almost similar, indicating that the addition of untreated HNTs has only a minor influence in the curing characteristics in practice even if the cure rate index presented in Table III is higher for the compound containing untreated HNTs.

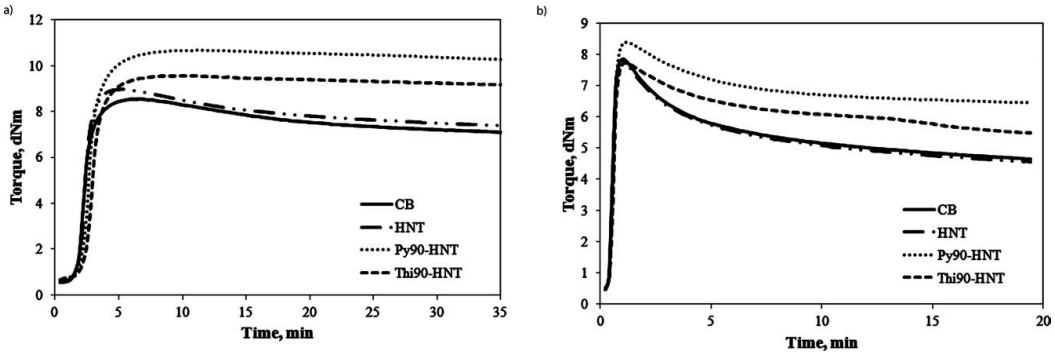

Figure 4. Development of the torque values of the NR/BR compounds filled with carbon black and HNTs measured at (a) 160°C and (b) 193°C.

Morphology

To visualize the dispersion of the HNTs in the rubber matrix, the morphology of the materials was investigated by SEM and TEM. The image of pristine HNTs is shown in Figure 5(a), showing the tube-like dimension and the agglomerated nature of the tubes. Owing to the high surface area of these very small particles, the tubes itself remain aggregated. In Figure 5(b), both carbon black as well as the relatively smaller unmodified HNT particles are clearly visible. The carbon black particles form a spherical aggregated structure, whereas the unmodified HNTs are homogenously dispersed through the rubber matrix. It is interesting to note in Figure 5(c,d) that in the presence of modified HNTs, the aggregated structure of CB becomes smaller compared to Figure 5(b). These investigations indicate that the compatibility between the two elastomers and carbon black is facilitated by modified HNT. The plasma polymer coatings reduce the hydrophilic character of the filler surface making it more compatible with the polymers and their chemical structure resembles the chemical structure of the polymers and also increase the compatibility to carbon black due to the presence of carbon–carbon double bonds which are also present on the carbon black surfaces. Very similar observations were also reported for plasma-modified silica as filler in elastomer blends: a remarkable improvement of the dispersion of the silica and filler polymer interaction was found.[15] However, this work was based on a 100% replacement of pristine silica by the plasma-treated filler. The results of this investigation show that it might be sufficient to add a small percentage of surface-modified filler. Another proof of this compatibilization effect is the Payne effect, which is reduced by the addition of HNTs. The Payne effect is the decrease of the storage modulus G' with increasing strain, as the interparticle forces between the filler particles are effective only over small distances between them. The higher the interparticle forces, the higher the Payne effect. In general, the value of the storage modulus remains unchanged with strain for an unfilled system, whereas for a filled system, a significant decrease can be observed. This nonlinear behavior was also observed in this study. Figure 6 illustrates the strain dependency of the storage modulus of the filled NR/BR matrix measured at 100°C. It can be observed that at very low strain amplitude ranges the value of G' remains constant up to a certain strain, and then the values decrease with further increase of strain. The CB-filled NR/BR have the highest Payne effect indicating the strongest filler–filler network. When 2.5 phr CB is replaced by 2.5 phr HNTs, the filler–filler interactions become weaker and the dispersion of the main filler is improved as a consequence of better rubber–filler compatibility. The fact that the thiophene-treated HNTs have a higher Payne effect than the other two HNT-containing samples might be caused by a HNT–CB interaction due to the peculiar coating on the HNT surface. Moreover, the plasma-modified HNT particles show a good dispersion in the rubber matrix, whereas the untreated HNTs are preferably located at the interface between the continuous and discontinuous phases.

Figure 7 shows TEM images of the composites. It is observed from Figure 7(a), that the unmodified HNTs remain as agglomerations in the matrix, whereas the modified HNTs are found to be well dispersed up to the level of single particles [Figure 7(b,c)]. The high surface polarity of the HNT particles favors their tendency to remain in the agglomerated form due to a significant contribution of filler–filler interactions together with the lack of interactions between the filler and the elastomer

Table III. Curing Characteristics Measured at 160°C and Swelling Degree of Nr/Br Compounds

	CB	HNT	Py90-HNT	Thi90-HNT
Scorch time T_{s2} (min)	2.1	2.2	2.3	2.5
Optimum curing time T_{90} (min)	3.5	3.4	4.3	4.2
Cure rate index (min^{-1})	71	83	50	59
Swelling degree	1.70 ± 0.05	1.62 ± 0.02	1.58 ± 0.04	1.61 ± 0.03

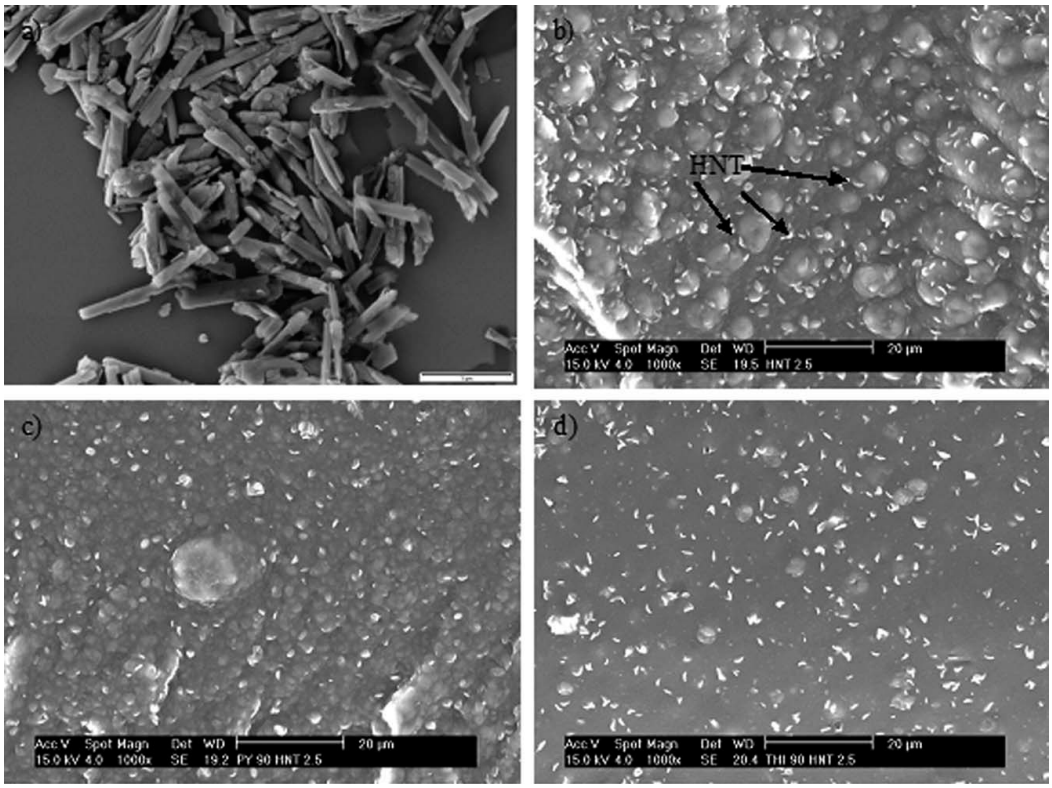

Figure 5. Scanning electron microscopic images of (a) pristine HNTs, and NR/BR compounds filled with carbon black and, (b) untreated, (c) pyrrole-modified and (d) thiophene-modified HNTs.

matrix. The plasma modification with pyrrole and thiophene leads to a decrease of the surface polarity and improves the dispersion of the HNTs. However, the HNT particles in the rubber matrix are found to be smaller in length as compared to the pristine particles shown in Figure 5(a): They are most probably ruptured during shear mixing and thus transformed into smaller particles. This reduces the aspect ratio and might result in a lower reinforcing activity. The breakage of the nanotubes is expected to result in easier dispersion of this filler but it is not influencing the filler–polymer interaction, as this is a surface effect and not depending on the shape and size of the particles.

Bound Rubber

The BDR value describes the amount of polymer which is physically or chemically bound to the filler. Figure 8 shows the BDR content values of compounds with untreated and plasma-modified HNTs. The compounds with plasma-pyrrole treated HNTs show the highest BDR content. This indicates a stronger polymer–filler interaction for the compounds including plasma-treated HNTs.

Mechanical Properties

Stress–strain measurements of the NR/BR composites were performed to investigate the effect of the plasma-modified HNTs on the physical properties. It is evident from Table IV, that incorporation of pyrrole-modified HNTs into the NR/BR matrix increased the 100% modulus by 13% and the 300% modulus by

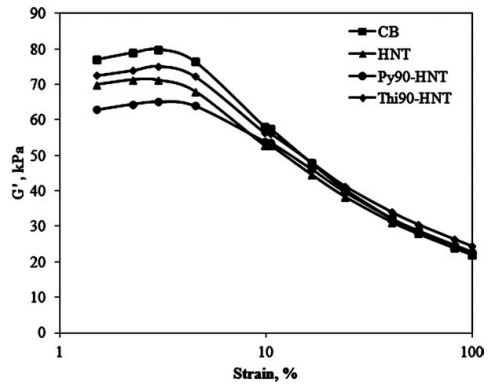

Figure 6. Strain dependence of the storage modulus G' at 100°C for carbon black and HNT filled rubber.

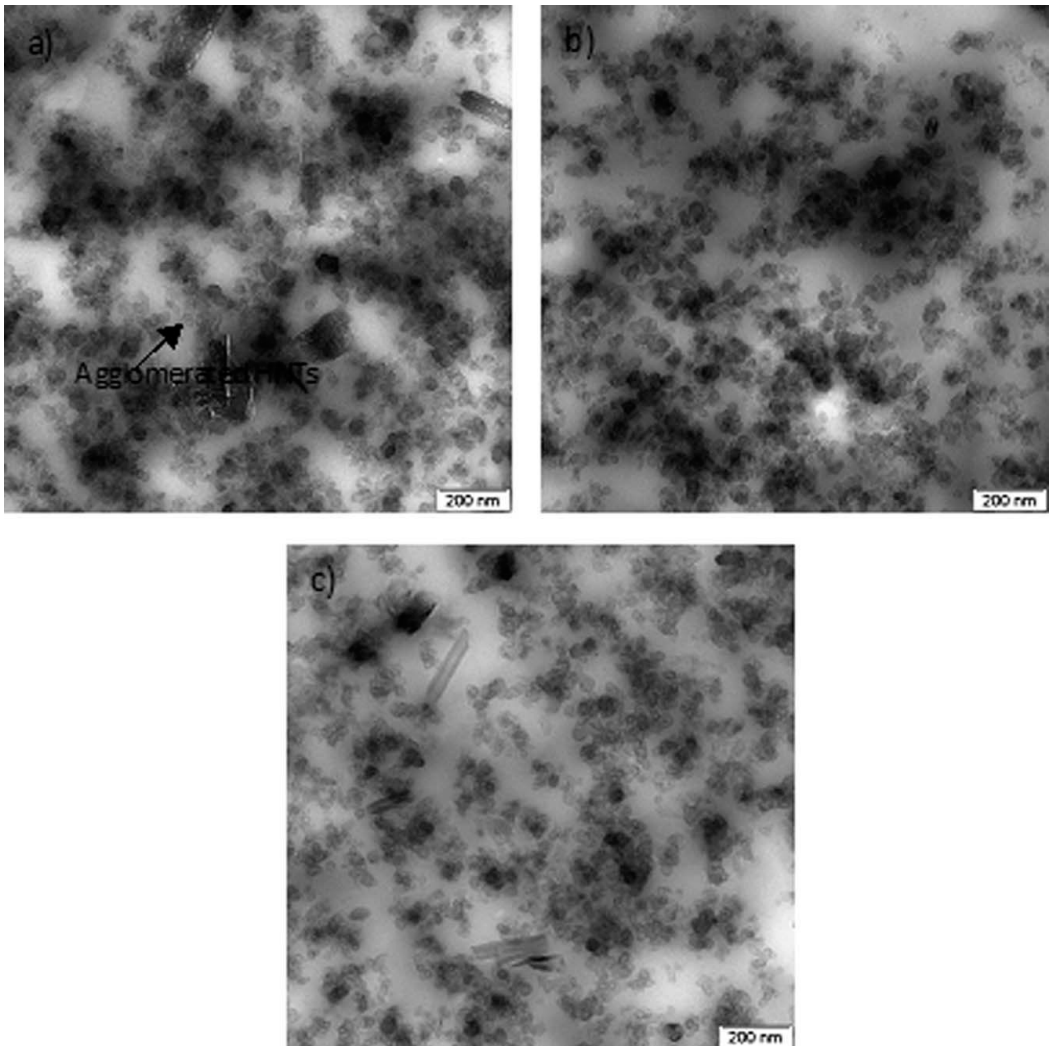

Figure 7. Transmission electron microscopic images of NR/BR filled with carbon black and (a) untreated HNTs, (b) pyrrole-modified HNTs, and (c) thiophene-modified HNTs.

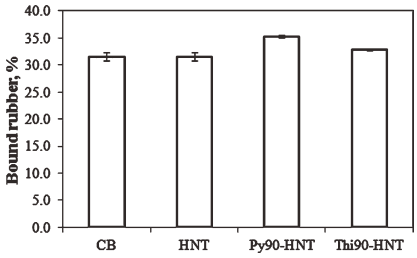

Figure 8. BDR content of the NR/BR compounds filled with carbon black and HNTs.

Table IV. Physical Properties of Carbon Black and HNT-Filled Rubber

Sample	Tensile strength (MPa)	Elongation (%)	100% Modulus (MPa)	300% Modulus (MPa)
CB	20.6	443	2.5	12.1
HNT	19.7	380	2.7	12.8
Py90-HNT	21.7	410	2.8	13.5
Thi90-HNT	23.0	445	2.6	13.0

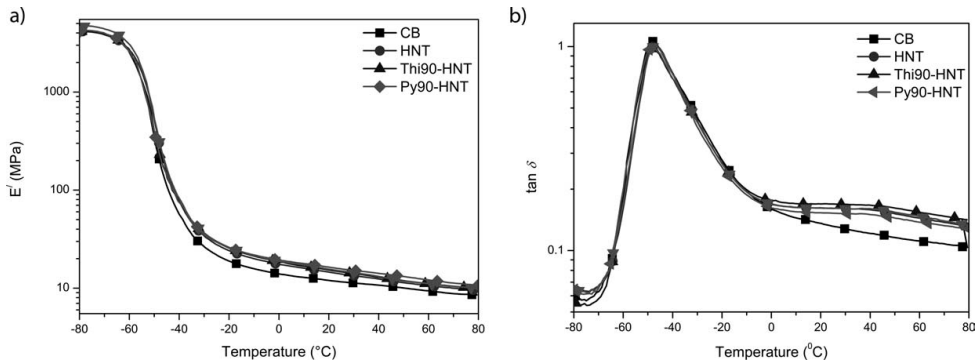

Figure 9. Temperature dependence of the (a) storage modulus (E') and (b) loss tangent (tan δ) of the crosslinked rubber.

12%, whereas the thiophene modification resulted in an increase of 5 and 7%, respectively. It is important to keep in mind that the total amount of filler on a weight-basis in all cases was kept constant at 42.5 phr. As the modulus is directly related to the volume fraction of the fillers, a lower volume fraction of the total amount of the fillers in the hybrid filler system would lead to inferior moduli value, particularly, when there is a considerable difference in density. In terms of tensile strength, the highest value was found when thiophene-modified HNTs were introduced together with the carbon black. This compound also showed the highest elongation at break value. This is an effect of the sulfur moieties on the surface of the HNTs, which enables them to crosslink with the polymer and form interpenetrating networks.

Figure 9 shows dynamic mechanical analysis (DMA) plots of the E' and tan δ values for the vulcanizates. As reference, the pure carbon black compound is also shown. From these measurements, it becomes clear that all HNT containing vulcanizates show higher storage moduli in the whole temperature region as compared to vulcanizates filled with 42.5 phr carbon black. It shows that the replacement of 2.5 phr of carbon black by modified HNTs enhances the rubber–filler interaction and that the material becomes less elastic. This observation also corroborates with the stress–strain data as discussed previously. At lower temperatures, a peak in the loss tangent appears around −48°C, which is the glass transition temperature of the rubber. As the position of the peak does not change, the addition of HNTs do not affect the glass transition temperature of the rubber matrix. Interestingly, at higher temperatures, an additional broad relaxation phenomenon is observed when the elastomer is filled with both, modified and unmodified HNTs. A higher tan δ in the temperature range just above 0°C is an indication for a better wet grip when used as tire tread material.[21] However, the tan δ at a temperature around 60°C is also higher compared to the carbon black filled material, and that indicates a higher rolling resistance. These differences in the loss modulus are a consequence of changes in the interaction between elastomer chains and fillers, as well as the morphology of the material. The addition of HNTs results in increased energy dissipation under these circumstances.

CONCLUSIONS

This study focused on the potential of surface modification of HNTs by plasma polymerization to overcome filler–filler interactions and to establish rubber–filler interactions.

HNTs can be surface coated by a plasma polymer film based on pyrrole or thiophene as monomers. This modification reduces the polarity of the filler and improves the compatibility of the system. As a consequence, agglomeration of HNT particles is hindered and dispersion in the polymer matrix is improved. The extent, to which the dispersion can be improved, depends on the monomer which is chosen for the plasma polymerization process.

The partial replacement of carbon black by modified HNTs influences the curing characteristics of the compound; it reduces reversion over a wide temperature range. Mechanical properties of the composite material are improved by the plasma treatment, with the polythiophene coating having the most effect due to the sulfur moieties on the surface of the HNTs, which can promote sulfur bridge to the rubber molecules. These improvements in rheological and mechanical properties clearly demonstrate the potential of HNTs with a tailored surface chemistry. In terms of dynamic properties, the addition of HNTs results in higher values of the loss angle, which means more energy dissipation. This is an indication for better wet skid resistance, however, at the same time for a higher rolling resistance.

ACKNOWLEDGMENTS

This work has been supported by the Finnish Funding Agency for Technology and Innovation (TEKES Grant No 40352/08). The authors thank S. Pohjonen and T. Lehtinen from the Tampere University of Technology for their technical help. We are also thankful to R. Boldt, Leibniz-Institute for Polymer Research, Dresden, for the TEM images. We are also thankful to Department of Elastomer

Technology and Engineering, University of Twente for allowing using their plasma reactor.

REFERENCES

1. Rooj, S.; Das, A.; Heinrich, G. *Eur. Polym. J.* **2011,** *47*, 1746.
2. Rooj, S.; Das, A.; Thakur, V.; Mahaling, R. N.; Bhowmick, A. K.; Heinrich, G. *Mater. Des.* **2010,** *31*, 2151.
3. Subramaniam, K.; Das, A.; Heinrich, G. *Comp. Sci. Technol.* **2011,** *71*, 1441.
4. Das, A.; Wang, D.-Y.; Leuteritz, A.; Subramaniam, K.; Greenwell, H. C.; Wagenknecht, U.; Heinrich, G. *J. Mater. Chem.* **2011,** *21*, 7194.
5. Das, A.; Stöckelhuber, K. W.; Wang, D.-Y.; Jurk, R.; Fritzsche, J.; Lorenz, H.; Klüppel, M.; Heinrich G. *Adv. Polym. Sci.* **2011,** *239*, 85.
6. Bokobza, L.; Rahmani, M.; Belin, C.; Bruneel, J.-L.; El Bounia, N.-E. *J. Polym. Sci.* **2008,** *46*, 1939.
7. Xu, D.; Sridhar, V.; Mahapatra, S. P.; Kim, J. K. *Appl. Polym. Sci.* **2009,** *111*, 1358.
8. Arroyo, M.; Lopéz-Manchado, M. A.; Herrero, B. *Polymer* **2003,** *44*, 2447.
9. Jia, Q.-X.; Wu, Y.-P.; Wang, Y.-Q.; Lu, M.; Zhang, L.-Q. *Compos. Sci. Technol.* **2008,** *68*, 1050.
10. Kim, M.-S.; Kim, G.-H.; Chowdhury, S. R. *Polym. Eng. Sci.* **2007,** *47*, 308.
11. Rooj, S.; Das, A.; Heinrich, G. *Polym. J.* **2011,** *43*, 285.
12. Ismail, H.; Pasbakhsh, P.; Ahmad Fauzi, M. N. *Polym. Test.* **2008,** *27*, 841.
13. Paskbakhsh, P.; Ismail, H.; Ahmad Fauzi, M. N.; Abu Bakar, A. *Polym. Test.* **2009,** *28*, 548.
14. Paskbakhsh, P.; Ismail, H.; Ahmad Fauzi, M. N.; Abu Bakar, A. *J. Appl. Polym. Sci.* **2009,** *113*, 3910.
15. Tiwari, M.; Noordermeer, J. W. M.; van Ooij, W. J.; Dierkes, W. K. *Polym. Adv. Technol.* **2008,** *19*, 1672.
16. Tiwari, M.; Noordermeer, J. W. M.; van Ooij, W. J.; Dierkes, W. K. *Chem. Technol.* **2008,** *81*, 276.
17. Tiwari, M.; Dierkes, W. K.; Datta, R. N.; Talma, A. G.; Noordermeer, J. W. M. *Rubber Chem. Technol.* **2009,** *82*, 473.
18. Nah, C.; Huh, M.-Y.; Rhee, J. M.; Yoon, T.-H.; *Polym. Int.* **2002,** *51*, 510.
19. Mathew, G.; Huh, M.-Y.; Rhee, J. M.; Lee, M.-H.; Nah, C. *Polym. Adv. Technol.* **2004,** *15*, 400.
20. Leblanc, J. L.; Hardy, P. *Kautsch. Gummi Kunstst.* **1991,** *44*, 1119.
21. Nordsiek, K. H. *Kautsch. Gummi Kunstst.* **1985,** *38*, 178.

Publication IV

Minna Poikelispää, Amit Das, Wilma Dierkes, Jyrki Vuorinen

The effect of partial replacement of carbon black by carbon nanotubes on the properties of natural rubber/ butadiene rubber compound

Journal of Applied Polymer Science, 130 (2013), 3153-3160

Journal of Applied Polymer Science

The Effect of Partial Replacement of Carbon Black by Carbon Nanotubes on the Properties of Natural Rubber/Butadiene Rubber Compound

Minna Poikelispää,[1] Amit Das,[1,2] Wilma Dierkes,[1,3] Jyrki Vuorinen[1]
[1]Department of Materials Science, Tampere University of Technology, Tampere, Finland
[2]Department of Elastomers, Leibniz Institute of Polymer Research Dresden, Dresden, Germany
[3]Department of Elastomer Technology and Engineering, University of Twente, Enschede, The Netherlands
Correspondence to: M. Poikelispää (E-mail: minna.poikelispaa@tut.fi)

ABSTRACT: The basic objective of this study is to investigate the mechanical properties of tyre tread compounds by gradual replacement of carbon black by multiwalled carbon nanotubes (MWCNTs) in a natural rubber–butadiene rubber-based system. A rapid change in the mechanical properties is noticed even at very low concentrations of nanotubes though the total concentration of the filler is kept constant at 25 phr (parts per hundred rubber). The correlation of the bound rubber content with MWCNT loading directly supports the conclusion that MWCNTs increase the occluded rubber fraction. Transmission electron microscopy reveals a good dispersion of the MWCNT up to a certain concentration. In the presence of MWCNT, a prominent negative shift of the glass transition temperature of the compound is found. Thermal degradation behavior, aging, and swelling experiments were also carried out to understand the resulting effect of the incorporation of MWCNT in the rubber matrix. © 2013 Wiley Periodicals, Inc. J. Appl. Polym. Sci. 000: 000–000, 2013

KEYWORDS: nanotubes; graphene and fullerenes; rubber; mechanical properties

Received 11 December 2012; accepted 14 May 2013; Published online
DOI: 10.1002/app.39543

INTRODUCTION

Carbon black (CB) is the mostly used filler in rubber compounds owing to its outstanding reinforcing properties based on the structure and physical bonding with the polymer. However, it has also drawbacks as, for example, in dynamic properties, which determine the key properties of many products such as tyres. Traditionally, silica is used to improve the dynamic properties of rubbers. The use of silica instead of CB improves friction properties of the rubber. Thus, silica-filled rubber is suitable for tyre applications as it causes lower rolling resistance when the material is used in tyre treads compared to CB-filled rubber. However, the use of silica has its drawbacks, too: The adhesion and interaction between the nonpolar rubber and the polar filler is poor. Therefore, surface modification is required to achieve the full advantages of silica. In addition, a good dispersion of silica particles into rubber matrix requires multiple mixing stages, which prolongs processing times and increases processing costs.[1]

The drawbacks of CB and silica might be prevented with new filler systems, guaranteeing a good dispersion and a good polymer–filler interaction. Since Toyota presented the nanoclay-filled polyamides in 1991, polymer research has been concentrating on nanocomposites. New types of nanofillers have been studied in rubber technology, too. Nanofillers, such as carbon nanotubes (CNTs) and layered silicates, are found to carry many benefits compared to conventional rubber fillers, CB, and silica. They have been reported to, for example, increase tensile strength, hardness, modulus, abrasion resistance, electrical conductivity, and chemical resistance.[2–4]

CNTs are widely investigated nanofillers in rubbers. Owing to its tubular form, multiwalled carbon nanotubes (MWCNTs) have a high aspect ratio and therefore good reinforcing effect. Thus, it has a good potential to work as reinforcing filler in rubber. However, MWCNTs tend to form agglomerates and entanglements owing to the specific structure and the high surface area of particles and therefore they have high filler–filler interaction. A successful application of nanofillers depends mainly on a good dispersion, but achieving a good dispersion of MWCNTs during melt mixing is extremely difficult. Most of the recently published studies have been done with solution mixing owing to better dispersion.[2,5–8] In addition, pretreatment of CNTs has proven to improve dispersion.[9,10]

Table I. Formulation of the NR/BR Compounds and Mixing Procedure

Ingredients	Type/producer	Amount (phr)
NR	SMR10	20
BR	Buna-cis-132/Dow Chemical	80
MWCNT	Baytubes C 150 P/Bayer	*x*
CB	N-234/Evonik	$25 - x$
6PPD	Lanxess	2.0
TMQ	Lanxess	1.0
ZnO	Grillo Zinkoxid GmbH	5.0
TDAE-oil	Vivatec 500/ Hansen & Rosenthal GmbH	8.0
Stearic acid	Oleon N.V	2.0
Ceresine wax	Statoil Wax GmbH	1.5
CBS	Lanxess	1.5
Sulfur	Solvay Barium Strontium GmbH	1.5

Abbreviations: 6PPD: *N*-(1,3-dimethylbutyl)-*N*′-phenyl-1,4-benzenediamine, TMQ: 2,2,4-trimethyl-1,2-dihydroquinoline, TDAE-oil: treated distillate aromatic extract oil, CBS: *N*-cyclohexyl-2-benzothiazolesulfenamide, x: 0.5, 1, 2, 2.5, 5, 7.5, 10, and 12.5 phr.

Some of the recent researches have combined CNTs with other fillers. It was found that the combination of graphene and CNTs improves the dispersion of CNTs as well as mechanical properties in silicone rubber.[11] Bokobza et al.[2] used the blend of CB and MWCNTs in styrene–butadiene rubber (SBR), and they achieved improvements in the stress–strain properties owing to improved polymer–filler interaction compared to the CB-filled compounds. Verge et al.[12] showed that good dispersion can be achieved with nitrile butadiene rubber (BR) even by melt mixing as acrylonitrile units form free radicals during the mixing process which are able to react and graft onto the CNT surface.[12] The synergistic effect of expanded graphite and MWCNTs in the formation of a filler network and improved mechanical properties of solution SBR (S-SBR) mixed in an internal mixer was observed by Das et al.[13]

In this study, CB was partially replaced by CNTs. The effect of MWCNT loading on properties of a natural rubber (NR)–BR composite, prepared by melt mixing, was investigated.

EXPERIMENTAL

Materials

The CNTs were Baytubes C 150 P, delivered by Bayer. The diameter of the multiwall nanotubes was 13–16 nm and the length varied between 1 and 10 μm. The other materials used in the compound and formulation are summarized in Table I.

Preparation of Nanocomposites

NR, BR, nanofillers, and other ingredients excluding curatives were mixed in a Krupp Elastomertechnik GK 1.5 E intermeshing mixer (50°C, 90 rpm) for 5 min. The curatives were added on an open two-roll mill. In the reference compound, only CB was used as filler in a concentration of 25 phr. In the MWCNT-containing compounds, a part of the CB (0.5, 1, 2, 2.5, 5, 7.5, 10, and 12.5 phr) was replaced by the same amount of MWCNTs.

Characterisations

The Mooney viscosity of the compounded material was measured in a MV 2000 Mooney Viscometer from Alpha Technologies. The measurement was carried out at 100°C including 1-min heating time and 4-min measuring time.

Curing studies and Payne effects were measured using an Advanced Polymer Analyzer 2000 from Alpha Technologies. Curing studies were carried out at 150°C for 25 min, and the optimum curing time was determined (*t*90, time taking to reach 90% of the ultimate rheometric torque). The compounds were then vulcanized at their *t*90 value (Table II). The Payne effect was studied in a strain sweep from 0.28 to 100% at 100°C which is the commonly used temperature for these measurements.

Tensile tests of the samples were carried out with a Messphysik Midi 10–20 universal tester according to ISO 37. Dynamic properties were studied with a Pyris Diamond DMA from PerkinElmer Instruments, operating in tension mode. The measurements were done from −80 to +80°C at a heating rate of 10°C min^{-1} and a frequency of 10 Hz.

The volume resistivity was measured according to standard ISO 1853. The sample was rectangular with dimensions of approximately 140 × 50 × 2 mm (length × width × thickness). The resistances were measured with a Sefelec teraohmmeter MP1500P. The voltage used in the measurements was 10 V.

The volume fraction of the rubber was determined by swelling studies. Specimens with diameter of 12 mm and a thickness 0.2 mm were kept in toluene for equilibrium swelling. The sample was weighted before and after immersion as well as after drying. The volume fraction (V_r) of the rubber was calculated by

$$V_r = \frac{(D - FI)\ \rho_r^{-1}}{(D - FI)\ \rho_r^{-1} + A_0\ \rho_s^{-1}} \quad (1)$$

where D is the weight of the dried sample, F is the weight fraction of insoluble components, I is the initial weight of the sample, ρ_r is the density of rubber, ρ_s is the density of solvent, and A_0 is the weight of absorbed solvent.[14]

The polymer–filler interaction was studied using a Kraus plot

$$\frac{V_{r0}}{V_{rf}} = 1 - m\left(\frac{\phi}{1-\phi}\right) \quad (2)$$

with

$$m = 3C\left(1 - V_{r0}^{\frac{1}{3}}\right) + V_{r0} - 1 \quad (3)$$

where V_{r0} is the volume fraction of the polymer in the solvent-swollen gum, V_{rf} is the volume fraction of polymer in the swollen-filled rubber, C is a characteristic constant of the filler, and θ is the volume fraction of filler in the rubber. The m-value describes the reinforcing ability of filler. It is negative for reinforcing fillers: the higher m, the better the polymer–filler interaction.[14,15]

Table II. Curing and Mechanical Properties of the CB/MWCNT-Filled Rubber

	Curing characteristics			Tensile characteristics			
MWCNT/CB	Scorch time ts2 (min)	Curing time t90 (min)	Torque S_{max} (dNm)	Tensile strength (MPa)	Elongation at break (%)	Modulus 100% (MPa)	Viscosity, ML (1 + 4)100°C
0/25	7.0	9.7	5.0	22.8 ± 2.6	593 ± 35	1.3 ± 0.05	43.6 ± 0.3
0.5/24.5	6.9	9.6	5.1	24.0 ± 2.9	622 ± 33	1.3 ± 0.05	45.2 ± 0.2
1.0/24.0	6.9	9.6	5.4	23.0 ± 1.0	622 ± 10	1.3 ± 0.05	46.2 ± 0.2
2.0/23.0	6.8	9.4	5.9	23.7 ± 2.9	584 ± 27	1.5 ± 0.05	50.8 ± 0.3
2.5/22.5	6.8	9.5	5.7	21.4 ± 1.9	599 ± 22	1.4 ± 0.04	47.7 ± 0.2
5.0/20.0	6.6	9.4	6.6	22.6 ± 1.7	577 ± 30	1.8 ± 0.03	51.6 ± 0.2
7.5/18.5	6.3	9.2	7.5	22.0 ± 1.4	560 ± 22	2.1 ± 0.04	56.2 ± 0.1
10.0/15.0	6.1	9.0	7.6	19.9 ± 1.3	540 ± 18	2.1 ± 0.06	59.6 ± 0.2
12.5/12.5	5.6	8.5	8.5	16.4 ± 0.5	467 ± 16	2.5 ± 0.12	61.9 ± 0.4

The state of dispersion of the CB and MWCNT particles in the NR/BR nanocomposites was investigated by transmission electron microscopy (TEM) using a JEM 2010 model. Ultra-thin sections were cut from the samples by an ultramicrotome (Leica Ultracut UCT) at −100° with a thickness of approximately 80–100 nm.

The thermal degradation kinetics of the compounds were measured by a Perkin-Elmer STA 6000 TGA in nitrogen atmosphere. The heating temperature was varied from 25 to 995°C and three different heating rates: 5, 10, and 15°C/min were used. The activation energy (E_a) was determined according to the Flynn–Wall–Ozawa method, which is based on the following equation:

$$\log\beta = -\frac{0.457E_a}{RT} + \log\frac{(AE_a)}{Rg(\mathrm{a})} - 2.315 \quad (4)$$

where β is the heating rate, E_a is the activation energy, R is the gas constant, T is the temperature in which the conversion is reached, α is the conversion degree, A is the exponential factor and $g(\mathrm{a}) = \int_0^{\mathrm{a}} \frac{d\mathrm{a}}{f(\mathrm{a})}$ is the integral conversion function. E_a is the slope of the line of log β versus 1/T.[16,17]

For ageing tests, compounds were kept in an oven at 70°C for 2, 7, 14, and 21 days. The elongation at break and stress at 100% strain (100% modulus, M_{100}) were measured on aged samples (three parallel measurements) according to ISO 37. The results were evaluated according to the Ahagon plot, which is used to describe the type of ageing using the 100% modulus and extension ratio at break (λ_b):

$$\lambda_b = AM_{100}^{-0.75} \quad (5)$$

where A is a constant characterizing the base formulation.[18,19]

RESULTS AND DISCUSSION

Raw CNTs exist in agglomerated form and are heavily entangled like felted threads. Therefore, dispersion of the tubes into single particles is very difficult to achieve. To control the dispersion, the rubber vulcanizates containing 5 and 10 phr were selected for TEM experiments. Figure 1 shows the morphology of the matrix. The coexistence of CB aggregates and the thread-like structures of the MWCNTs can easily be seen in all figures. The large areas of aggregated and agglomerated MWCNT were not observed in the compound filled with 5 phr MWCNT and 20 phr CB. Relatively large clusters of agglomerated MWCNT were detected in the compounds filled with 10 phr MWCNT and 15 phr CB, clearer in the smaller scale image in Figure 1(d). An explanation for this effect is that the dispersion is getting worse beyond a certain loading as the distance between nanofiller particles decreases and their tendency to form agglomerates increases. Thus, it can be concluded that the inclusion of at least up to 5 phr MWCNT could be done with the existing mixing and processing technology of rubber. MWCNTs are dispersed around CB particles. Thus, CB acts as a separator between MWCNT which facilitates dispersion. Mooney viscosities of the compounds are listed in Table II. The viscosity of the compounds increased proportionally with MWCNT concentration. The surface area of MWCNTs is higher than that of CB, which enables improved interaction with the rubber chains, resulting into a higher reinforcement effect. This fact corroborates the data obtained from bound rubber measurements. Bound rubber is the amount of rubber which is not extractable from an uncured rubber compound. The higher the bound rubber content, the higher the occluded rubber fraction. This is the rubber portion which suffers less from external stress. As shown in Figure 2, the bound rubber increases slightly up to a certain loading of MWCNT; beyond that the values remain almost stable. As shown in Figure 1, the MWCNTs are well dispersed up to a certain concentration, exposing their complete surface area to the rubber chains. After passing a particular concentration, the tubes are no more well dispersed, resulting in a lower degree of filler–polymer interaction and therefore the bound rubber remains unaltered at higher MWCNT concentrations. Figure 2 also shows the difficulties encountered in the BR measurements, especially for lower concentrations of nanotubes: the variation between single measurements is rather large.

The results of the curing studies are summarized in Table II. Scorch time decreases when CB is replaced by MWCNTs. Generally, addition of CB to rubber increases the rate of the curing reaction[20]; however, an explanation for this effect is not given so far. In the present case, one of the reasons for the shorter

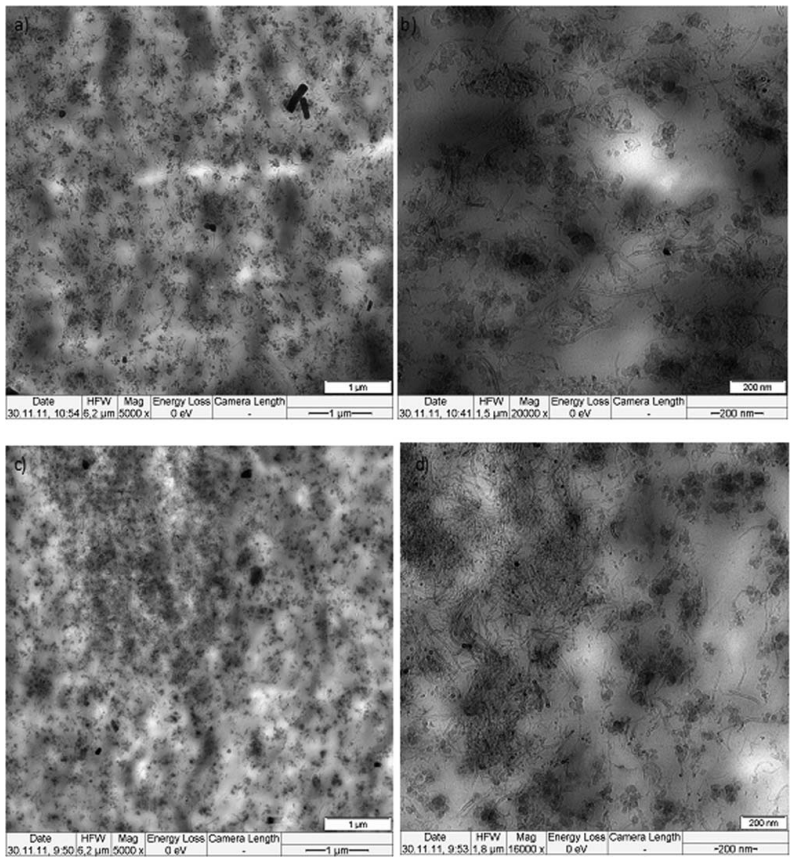

Figure 1. TEM images of the composites containing 5 phr MWCNT (a, b) and containing 10 phr MWCNT (c, d).

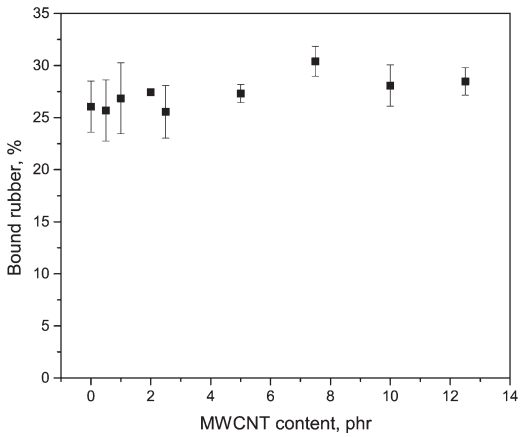

Figure 2. Variation of the bound rubber content with the increase of MWCNT concentration in the CB-filled NR/BR compound. The total amount of fillers was kept constant at 25 phr.

scorch time might be impurities in the MWCNTs: they contain about 10% of metallic impurities from the synthesis by vapour growth deposition. These metals in the tips of MWCNTs could participate in the sulfur vulcanization reaction and enhance the crosslinking reaction rate.[21] Another explanation is the exceptional high value of thermal conductivity of MWCNTs: the nanotubes can more efficiently transport thermal energy through the matrix, resulting in a faster temperature increase of the material and thus shorter scorch time. A decrease in curing time is also observed, but the change is mainly owing to the reduction in scorch time; the curing rate is not influenced by the presence of MWCNTs. The maximum torque values increase when the amount of MWCNTs is increased, indicating a higher reinforcement effect of MWCNTs compared to CB.

Gradual replacement of CB by the same weight percentage of MWCNTs practically increases the total volume fraction of the fillers, which directly affects the moduli values. This is reflected in the properties of the vulcanizates with higher MWCNT loading: Modulus at 100% elongation starts to increase after incorporation of 2 phr MWCNTs, and a nearly twofold increase in 100% modulus is found at 12.5 phr MWCNTs as compared to

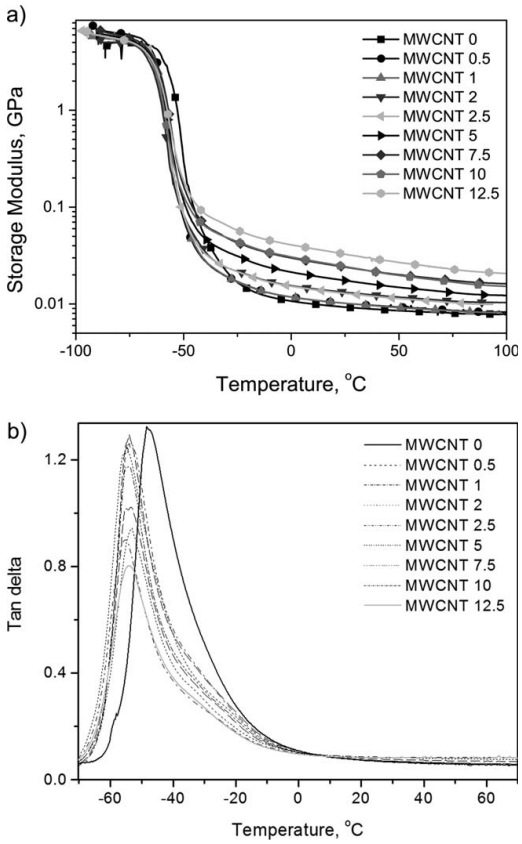

Figure 3. Temperature dependence of the (a) storage modulus and (b) loss tangent of the CB and MWCNT-filled compounds.

the composite containing only CB. The higher surface area of the MWCNTs and thus the increased interaction with the polymer also results in an increase of 100% modulus, tensile strength, and elongation at break when compared to the compound filled only with CB and as long as the MWCNT are well dispersed (Table II). When the amount of MWCNTs exceeded 5 phr, tensile strength as well as elongation at break starts to decrease again owing to insufficient dispersion of MWCNTs.

Analysis of the dynamic mechanical spectra can also help to understand the reinforcement effect of elastomeric materials. Figure 3 shows the storage modulus (E') and tan δ values of the compounds as a function of temperature. It is observed that within the rubbery plateau area, MWCNTs increase the E' values of the compounds and make the material stiffer. At the same time, a prominent reduction of the tan δ peak is also observed at higher MWCNT loadings, explaining the restricted motion of the rubber chains adhering to the MWCNT surface. A strong rubber–filler interaction is the reason for this behavior, which was also seen in the bound rubber experiments. It is also noticed that MWCNTs decreased the glass transition temperature (T_g) from -48 to -53°C in this study. In most of the literature, it is claimed that the T_g increases when fillers, which interact with the polymer chains very firmly, are added. However, plenty of reports can be found describing a negative shift of the T_g of the polymer filled with different types of nanosized fillers. Allaoui and El Bounia[22] showed that the T_g of CNT-filled epoxy is lower than that of unfilled epoxy in many studies. The decrease in T_g was explained with lower curing degree. They analyzed, published elsewhere, T_g values of CNT/epoxy composites and stated that especially single-wall CNTs decrease T_g of epoxy; for MWCNTs a clear trend was not found. However, in rubber the analogy with epoxy cannot be drawn. On the contrary to the existence of a glassy-like polymer, the existence of a very thin liquid-like polymer film near to surface of MWCNT can also be envisaged to give a possible explanation for negative shift of T_g.[23] The graphitic surface of the MWCNT which energetically is not favorable to adsorb the macromolecular chains could be the reason behind it.

The dependence of certain dynamic properties on the strain amplitude at low deformation range can help to understand the dispersion state of the fillers in a soft rubber matrix. It describes the filler–filler interactions between the filler particles: the higher the filler–filler interaction, the higher the modulus. But as these interactions are effective only on short distances, the modulus quickly decreases with increasing strain. This is called the Payne effect. This dependency is very strong when the fillers form a three-dimensional network within the rubber matrix. Reasonably, well-dispersed filler particles do not contribute as much as poorly dispersed fillers to the network, thus to the modulus. This effect is generally quantified by measuring a storage modulus as a function of strain. Figure 4(a) shows the strain dependency of the storage modulus of the MWCNT/CB-filled NR/BR matrix measured at 100°C, and Figure 4(b) shows storage modulus values at low strain (0.56%), illustrating the differences in Payne effect. It is evident from the figures that filler–filler interaction increases when the concentration of MWCNTs increases. The storage modulus at low strain is gradually increasing, illustrating strong network formation by the MWCNTs as CB is successively replaced. In general, a rubber matrix filled with a particular volume fraction of fillers shows a lower Payne effect when the fillers are better dispersed. An example for this effect is the addition of a silane coupling agent to a silica-filled system, leading to a decrease of the Payne effect as the rubber–filler interaction develops at the expense of the filler–filler interaction.[24] But in the case of MWCNTs with extremely high anisotropic character, the filler–filler interaction increases when the agglomerates are dispersed into individual tubes, as these latter form an interconnecting network throughout the matrix. Subramaniam et al.[25] proposed this mechanism and they observed that the well-dispersed tubes could show a strong Payne effect and badly dispersed tubes yield little effect in the strain dependence of the modulus values.

MWCNTs are known to increase electrical conductivity of polymers. It is obvious that higher amounts of MWCNTs decrease the resistivity of the composites. Figure 5 shows the dependence of DC electrical resistivity on MWCNT content. As the sample without MWCNT contained 25 phr CB, a percolated network of CB particles was already established, and thus the addition of

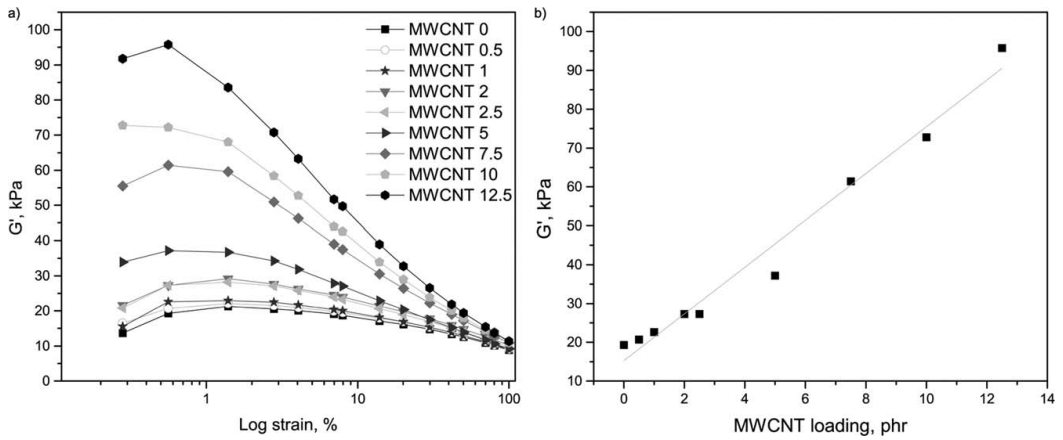

Figure 4. (a) Storage modulus of the compounds as a function of strain at 100°C and (b) storage modulus of the compounds at 0.56% strain with various concentrations of MWCNTs.

MWCNTs was not reflected by showing a rapid decrease of the resistivity. Nevertheless, after partial replacement of CB by MWCNTs, the composites show a decrease in resistivity, indicating the earlier discussed filler–filler network.

The volume fraction of the polymers can be calculated from swelling studies, and it is related to crosslink density. The volume fractions of the polymer in the MWCNT/CB-filled NR/BR compounds are listed in Table III, and it is obvious that the volume fraction of the compounds containing MWCNTs is higher than the fraction of the compound containing only CB. In these compounds, CB was partially replaced by MWCNTs. As MWCNTs have lower density than CB, the volume fraction of fillers increased with the addition of MWCNTs, even if the total amount of fillers was kept constant. The lower degree of swelling indicates higher crosslink density and higher reinforcement. However, it is observed that after addition of 7.5 phr of MWCNT, the degree of swelling does not change anymore with the increase in MWCNT content, indicating decreased in crosslink density. This can also be seen in Figure 6(a), where the Kraus plots of the CB/MWCNT-filled NR/BR compounds are presented. The slope of the curves represents the polymer–filler interaction parameter. According to these results, with increasing MWCNT content the slope becomes steeper up to 10 phr, indicating higher rubber–filler interaction. With 12.5 phr MWCNT loading, the slope decreases substantially owing to an increased amount of agglomerates. It needs to be mentioned here that a higher amount of MWCNT not only increases the reinforcement of the rubber matrix owing to the higher volume fraction of the MWCNTs, but it simultaneously suffers from poor dispersion of the tubes as observed from TEM images. It would be very difficult to draw a clear conclusion from the swelling data alone, but together with the results mentioned above, the increase in higher reinforcement effect can be easily seen.

The activation energies of the thermal degradation of the compounds were calculated according to the Flynn–Wall–Ozawa method. Figure 6(b) shows the degradation kinetics and the

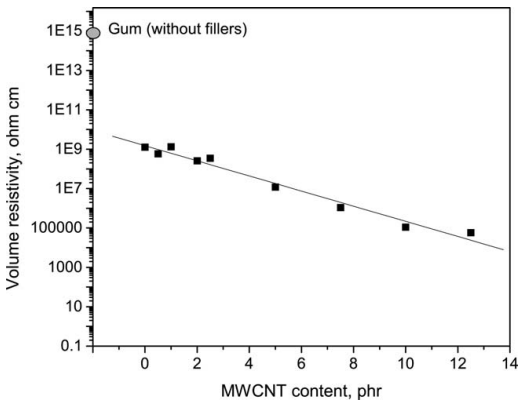

Figure 5. Volume resistivity of MWCNT/CB-filled NR/BR compounds.

Table III. Volume Fractions of the Rubber in a Swollen Network

MWCNT/CB concentration	Volume fraction (–)
0/25	0.173
0.5/24.5	0.185
1/24	0.198
2/23	0.185
2.5/22.5	0.190
5/20	0.204
7.5/17.5	0.210
10/15	0.197
12.5/12.5	0.202

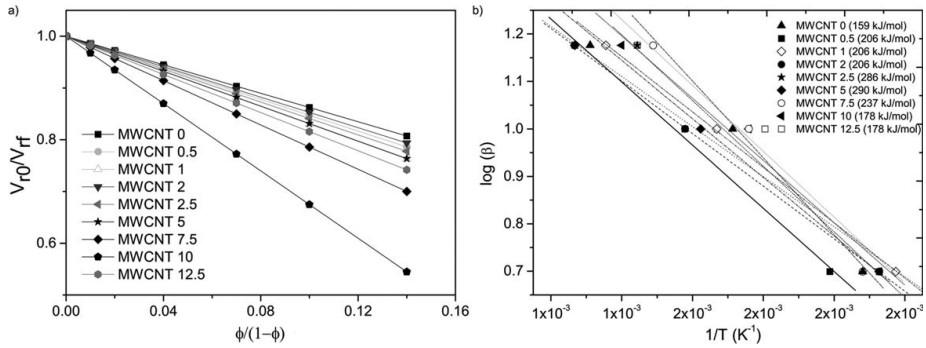

Figure 6. (a) Kraus plot and (b) Flynn–Wall–Ozawa plots of MWCNT and CB-filled NR/BR compounds.

activation energies at 40% conversion level of the MWCNT/CB-filled compounds. The activation energy varied from 159 to 286 kJ/mol with different MWCNT loadings. The activation energy increased gradually up to a 5-phr MWCNT loading. At higher MWCNT loadings, it decreased again most probably owing to the increasing amount of agglomerates which gives a more heterogeneous character to the rubber matrix. This prevents interaction with the rubber chains and makes the matrix degrade easily. Ageing of rubbers changes mechanical properties of rubber. Typical changes are an increase in modulus and decrease in elongation at break (ε), which is also valid with these compounds as summarized in Table IV. In many applications, it is important to be able to foresee the period that a rubber can be used under service conditions. Ahagon et al.[18] observed that the modulus at 100% strain and elongation at break can be utilized in the prediction of the life cycle of a tyre. If aging is owing to further crosslinking, the slope of the plot of the logarithm of the extension ratio (λ_b) versus the logarithm of the modulus at 100% strain (M_{100}) should be about −0.75. In Figure 7, the corresponding plots are shown. As shown in Figure 7, it is observed that the slopes are not exactly matching with each other and that they slightly deviate from the value −0.75. The slopes lie in the range from −0.58 to −1.20. No regular trend was found when CB is replaced by MWCNTs, and the presence of MWCNT does not seem to influence the aging behavior. The average value of the slope is found to be approximately 0.84. From this result, it can be concluded that ageing of MWCNT/CB-filled NR/BR compounds at 70°C is dominated by the formation of crosslinks and not by destructive degradation of the bonds.

Table IV. Elongation at Break and 100% Modulus Values of the Compounds After Ageing

MWCNT/CB content		Ageing 0 Days	Ageing 2 Days	Ageing 7 Days	Ageing 14 Days	Ageing 21 Days
0/25	ε (%)	616 ± 40	599 ± 22	514 ± 5	511 ± 50	495 ± 11
	M_{100} (MPa)	1.28 ± 0.06	1.50 ± 0.03	1.51 ± 0.04	1.56 ± 0.01	1.77 ± 0.06
0.5/24.5	ε (%)	618 ± 28	627 ± 5	510 ± 2	502 ± 12	531 ± 1
	M_{100} (MPa)	1.36 ± 0.06	1.38 ± 0.12	1.58 ± 0.18	1.7 ± 0.08	1.8 ± 0.08
1.0/24.0	ε (%)	634 ± 17	567 ± 22	512 ± 2	502 ± 10	510 ± 10
	M_{100} (MPa)	1.43 ± 0.01	1.48 ± 0.04	1.83 ± 0.02	1.85 ± 0.08	1.83 ± 0.02
2.0/23.0	ε (%)	561 ± 2	562 ± 17	446 ± 61	503 ± 14	502 ± 25
	M_{100} (MPa)	1.67 ± 0.04	1.73 ± 0.02	1.97 ± 0.02	2.15 ± 0.07	2.10 ± 0.04
2.5/22.5	ε (%)	599 ± 50	520 ± 41	528 ± 51	530 ± 32	505 ± 14
	M_{100} (MPa)	1.53 ± 0.01	1.63 ± 0.02	1.84 ± 0.06	1.97 ± 0.07	2.05 ± 0.02
5.0/20.0	ε (%)	601 ± 22	566 ± 46	522 ± 38	482 ± 52	428 ± 40
	M_{100} (MPa)	1.86 ± 0.09	1.94 ± 0.30	2.19 ± 0.01	2.32 ± 0.08	2.48 ± 0.01
7.5/18.5	ε (%)	622 ± 13	576 ± 54	504 ± 26	400 ± 13	461 ± 11
	M_{100} (MPa)	2.26 ± 0.03	2.37 ± 0.13	2.91 ± 0.01	3.15 ± 0.04	3.06 ± 0.18
10.0/15.0	ε (%)	512 ± 4	512 ± 33	460 ± 28	349 ± 42	391 ± 49
	M_{100} (MPa)	2.21 ± 0.05	2.35 ± 0.08	2.76 ± 0.02	2.87 ± 0.08	2.95 ± 0.10
12.5/12.5	ε (%)	439 ± 24	381 ± 18	371 ± 35	306 ± 37	299 ± 18
	M_{100} (MPa)	2.66 ± 0.04	2.84 ± 0.14	3.06 ± 0.03	3.48 ± 0.10	3.2 ± 0.19

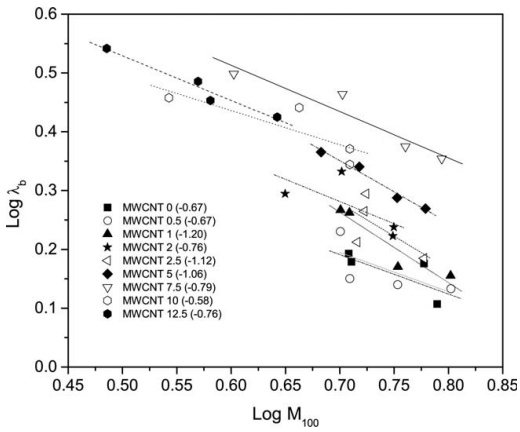

Figure 7. Ahagon plot of the aged samples.

CONCLUSIONS

Replacement of a small amount of CB by MWCNTs enhanced the mechanical properties of the model tread compound significantly. Up to 5 phr MWCNT loading, the dispersion of the tubes was found to be very good. The presence of CB facilitated the dispersion of the tubes in the soft rubber matrix. As the rubber was already filled with CB, the filler concentration was above the percolation threshold though a strong filler–filler network was formed after addition of MWCNT as indicated a by strain sweep analysis. As a consequence, the addition of MWCNTs increased the electrical conductivity. The partial replacement of CB by MWCNT enhanced the rubber–filler interaction up to a certain concentration, which was very easily reflected in a Kraus plot analysis. Aging studies indicated a regular formation of new crosslinks which was shown by Ahagon plots.

ACKNOWLEDGEMENT

This study has been supported by the Finnish Funding Agency for Technology and Innovation (TEKES, Grant No. 40352/08). The authors thank Mrs. S. Pohjonen and Mr. T. Lehtinen from the Tampere University of Technology for their technical help. The authors are also thankful to Mrs. R. Boldt, Leibniz-Institute for Polymer Research, Dresden, for the TEM images.

REFERENCES

1. Noordermeer, J. W. M.; Dierkes, W. K. Rubber Technologist's Handbook; White, J., De, S. K., Naskar, K., Eds.; Smithers Rapra, Shawbury, Shrewsbury: Shropshire, United Kingdom, **2009**; Vol. *2*, Chapter 3, p 59.
2. Bokobza, L.; Rahmani, M.; Belin, C.; Bruneel, J.-L.; El Bounia, N.-E. *J. Polym. Sci.* **2008**, *46*, 1939.
3. Subramaniam, K.; Das, A.; Heinrich, G. *Comp. Sci. Technol.* **2011**, *71*, 1441.
4. Xu, D.; Sridhar, V.; Mahapatra, S. P.; Kim, J. K. *Appl. Polym. Sci.* **2009**, *111*, 1358.
5. Jiang, H.-X.; Ni, Q.-Q.; Natsuki, T., *Key Eng. Mater.* **2011**, *464*, 660.
6. Bokobza, L. *Polym. Adv. Technol.* **2012**, *23*, 1543.
7. Zhou, X.; Xhu, Y.; Liang, J.; Yu, S.; *J. Mater. Sci. Technol.* **2010**, *26*, 1127.
8. De Falco, A.; Goyanes, S.; Rubiolo, H.; Mondragon, I.; Marzocca, A. *Appl. Surf. Sci.* **2007**, *254*, 262.
9. Sui, G.; Zhong, W. H.; Yang, X. P.; Yu, Y. K.; Zhao, S. H. *Polym. Adv. Technol.* **2008**, *19*, 1543.
10. Shanmugharaj, A. M.; Bae, J. H.; Lee, K. Y.; Noh, W. H.; Lee, S. H.; Ryu, S. H. *Compos. Sci. Technol.* **2007**, *67*, 1813.
11. Hu, H.; Zhao, L.; Liu, J.; Liu, Y.; Cheng, J.; Luo, J.; Liang, Y.; Tao, Y.; Wang, X.; Zhao, *J. Polymer* **2012**, *53*, 3378.
12. Verge, P.; Peeterbroeck, S.; Bonnaud, L.; Dubois, P. *Compos. Sci. Technol.* **2010**, *70*, 1453.
13. Das, A.; Kasaliwal, G. R.; Jurk, R.; Boldt, R.; Fischer, D.; Stöckelhuber, K. W.; Heinrich, G. *Compos. Sci. Technol.* **2012**, *72*, 1961.
14. Paul, K. T.; Pabi, S. K.; Chakraborty, K. K.; Nanodi, G. B., *Polym. Comp.* **2009**, *30*, 1647.
15. Krauss, G. *J. Appl. Polym. Sci.* **1963**, *7*, 861.
16. Flynn, J.; Wall, L. *J. Polym. Sci. Part B: Polym. Lett.* **1966**, *4*, 323.
17. Ozawa, T. *Bull. Chem. Soc. Jpn.* **1965**, *38*, 1881.
18. Ahagon, A.; Kida, M.; Kaidou, H. *Rubber Chem. Technol.* **1990**, *63*, 683.
19. Kaidou, H.; Ahagon, A. *Rubber Chem. Technol.* **1990**, *63*, 698.
20. Franta, I., Ed. Elastomers and Rubber Compounding Materials; Elsevier: Amsterdam, **1989**.
21. Kummerlöwe, C.; Vennemann, N.; Yankova, E.; Wanitschek, M.; Größ, C.; Heider, T.; Haberkorn, F.; Siebert, A. *Polym. Eng. Sci.* **2012**, *53*, 849.
22. Allaoui, A.; El Bounia, N. *Express Polym. Lett.* **2009**, *3*, 588.
23. Keddie, J. L.; Jones, R. A. L.; Cory, R. A. *Europhys. Lett.* **1994**, *27*, 59.
24. Reuvekamp, L. A. E. M.; Ten Brinke, J. W.; Van Swaaij, P. J.; Noordemeer, J. W. M. *Rubber Chem. Technol.* **2002**, *75*, 187.
25. Subramaniam, K.; Das, A.; Steinhauser, D.; Klüppel, M.; Heinrich, G. *Eur. Polym. J.* **2011**, *47*, 2234.

Publication V

Maija Hoikkanen, Minna Poikelispää, Amit Das, Uta Reuter, Wilma Dierkes, Jyrki Vuorinen

Evaluation of mechanical and dynamic mechanical properties of multiwalled carbon nanotube-based ethylene-propylene copolymer composites mixed by masterbatch dilution

Journal of Composite Materials, 50 (2016) 4093-4101

Article

JOURNAL OF COMPOSITE MATERIALS

Journal of Composite Materials
0(0) 1–9

DOI: 10.1177/0021998316631812
jcm.sagepub.com

SAGE

Evaluation of mechanical and dynamic mechanical properties of multiwalled carbon nanotube-based ethylene–propylene copolymer composites mixed by masterbatch dilution

Maija Hoikkanen[1], Minna Poikelispää[1], Amit Das[1,2], Uta Reuter[2], Wilma Dierkes[1,3] and Jyrki Vuorinen[1]

Abstract

A two-step masterbatch mixing technique was studied for preparation of carbon nanotube-filled ethylene–propylene diene elastomer compounds, and compared to conventional one-step mixing process. In the two-step process, a masterbatch compound with carbon nanotube content of 50 parts per hundred was prepared by melt-mixing ethylene–propylene diene elastomer. This material was then compounded with pristine ethylene–propylene diene elastomer and composites with different carbon nanotube concentrations were compared. The aim of this study is to compare the efficiency of two different mixing processes on the dispersion of carbon nanotubes and to facilitate the handling of carbon nanotubes, as the masterbatch can be prepared in a controlled way and used for further dilution without the problems related to carbon nanotube processing. The compound properties were studied with emphasis on mechanical characterization and dynamic mechanical thermal analysis. Masterbatch mixing resulted in the similar mechanical properties of the composites compared to the direct mixing method. At the relatively low loadings of carbon nanotubes, the considerable improvements of the mechanical properties were observed. The aspect ratio of the carbon nanotubes determined by transmission electron microscope was found to be similar to the one calculated from the Guth equation. It showed a considerable reduction in aspect ratio independent of the used mixing method.

Keywords

Carbon nanotube, masterbatch mixing, rubber, EPDM

Introduction

Carbon nanotubes (CNTs) have high potential for reinforcement due to their small dimensions, high aspect ratio, and unique properties arising from their tube-like structure. However, their application in a polymer, more specifically in rubbers, is hampered due to dispersion problems, as well as health and safety issues caused by the small particle size of the nanotubes. In many studies, solution mixing was used to improve dispersion, but this is a rather slow method and industrially not viable. Thus, for large-scale use, traditional mixing method where rubber compound is prepared by solid state and dry mixing of fillers, rubbers and all other additives in internal mixer or open two-roll mill is more practical method. The masterbatch dilution technique is one of the methods whereby a fine dispersion and distribution of different nanosized fillers could be realized. This approach has been used previously for the preparation of nanoclay-based rubber nanocomposites.[1] In this work, a polar

[1]Department of Materials Science, Tampere University of Technology, Finland
[2]Leibniz Institute of Polymer Research Dresden, Germany
[3]Department of Elastomer Technology and Engineering, University of Twente, the Netherlands

Corresponding author:
Minna Poikelispää, Department of Materials Science, Tampere University of Technology, P.O. Box 589, 33101 Tampere, Finland.
Email: minna.poikelispaa@tut.fi

rubber, that is, carboxylated nitrile rubber (XNBR), was used as a matrix for the nanoclay masterbatch. This nanoclay-XNBR compound was then further diluted in a solution butadiene rubber matrix.[1] In another study, a similar type of XNBR-nanoclay masterbatch was exploited in the preparation of styrene butadiene/butadiene rubber (SBR/BR) nanocomposites.[2] In this study, it is reported that the final composites prepared in an internal mixer showed better mechanical properties compared with the composites prepared by a two-roll mixing mill or solution mixing.[2]

During rubber mixing process, a huge amount of fine chemicals and fillers are handled and due to this the working environment becomes poor: the chemicals can be found in the air and nearby areas. Therefore, the workers who are directly handling the CNTs in the mixing room can be affected by small nanoparticles by inhalation. There are reports about the toxicity of CNTs to the human health.[3,4] Precautions are needed to avoid possible penetration of CNTs into the human body by inhalation, by direct skin contact, by food and drinking water. These nanoparticles, when exposed to a considerable amount, can affect microorganisms, plants, and animals.[3,4]

To avoid these problems, the masterbatch dilution approach could be used. This technique allows preparing a masterbatch with a high CNT loading and further diluting it with the matrix material to the desired loading. Thus, it offers eco-friendlier and healthier compounding of rubber filled with CNTs.

Kummerlöwe et al.[5] prepared CNT masterbatches with two different types of rubbers, and finally it was diluted with SBR or nitrile rubber. It is reported that direct melt mixing of CNTs with S-SBR and NBR can establish a very low percolation threshold of 0.2 and 1 wt% CNTs, respectively.

In the present study, the application of the masterbatch technique for multi-walled CNT filled ethylene–propylene diene rubber (EPDM) and the effects of this mixing method on the resulting compound properties were studied. EPDM was selected as the elastomer matrix since it has good environmental resistance but relatively low mechanical properties which could thus be improved by the CNT addition. Furthermore, EPDM-CNT based materials have potential applications in electronics, for example, in flexible sensors.[6,7]

Experimental

Compounding and sample preparation

EPDM rubber (Keltan 512, Lanxess/DSM, the Netherlands) was used for the preparation of the masterbatch and the final compounds. Multiwall CNTs (NC7000) were purchased from Nanocyl, Belgium and used as received.

Table 1. Calculated CNT content of the test compounds and TGA results.

Sample name	Mixing method	CNT content (phr) Calculated	CNT content (phr) TGA result
EPDM_0	Masterbatch	0	0
EPDM_3	Masterbatch	3.2	3.3
EPDM_6	Masterbatch	6.3	6.3
EPDM_9	Masterbatch	9.3	8.7
Reference_6	Direct mixing	6.3	5.9

The masterbatch of EPDM and CNT was first prepared by mixing them 4 min in an internal mixer (Brabender N 350 E, rotor speed 70 r/min, starting temperature 50°C) with a composition of 2:1, that is, the CNT content of 50 parts per hundred (phr). A certain amount of this masterbatch was then further mixed in a separate step with pristine EPDM to CNT concentrations given in Table 1. After 2 min mixing 2 phr ZnO and 5 phr stearic acid were incorporated. The second mixing step was performed in the same mixer than the masterbatch with the similar mixing parameters. The compound was dumped at the temperature of 160°C or after 5 min mixing. Finally, 2 phr dibutyldithiocarbamate (ZDBC) and 1 phr N-cyclohexyl-2-benzothiazolesulfenamide (CBS) and 1 phr sulphur were added on a two-roll mixing mill. A reference sample was prepared by direct mixing of CNTs with EPDM for comparison (reference, 6 phr). Vulcanized samples with thickness of 2.2 mm were prepared by curing at 160°C during their respective curing time.

Characterization

The curing behavior and the strain sweep analysis of the compounds were studied with the Advanced Polymer Analyzer (APA 2000, Alpha Technologies). Curing studies were performed at 160°C at 0.2° strain and 1.7 Hz frequency. The strain sweep was done with amplitudes from 0.28% to 140% at 100°C.

Thermogravimetric analysis (TGA) was done with a Perkin Elmer STA 6000. The measurements were conducted in air at a heating rate of 10 K/min from 30°C to 995°C.

Tensile properties were determined according to ISO 37 using a dumbbell specimen type 1. The tests were performed with a Messphysik Midi 10-20 universal tester, a contact extensometer and at a crosshead velocity of 500 mm/min. The Shore A hardness was recorded according to ASTM D 2240–00 with an AFFRI

Hardness tester, stand Type 1, at 15 s. Five parallel measurements were taken for tensile and hardness properties.

The thermomechanical behavior of the cured compounds was studied by dynamic mechanical thermal analysis (DMTA). The measurements were done on a Perkin Elmer Pyris Diamond DMTA and were performed in the range from −80°C to +70°C at a rate of 3 K/min and frequency of 1 Hz. They were started in force control in the glassy state and changed to displacement control after the initial reduction of the modulus due to the glass transition. The displacement limit was set to $\Delta L = 40\,\mu m$ and with a sample length of 20 mm, the sample experienced 0.2% maximum strain during the measurement.

The tensile stress softening behavior (Mullins effect) was studied with a Zwick Z 010 according to DIN 53504/S2/200 with an optical extensometer. The prestress was 0.4 Newton, and the crosshead speed was 200 mm/min. The samples were first stretched up to 100% elongation and then released. This cycle was repeated three times after which the samples were stretched to failure. Transmission electron microscopic images were taken by a Libra 120 transmission microscope at an acceleration voltage of 120 kV. Samples were sliced by ultramicrotomy at the temperature of 140°C. The aspect ratios of CNTs for the analyzed samples were calculated from the well-dispersed areas of all high-resolution (original magnification 20,000×) images using ImageTool 3.00.

To study the aspect ratio analytically, Young's modulus values were fitted to two well-established mechanical models. The models were selected to have a single fitting parameter, the aspect ratio. The output of the models in each case is the filled compound (composite) modulus, E_c, as the function of the filler volume fraction, V_f.

When starting from the hydrodynamic effect caused by rod shaped fillers (Guth equation[8]) with aspect ratio of filler f in a matrix with modulus E_m, the modulus of the composite E_c can be calculated as

$$E_c = E_m\left(1 + 0.67fV_f + 1.62f^2V_f^2\right) \quad (1)$$

Composite models based on stress and strain distribution calculations were the second approach taken into account. The semi-empirical Halpin–Tsai model[9] for short-fiber reinforced composites was applied in the form of following equation

$$\frac{E_c}{E_m} = \frac{1 + 2f\eta V_f}{1 - \eta V_f} \quad (2)$$

where f is the aspect ratio, $\eta = \frac{E_{filler}/E_m - 1}{E_{filler}/E_m + 2f}$ and E_{filler} is the Young's modulus of the filler. Equation (2) has previously been used for CNT reinforced SBR, and following that approach, a CNT modulus value of $E_{filler} = 1000\,GPa$ has been used.[10]

Beyond the modeling based on tensile testing data yielding the aspect ratio, also (DMTA) data was fitted for understanding the thermorheological behavior of the compounds. The approach used was based on finding the constants for the Havriliak–Negami equation (equation (3))[11]

$$E*(\omega) = E_\infty + \frac{E_0 - E_\infty}{[1 + ([i\omega\tau])^\alpha]^\beta} \quad (3)$$

where E^* is the complex modulus, ω is the angular frequency, and τ is the relaxation time, E_∞ and E_0 the high and low frequency limits, correspondingly, and α and β curve shape parameters.

This method has previously been applied to study the α-transition (T_g) of plasticized polyvinylchloride (PVC) and carbon black (CB) filled neoprene,[12] unfilled copolyester and its nanosilicate filled variant,[13] and polycarbonate and polyether ether ketone thermoplastics.[14] Besides the glass transition (α transition), also secondary transitions below T_g of ethylene–norbornene copolymers[15] have been studied with this approach.

Results and discussion

To determine the amount of CNTs which was effectively transferred into the rubber composites by masterbatch dilution process, TGA was done. The results obtained from this experiment are shown in Figure 1. Degradation of the composite took place in two steps: the first degradation step occurs in between 400°C and 550°C which is associated with the degradation of the polymer chains, and the second step takes place between 550°C and 650°C. This second degradation process can be ascribed to the oxidative decomposition of CNTs. The residue which is left in the pan is the amount of inorganic ingredients used in the compounding recipe. Based on the TGA data, the experimentally obtained CNT contents correspond well to the amount which was considered in the mixing process as seen in Table 1.

The most interesting observation of the TGA study was the overall increase in the degradation temperature of the rubber polymer. The thermal stability of the composites was found to improve nearly 10°C compared with the gum compound. This effect is found for all CNT-filled composites indicating good rubber-filler interaction.

To understand the effect of the addition of CNTs on the curing behavior, rheometric studies were performed (Figure 2). The curing parameters obtained from the

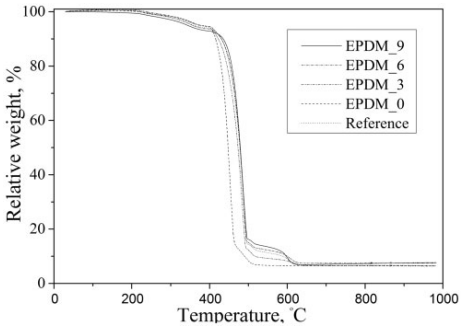

Figure 1. Thermal decomposition of the CNT-filled EPDM compounds.

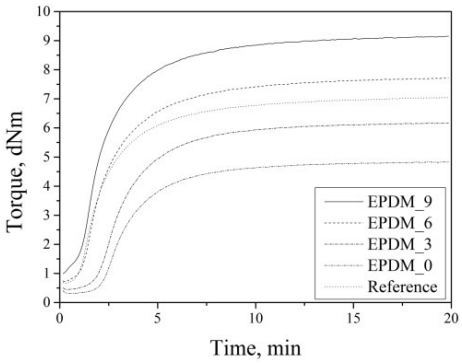

Figure 2. The effect of the CNT concentration and the mixing method on curing behavior of EPDM.

curves are presented in Table 2. The cure rate index (CRI) which is a measure of the fastness of the cure can be calculated with the equation

$$CRI = \frac{100}{t_{90} - t_2} \tag{3}$$

where t_{90} is the optimum curing time and t_2 is the scorch time.

As can be seen in Figure 2, the increase in the rheometric torque of pure EPDM rubber is lower compared with filled compounds. With the increasing CNT concentrations, the torque values are increasing. Generally, presence of reinforcing fillers in soft rubber compounds enhances the rheometric torque which is explained by strong rubber–filler interactions. Besides the hydrodynamic effect of the filler particles, the formation of filler–filler network also contributes to higher torque values, and the effect can be observed from the minimum rheometric torque level.

Table 2. Curing data.

Name	t_2, min	t_{90}, min	CRI, 1/min	Delta torque, dNm
EPDM_0	1.6	7.6	16.7	4.5
EPDM_3	1.3	7.2	16.9	5.6
EPDM_6	0.7	6.7	16.7	7.0
EPDM_9	0.4	6.2	17.2	8.2
Reference	0.7	6.4	17.5	6.4

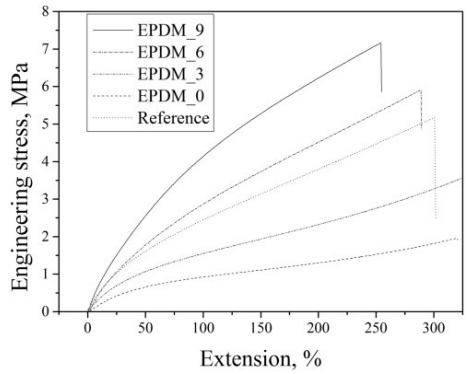

Figure 3. The effect of the CNT concentration and the mixing method on stress–strain behavior of EPDM.

The CRI (Table 2, column 4) increases at higher CNT concentrations. This indicates that the CNTs accelerate curing. In addition, the scorch time shortening with increasing CNT loading is notable; it is possible that this is due to remaining metal catalysts (e.g., Fe, Co, Ni)[16] from CNT production interfering with the onset of the curing reaction.[5] The reference compound shows higher CRI values than the corresponding masterbatch compound. Thus, the mixing method has some influence on the curing kinetics. As previously discussed by Kummerlöwe et al.[5] for CNT-filled NBR and SBR, competing mechanisms affect the cure process when CNTs are added, and the influencing factors include increased thermal conductivity, adsorption of accelerators and polymers on the CNT surface, and also the residual metal contaminants and CNT surface functionalities,[5] making it difficult to separate the effects.

Typical stress–strain curves of the masterbatch compounds and the reference are shown in Figure 3. The tensile properties derived from these curves are given in Table 3. The Young's modulus was calculated from the stress–strain curve within the linear range used for the slope determination (2–12% elongation for all materials).

Table 3. The mechanical properties of the CNT-filled EPDM compounds.

Sample	Tensile strength (MPa)	Elongation at break (%)	100% modulus (MPa)	Young's modulus (MPa)	Hardness (Shore A)
EPDM_0	2.1 ± 0.1	280 ± 30	1.0 ± 0.1	2.2 ± 0.1	42 ± 2
EPDM_3	3.5 ± 0.1	300 ± 20	1.6 ± 0.1	3.1 ± 0.5	49 ± 1
EPDM_6	5.5 ± 0.2	290 ± 20	2.7 ± 0.1	4.8 ± 0.3	53 ± 2
EPDM_9	7.0 ± 0.3	270 ± 10	3.9 ± 0.3	6.5 ± 0.4	57 ± 1
Reference	5.1 ± 0.2	290 ± 10	2.4 ± 0.1	4.5 ± 0.1	54 ± 1

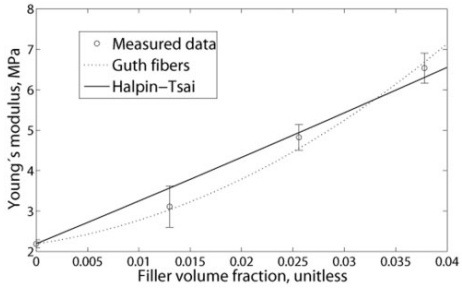

Figure 4. Young's modulus values of CNT-filled EPDM fitted with Guth and Halpin–Tsai equations.

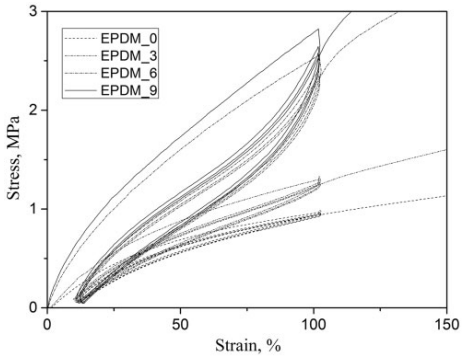

Figure 5. Cyclic stress–strain curves of the CNT-filled EPDM rubbers.

Table 4. Hysteresis areas, arbitrary units.

Sample	1st/2nd	2nd/3rd	3rd/4th
EPDM_0	5.6	0.8	1.1
EPDM_3	11.2	1.6	1.14
EPDM_6	46.0	3.9	2.01
EPDM_9	51.6	5.0	1.60

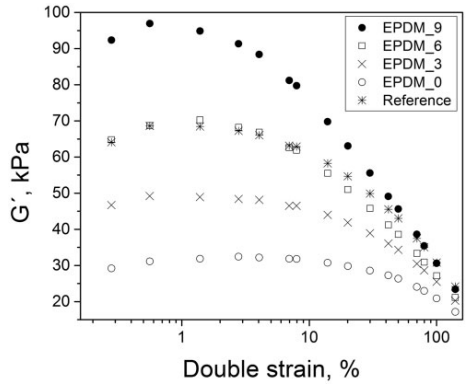

Figure 6. Storage moduli of the EPDM compounds as a function of dynamic strain (strain sweep analysis).

It is clear from the Table 3 that with the increasing content of CNTs the tensile strength of the composites increases whereas the elongation at break values do not alter much. As expected, the stress at 100% strain increased monotonically with the increase in the filler content. A 4-fold increase in the 100% modulus can be observed when the EPDM was filled with 9 phr of CNTs. Similarly, the Young's modulus increased steadily with increasing filler content. As far as the tensile properties of directly mixed compounds (reference) are compared with EPDM_6, significant variation could not be observed as the tensile strength values and other properties remain almost unaltered. This observation leads to the conclusion that the reinforcing effect of CNTs is not affected by the two-step mixing process. Particularly, a longer mixing time could break or damage the CNTs resulting in shorter tubes with a lower aspect ratio. Though the total mixing time of masterbatch procedure is longer than of the direct mixing process, the tubes apparently did not suffer much from the extra high shear mixing period. Shore A hardness values are not influenced by the way of mixing as seen in Table 3. Again it indicates that the

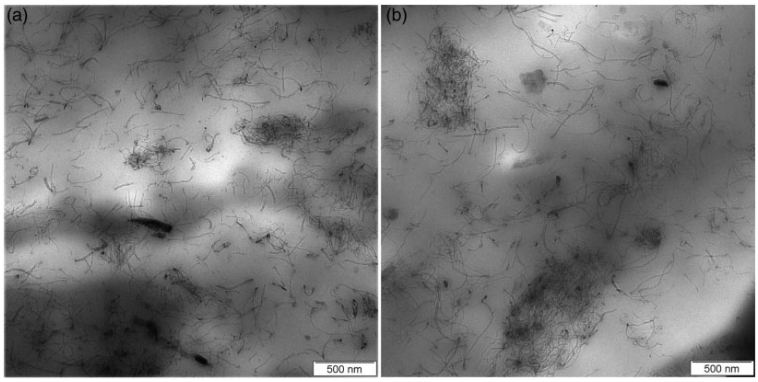

Figure 7. TEM images of the samples prepared by different mixing processes. (a) EPDM_6, masterbatch-mixing, (b) directly mixed reference.

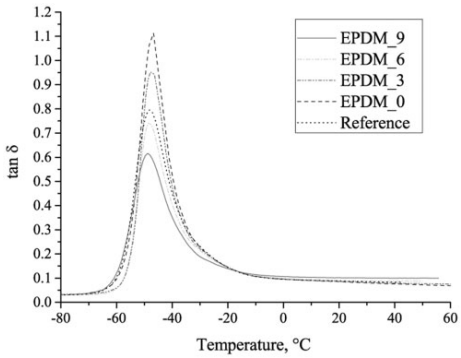

Figure 8. Loss angle (tan δ) of EPDM compounds as a function of temperature.

Table 5. Calculated values for the Havriliak–Negami parameters.

Sample	α	β	E_∞, GPa	E_0, MPa
EPDM_0	0.61	0.21	3.4	11
EPDM_3	0.62	0.19	3.7	21
EPDM_6	0.55	0.23	4.3	42
EPDM_9	0.51	0.23	4.9	73
Reference	0.57	0.22	3.4	29

masterbatch dilution process did not affect the reinforcing capabilities of CNTs.

Calculated moduli values using Guth and Halpin–Tsai models were compared to the measured Young's moduli of the compounds (Figure 4). It can be seen that the Guth's model gives mathematically the best fit. One difference between the Halpin–Tsai and the Guth model is that the modulus predicted by the former for high filler loadings is fixed for a volume fraction of 1.00. Therefore, at higher filler concentrations Halpin–Tsai model predicts lower modulus values than measured values. Guth's model does not have this anchoring and the results corresponds better the experimentally measured values.

The tensile stress softening of the compounds can be seen in the curves presented in Figure 5. The hysteresis, that is, stress–strain difference between consecutive stretch paths, was quantified and the results are shown in Table 4. It was found that the higher the CNT content, the greater the hysteresis loss, as expected for filled compounds, and leading to lower resilience. Several mechanisms have been suggested contributing to the large stress softening in CNT reinforced elastomers. The main causes include the breakage of the CNT filler network during the first extension, the reduction of the number of the elastically active polymer chains, which is typically called Mullins effect in CB filled systems, and the changing orientation of the CNTs. The latter one has been suggested being observable in an increase in the effective modulus.[17] In this context, it is interesting to discuss the observation that mechanical properties are arising from the reinforcing effect of the CNTs at lower concentrations when compared to conventional fillers like CB and silica,[17] as the formation of a percolating network will influence the stress–strain behavior. As illustration, for a CNT reinforced SBR/BR blend the electrical percolation limit was shown to lie between 1 and 2 phr for CNTs with an aspect ratio of 50–60.[18] Such low percolation limits have been confirmed for other elastomeric systems as well. Another example is SBR filled with different types of CNTs, where the percolation limits

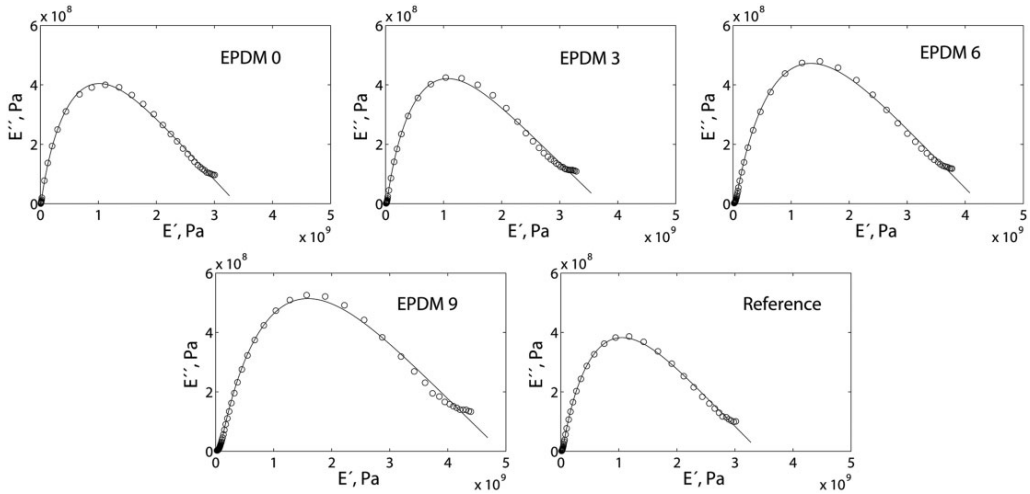

Figure 9. Cole-Cole plots of (a) EPDM_0, (b) EPDM_3, (c) EPDM_6, (d) EPDM_9, (e) reference. The values were obtained from dynamic mechanical thermal analysis of the rubber samples.

were less than 1 phr.[19] In the latter study, it was also noticed that besides the aspect ratio, the nature of the CNTs and their ultimately structural quality affect this limit as well.[19]

The extent of filler–filler interactions as measured by the Payne effect is shown in Figure 6. This effect can directly be correlated with the strength of the filler–filler network in a soft rubber matrix. It is measured by calculating the difference between the storage modulus at low strain (maximum value) and at high strain. It is observed that the strain dependence on directly mixed compounds is identical to the correlation measured for the masterbatch-diluted material, indicating a similar filler–filler network structure.

Based on the TEM imaging (Figure 7), both, the EPDM_6 and the directly mixed reference, contained well-dispersed CNTs as well as agglomerates. From direct TEM analysis, calculated average aspect ratios were similar to the masterbatch and directly mixed materials, 25 ± 11 ($n = 212$, EPDM_6) and 26 ± 14 ($n = 229$, reference), respectively. Thus, the mixing method did not affect the aspect ratio. The aspect ratio was also determined by the equations described by Guth (equation (1)), and verified with Halpin–Tsai equation (equation (2)).

The aspect ratios obtained from the fitting were: $L/d = 25$ from the Guth equation, $L/d = 116$ according to the orthotropic Halpin–Tsai equation whereas the initial aspect ratio given by the supplier was 158. Thus, it seems that the CNT tubes are broken during the mixing of the compounds resulting in a lower aspect ratio. It is also possible that the modeling describes mainly the length of the effectively reinforcing sectors of the CNTs rather than the actual length. Moreover, it is interesting to note that the value obtained by the Guth equation resembles the values determined directly from TEM images.

Based on the DMTA measurements (tan δ curves shown in Figure 8), only small differences were found between the glass transition temperature (T_g) values of the different compounds. The T_g values based on the tan δ curve of all compounds are found to be similar $\sim -48^{\circ}C$.

According to the fitting of the Havriliak–Negami equation (equation (3)) to the data obtained by dynamic mechanical analysis we have followed the procedure as described by Szabo and Keough.[12] The fitting yielded the values of the Havrialiak–Negami parameters α, β, E_∞, and E_0 and is shown in Table 5. The graphical representations of the fitted curves together with experimental data are also shown in Cole–Cole plots[20] (Figure 9). The parameters show a good fit for tan δ on the high frequency end, but deviate from the experimental values at the low frequency end.

With the increase of the CNT content α value is lower (asymmetric nature of the Cole–Cole plot), but there is no clear effect on the β value (the broadness of the Cole–Cole plot). This indicates that the low frequency behavior, that is, intermolecular motion, of the CNT filled EPDM is affected by the CNT content (change in α), while the high frequency behavior, that is, small scale molecular motions, is not affected.[13,17,21] Thus, presence of small amount of CNT affects the molecular dynamics in the rubbery region. The E_0 and E_∞ values increase when raising the CNT content. The directly mixed reference has α and β values close to the masterbatch mixed

compound EPDM_6, but the E_0 and E_∞ are notably lower. Thus, based on the Havriliak–Negami parameters, it can be said that presences of small amount of CNTs affect the molecular motion during the glass to rubber transition of the polymer chains.

Conclusions

The masterbatch mixing process allows the preparation of the compounds with the high level of CNTs which can be embedded in the continuous carrier setting free CNTs to a much smaller extent in the second step, the dilution to the desired concentration. The preparation of the CNT-elastomer composites is thus more controlled and less problematic in comparison with the conventional one-step mixing process. Furthermore, weighting and handling of the neat masterbatch is easier and filling of the mixer takes place faster and is cleaner.

The extra mixing step of masterbatch mixing does not negatively influence the properties of the composite compared to the direct mixing method: Based on the mechanical and thermal characterization, the properties of the masterbatch mixed compounds are very similar to what is obtained with direct mixing. Therefore, the masterbatch technique is useful to get better and healthier working environment.

Micromechanical fitting provided an estimation of the aspect ratio in the cured compound to be 25, which was supported by the TEM image analysis. This value is significantly lower than the original value of the CNTs indicating the breakage of the nanotubes during the mixing process. The filler–matrix and filler–filler interaction increase when the compound becomes more loaded, as seen in the Payne effect. Based on the Havriliak–Negami fitting with the data obtained from dynamic mechanical analysis, the CNT affects the molecular motion in the rubbery region.

Declaration of conflicting interests

The author(s) declared no potential conflicts of interest with respect to the research, authorship, and/or publication of this article.

Funding

The author(s) disclosed receipt of the following financial support for the research, authorship, and/or publication of this article: This work was financially supported by Finnish Funding Agency for Technology and Innovation (TEKES) under project #40352/08.

References

1. Das A, Jurk R, Stöckelhuber KW, et al. Nanoalloy based on clays: intercalated-exfoliated layered silicate in high performance elastomer. *J Macromol Sci Part A Pure Appl Chem* 2008; 45: 144–150.
2. Ghosh S, Sengupta RA and Heinrich G. High performance nanocomposite based on organoclay and blends of different types of SBR and BR. *Kaut Gummi Kunsts* 2011; 1–2: 48–54.
3. Mercer RR, Hubbs AF, Scabilloni JF, et al. Pulmonary fibrotic response to aspiration of multi-walled carbon nanotubes. *Part Fibre Toxicol* 2011; 8: 21.
4. Tkach AV, Shurin GV, Shurin MR, et al. Direct effects of carbon nanotubes on dendritic cells induce immune suppression upon pulmonary exposure. *ACS Nano* 2011; 5: 5755–5762.
5. Kummerlöwe C, Vennemann N, Yankova E, et al. Preparation and properties of carbon nanotube composites with nitrile- and styrene-butadiene rubbers. *Polym Eng Sci* 2013; 53: 849–856.
6. Kim JH, Kim YJ, Baek WK, et al. Flexible strain sensor based on carbon nanotube rubber composites. *Nanosens Biosens Info-Tech Sens Syst* 2010; 7646. DOI: 10.1117/12.847364.
7. Kim JH, Kim J, Kang I, et al. A strain positioning system using carbon nanotube flexible sensors for structural health monitoring. *2010 International Conference on Nanotechnology and Biosensors IPCBEE* 2011; 2: 38–41.
8. Guth E. Theroy of filler reinforcement. *J Appl Phys* 1945; 16: 20–25.
9. Halpin JC. Stiffness and expansion estimates for oriented short fiber composites. *J. Compos Mater* 1969; 3: 732–734.
10. Saatchi MM and Shojaei A. Mechanical performance of styrene-butadiene-rubber filled with carbon nanoparticles prepared by mechanical mixing. *Mater Sci Eng A* 2011; 528: 7161–7172.
11. Havriliak S and Negami S. A complex plane analysis of α-dispersions in some polymer systems. *J Polym Sci C* 1966; 14: 99–117.
12. Szabo JP and Keough IA. Method for analysis of dynamic mechanical thermal analysis data using the Havrialiak–Negami model. *Thermochim Acta* 2012; 392–393: 1–12.
13. Kalgaonkar RA, Nandi S, Tambe SS, et al. Analysis of viscoelastic behavior and dynamic mechanical relaxation of copolyester based layered silicate nanocomposites using Havriliak–Negami model. *J Polym Sci B* 2004; 42: 2657–2666.
14. Setua DK, Gupta YN, Kumar S, et al. Determination of dynamic mechanical properties of engineering thermoplastics at wide frequency range using Havriliak–Negami model. *J Appl Polym Sci* 2006; 100: 677–683.
15. Makrocka-Rydzyk M, Nowaczyk G, Glowinkowski S, et al. Dynamic mechanical study of molecular dynamics in ethylene–norbornene copolymers. *Polymer* 2010; 51: 908–912.
16. Rama R (ed). *Handbook of innovation in the food and drink industry*. New York: Haworth Press, 2008.
17. Bhattacharyya S, Sinturela C, Bahloula O, et al. Improving reinforcement of natural rubber by networking of activated carbon nanotubes. *Carbon* 2008; 46: 1037.
18. Das A, Stöckelhuber KW, Jurk R, et al. Modified and unmodified multiwalled carbon nanotubes in high

performance solution-styrene-butadiene and butadiene rubber blends. *Polymer* 2008; 49: 5276–5283.
19. Tsuchiya K, Sakai A, Nagaoka T, et al. High electrical performance of carbon nanotubes/rubber composites with low percolation threshold prepared with a rotation-revolution mixing technique. *Compos Sci Technol* 2011; 71: 1098–1104.
20. Cole KS. Electric phase angle of cell membranes. *J Gen Physiol* 1932; 15: 641–649.
21. Havriliak S Jr. Chain dynamic parameters for some actylic polymers. *Coll Polym Sci* 1990; 268: 426–439.

Publication VI

Maija Hoikkanen, Minna Poikelispää, Amit Das, Mari Honkanen, Wilma Dierkes, Jyrki Vuorinen

Effect of multiwalled carbon nanotubes on the properties of EPDM/NBR dissimilar elastomer blends

Polymer-Plastics Technology and Engineering, *54 (2015) 402-410*

Polymer-Plastics Technology and Engineering, 54: 402–410, 2015

ISSN: 0360-2559 print/1525-6111 online
DOI: 10.1080/03602559.2014.958775

Effect of Multiwalled Carbon Nanotubes on the Properties of EPDM/NBR Dissimilar Elastomer Blends

Maija Hoikkanen[1], Minna Poikelispää[1], Amit Das[1,2], Mari Honkanen[1], Wilma Dierkes[1,3], and Jyrki Vuorinen[1]

[1]*Department of Materials Science, Tampere University of Technology, Tampere, Finland*
[2]*Leibniz Institute of Polymer Research Dresden, Dresden, Germany*
[3]*Department of Elastomer Technology and Engineering, University of Twente, Enschede, The Netherlands*

GRAPHICAL ABSTRACT

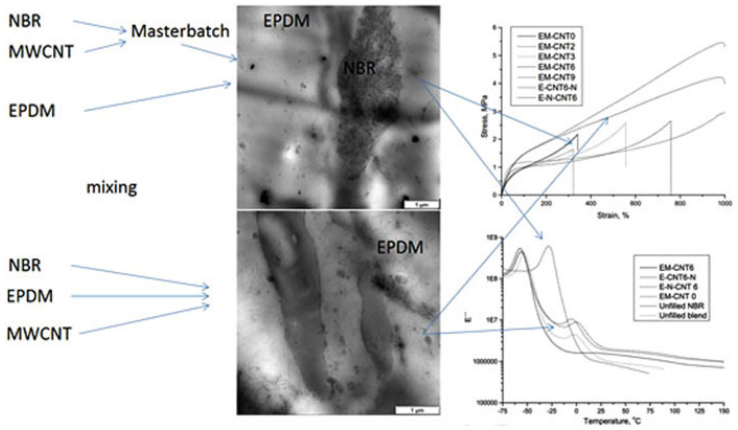

In the presence of multiwalled carbon nanotubes (MWCNT), polar nitrile-butadiene rubber (NBR) and nonpolar ethylene propylene diene rubber (EPDM) blends were prepared following a melt mixing method. For the preparation of MWCNT filled EPDM/NBR blends, two mixing methods were used: direct mixing and the masterbatch dilution method. Various physical, mechanical, and morphological properties are explored to elucidate the dispersion behavior of MWCNTs. It was concluded that the preparation method influences the dispersion of the nanotubes in different rubber phases and the properties of these blends are controlled by the degree of dispersion of the nanotubes in the two phases.

Keywords Compatibilization; Co-vulcanization; Elastomer blends; Mechanical properties; MWCNT

INTRODUCTION

Carbon nanotubes (CNTs) have a high potential as nanoscaled reinforcing filler for rubber compounds due to their high aspect ratio and unique properties arising from the rigid chemical structure of the carbon network. However, the mixing of these carbon based nanofillers with elastomers is not as easy as mixing with carbon black due to different reasons: The first and main reason is that CNTs tend to form bundles and agglomerates, making dispersion of the tubes in a soft polymer matrix very difficult. To achieve the desired mechanical properties of the elastomeric composites, these difficulties need to be overcome. A lot of research has been done to solve this problem, but until now an effective and industrially viable technique for the dispersion of CNTs in rubber is still missing.

Address correspondence to Prof. Jyrki Vuorinen, Tampere University of Technology, Department of Materials Science, P.O. Box 589, 33101 Tampere, Finland. E-mail: jyrki.vuorinen@tut.fi

Most methods were developed on the basis of solution mixing, but for industrial applications this is not feasible.

The masterbatch dilution technique is a promising way to disperse CNTs in a rubber matrix. This approach has been previously used for nanocomposites of montmorillonite layered silicate in solution styrene butadiene rubber (S-SBR), where the silicate was first preblended with carboxylated nitrile rubber (XNBR),[1,2] a rather polar rubber which was used as carrier to bring more exfoliated and intercalated silicate into the relatively nonpolar S-SBR rubber. It was reported that the presence of XNBR in the final compound did not affect the mechanical properties of the composites since the concentration of this polymer was very low.

The same principle was also explored in a different system of a layered silicate-XNBR masterbatch in a SBR/butadiene rubber (BR) nanocomposite, and the effects of several material parameters and mixing techniques were evaluated.[3] Finally, it was found that an internal mixer provided the best mechanical properties of the final SBR/BR nanocomposite compared to two-roll and solution mixing techniques.[2] Until now the masterbatch dilution technique has not been explored with the dispersion of MWCNTs in soft rubbers.

As the toxicity of these nanoparticles for the human body [4,5] is an issue, precautions are needed to avoid contamination of the working area with these nanoparticles. In this process, only during the preparation of the highly filled masterbatch carbon nanotubes can be set free. However, this blending step is highly controlled in order to minimize contamination of the environment. Later, this masterbatch is diluted to a desired level. In this work, the masterbatch dilution method was adopted, and a suitable mixing approach of MWCNTs in a soft rubber matrix was elaborated.

Besides, a potential compatibilization effect of MWCNTs in this blend is one of the research topics of this article. A few examples can be found where the compatibility effect of different type of fillers is discussed. For instance, polychloroprene (CR)/ethylene propylene diene rubber (EPDM) reinforced with layered silicates showed no change in the glass transition temperatures (Tg) either of the elastomers by the addition of the silicates.[6] A similar kind of report can be found for EPDM/nitrile rubber (NBR) blends with a conventional carbon black filler [7] and nanosized silica.[8]

However, a contrary effect was reported on compatibilization of EPDM/CR by quarternary ammonium salt modified montmorillonite nanosilicate,[9] diminishing the difference between the glass transition temperatures of the elastomers. In this case, the nanosilicate was located in both, the bulk and the interface between the two polymers, reducing the interfacial energy.[9] In this present article, the dispersion of carbon nanotubes by masterbatch dilution process is explored. Additionally, the effects of carbon nanotubes on the rubber blend compatibility were also studied.

EXPERIMENTAL

Compounding and Sample Preparation

EPDM, Keltan 512 (Lanxess), and NBR, Europrene N3330 (Versalis S.p.A), were used in this study. Multiwall carbon nanotubes (NC7000) were purchased from Nanocyl (Belgium), and used as received. Based on the manufacturer's information, the average MWCNT diameter is 9.5 nm, and the length is 1500 nm.[10]

The compounds prepared from the masterbatch as well as the directly mixed ones are shown in Table 1. As curative system, 5 phr ZnO, 2 phr stearic acid, 2 phr Zinc dibutyldithiocarbamate (ZDBC), 1 phr N-Cyclohexyl-2-benzothazolesulfenamide (CBS) and 1 phr sulphur were added to each compound. All chemicals used were typical grades for industrial rubber manufacturing.

For the masterbatch series, the masterbatch of NBR and MWCNTs was first prepared in an internal mixer (Brabender

TABLE 1
Composition of the EPDM/NBR compounds

Sample Name*	EPDM, phr	NBR, phr	NBR-CNT Masterbatch, phr	CNT, phr	Final CNT content, Phr
EM-CNT 0	100	0	0	0	0
EM-CNT 2	96.8	0	4.8	0	1.6
EM-CNT 3	93.6	0	9.6	0	3.2
EM-CNT 6	86.8	0	19.5	0	6.3
EM-CNT 9	80.4	0	28.9	0	9.3
E-CNT 6-N**	87	13	0	6.3	6.3
E-N-CNT 6**	87	13	0	6.3	6.3
E-N-gum	87	13	0	0	0
EM-CNT 6 2 steps	87	0	19.5	0	6.3
N-gum	0	100	0	0	0

*EM stands for EPDM mixed with NBR-MWCNT masterbatch.
**Different mixing sequences.

N 350 E) with a composition of 2:1 in weight. The masterbatch was then further blended with EPDM. The resulting compounds had MWCNT contents ranging from 1 phr to 9.3 phr. The mixing protocol of the dilution stage was as follows: Rotor speed: 70 rpm; Start temperature: 50°C; Dump temperature: 160°C; or Maximum time: 5 min (6 min in the case of the unfilled blend).

Finally, the curatives were added in an open two-roll mill. All the directly mixed filled compounds were prepared with MWCNT contents of 6 phr. With this particular loading, two different blends with identical composition were prepared. The mixing sequence of the blend of the compound named E-CNT 6-N was EPDM – MWCNTs - NBR, whereas for E-N-CNT 6 compound the sequence was EPDM – NBR – MWCNTs.

As the differences in the curative affinity of the elastomers may affect the respective elastomer cross-link densities, a compound was prepared in two steps: a NBR-MWCNT masterbatch was mixed with sulphur before the addition of EPDM, which was premixed with accelerators (EM-CNT 6 2 steps). Cured samples with a thickness of 2.3 ± 0.1 mm were prepared by compression molding at 160°C with their respective curing time ($t_{90} + 2$ min).

Characterization

The curing behavior and the Payne effect of the uncured compounds were studied with an Advanced Polymer Analyzer (APA 2000, Alpha Technologies). Curing studies were performed at 160°C at ±0.2° strain and 1.7 Hz frequency. The Payne effect was studied with a strain sweep from 0.28% to 140% at 100°C.

The MWCNT content was checked by thermogravimetry (TGA). Perkin Elmer STA 6000 equipment was used for the measurements, which were conducted in air with a heating ramp from 30°C to 995°C at rate of 10 K/min. The amount of MWCNTs was determined from the weight loss step measured at 550–650°C.

Tensile properties were determined according to ISO 37 with a dumbbell specimen type 1. Tests were performed with a Messphysik Midi 10-20 universal tester and contact extensometer. The Shore A hardness was recorded according to ASTM D 2240 – 00 with an AFFRI Hardness tester, stand Type 1, at 3 sec. Five parallel measurements were taken for tensile and hardness values. For comparing the surface properties of the cured rubber, the water contact angles were measured with 5-µl drops of 18.2 MΩ water. The water drop profiles were recorded with a goniometric system (Photocomp, Finland).

The apparent cross-link densities for the compounds were determined by swelling experiments. Approximately 0.4 g samples were cut from the vulcanized sheets and weighted. The samples were immersed in toluene for 96 h and reweighted in saturated swollen state, after which the samples were dried at room temperature for 72 h and the dry weight was then re-checked. The swelling value, Q, the ratio of the uptake of toluene in the sample to the original sample elastomer mass, was calculated. The reciprocal of the swelling value, 1/Q, equals the apparent cross-link density. Two specimens per compound were studied.

The thermo-mechanical behavior of the cured compounds was examined by dynamic mechanical thermal analysis (DMTA). The measurements with a Perkin Elmer Pyris Diamond were performed from −80°C to + 70°C at a heating rate of 3 K/min and a frequency of 1 Hz. The DMTA measurements were started in force control in the glassy state, and changed to displacement control after initial reduction of the modulus corresponding to the glass transition. The displacement limit was set to $\Delta L = 40$ µm, and with sample length of 20 mm, the samples experienced 0.2% maximum strain during the measurement.

A field emission scanning electron microscope (FESEM), Zeiss ULTRAplus, was used to analyse the fracture surfaces of selected compounds. The failure surfaces were prepared by a Charpy impact hammer hit on liquid nitrogen cooled rubber strips. Transmission electron microscopy images were taken with the instrument Limca 200MS (Germany). The images were taken at an acceleration voltage of 200 kV. The ultra-thin sections of the samples were prepared with a Leica Ultracut UTC at −120°C (under liquid nitrogen).

RESULTS AND DISCUSSION

The plots of thermal degradation behavior are shown in Fig. 1. The TGA data confirmed the MWCNT content to be very close to expected concentrations. However, the MWCNT content in the directly mixed compounds is in every compound a bit lower than calculated, while for the masterbatch specimens there is no such tendency. This means that in the masterbatch dilution technique the transfer of MWCNTs is more quantitatively, whereas for direct mixing some MWCNTs are lost during mixing. It is observed that the composites are decomposing in several steps. The temperature range for main chain degradation of EPDM filled with MWCNTs is always higher than that of pure EPDM: The

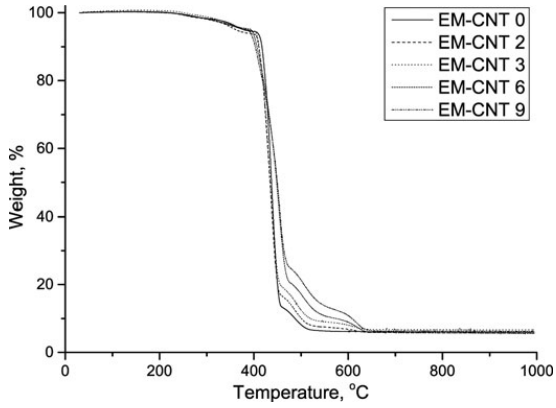

FIG. 1. Thermogravimetric analysis of vulcanised rubber compounds.

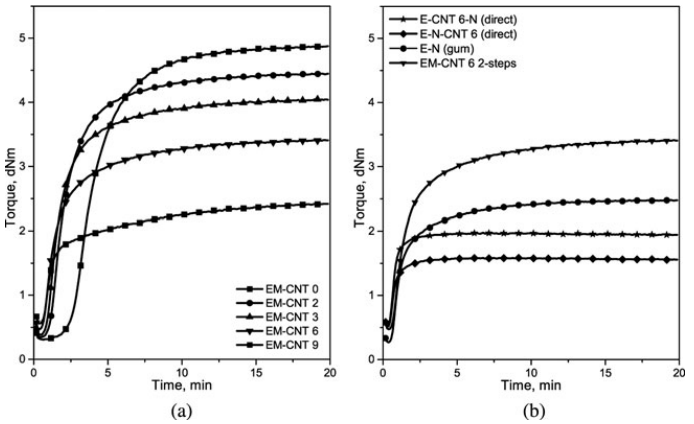

FIG. 2. Rheometric curves of EPDM/NBR filled with MWCNTs measured at 160°C a) masterbatch mixing, b) reference compounds.

active surface of MWCNTs is interacting with the rubber chains and enhancing the thermal stability.

Curing curves of the compounds are presented in Fig. 2. As can be seen from Fig. 2a, the maximum rheometric torque of pure EPDM rubber is higher compared to the MWCNT-filled composites. Thus, with the increase of masterbatch content, the torque is decreasing. Generally, increased filler loading increases the torque, the maximum value but also the minimum value. However, in this case, the carrier of the fillers, polar NBR, affects the morphology of the blend: a heterogeneous blend morphology is formed with the nonpolar EPDM.

The curatives are expected to have a higher affinity to the polar polymer, resulting in an over proportional high concentration in NBR and a low concentration in EPDM. EPDM, the major phase, is successively more undercured, and the final torque is therefore decreased.[11] With the increase of the masterbatch content, the onset of cure is shortening. Some reports are found where the MWCNTs enhanced the rate of the sulphur vulcanization process.[12] It was described that the presence of a about ~10 wt.% of metal oxides in the MWCNTs facilitated the sulphur vulcanization process.

To understand the effect of the dilution technique on the dispersion and reinforcing behavior, some compounds were prepared by the direct mixing technique for comparison. The rheograms of these compounds are shown in Fig. 2b. A relatively low torque value is observed for the EPDM-NBR blend. The composition of these blends was similar to the masterbatch mixed compound EM-CNT 6. However, incorporation of MWCNTs directly to the compounds significantly affects the final vulcanization stage by lowering the torque values. A substantial amount of curatives end up in or migrats to one of the two phases, or are adsorbed on the filler, causing this effect. Filler distribution is also expected to be inhomogeneous.

Even if the addition of the curatives in the masterbatch dilution mixes was done at the end of the mixing process, it did not affect the curing properties as much as it did for the directly mixed compounds. To study the curative migration, a compound (EM-CNT 6 2-steps) was made in which the accelerators were incorporated in the EPDM rubber at the very beginning of the mixing process, and sulphur was mixed with the NBR/MWCNTs masterbatch before the addition of the EPDM/accelerator blend. This premixing forces the polar accelerators into the less polar rubber, EPDM. In this case, no change in the curing is process is noticed.

Dynamic viscoelastic responses such as storage modulus and loss modulus of the filled elastomeric materials depend not only on temperature and frequency applied to the materials, but also on the magnitude of strain. These strain-dependent dynamic properties can only be found in filled rubbers. At a certain strain, the filler-filler network is broken and a decrease of the storage modulus is observed. The difference between the storage modulus at low deformation and storage modulus at higher deformation is called the Payne effect. A gum rubber without any filler generally does not show such an effect. Measurement of strain sweep analysis indicates how strong the filler-filler network is.

This nonlinear strain-dependency of the composites was also investigated and the results are shown in Fig. 3. It is observed that the storage modulus at low strain increases with increasing masterbatch content indicating a stronger filler-filler network due to a higher amount of MWCNTs. Therefore, a relatively low quantity of MWCNTs can establish filler-filler networks, and the effect is reflected in the strain sweep measurements. It is worth mentioning that for classical carbon black-filled compounds, the Payne effect can only be seen at high concentrations of carbon black (more than 20 phr). But in this case the effect is noticed at lower filler loadings. As far as the Payne effect of the unfilled EPDM/NBR blend is concerned, the Payne effect was not observed (Fig. 2b), which is expected for unfilled compounds.

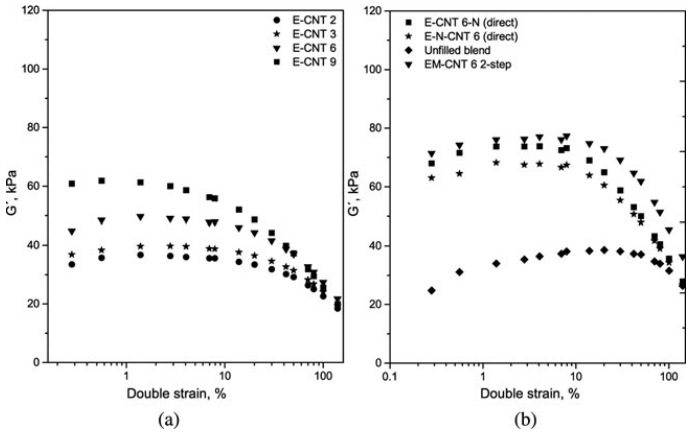

FIG. 3. Strain sweep analysis of the EPDM/NBR compounds filled with MWCNTs.

A different behavior was noticed when the compounds were produced in different ways. The directly mixed compounds showed higher Payne effects than the compounds mixed via the masterbatch method. Thus, the MWCNT-MWCNT interaction is smaller in the compounds produced by the masterbatch method. The compounds did not show a percolated network, which was revealed by DC electrical conductivity studies: all compounds showed resistivities in the range of 10^{12} ohm*cm. Thus, the filler-filler network developed here did not form a continuous network throughout the rubber, but was localized in certain regions of the matrix.

The trend seen for the masterbatch mixed compounds is in contradiction with the results of Subramaniam et al.[13]. In this article, it is described that a better dispersion results in a higher Payne effect due to tubular nature of the fillers. However, in the present case a dissimilar polymer blend was used, in which the tubes are not dispersed throughout the complete matrix, but the MWCNTs were preferentially located in some regions of the matrix resulting in high local concentrations in some particular areas of the rubber matrix. Additionally, the Payne effect is well defined for fillers in single polymers; it is not very clear how the Payne effect has to be interpreted in blends.[14]

The hardness values of the composites changed after addition of MWCNTs. With addition of 9 phr MWCNTs the Shore A hardness increased by 5 units (Table 2). The hardness values of the directly mixed compounds are even higher than the masterbatch mixed compounds with the same loading of MWCNTs.

The results from stress-strain experiments are also presented in Table 2. It is clear from the table, that the tensile strength, 100% modulus, and 200% modulus did not alter much, but elongation at break was increased tremendously with higher amounts of MWCNTs. As the masterbatch compounds contain MWCNTs and NBR, the formed vulcanizates with EPDM are rubber blends. A typical characteristic of a rubber blend is higher elongation at break values, and in the present case the masterbatch diluted compounds are showing higher elongation at break values due to its blend morphology.

As far as the mechanical properties of the directly mixed compounds are concerned, the moduli values and tensile

TABLE 2
Mechanical properties of the composites

Mix	Tensile strength, MPa	Elongation at break, %	100% Modulus, MPa	300% Modulus, MPa	Hardness, Shore A	Cross-linking density 1/Q
EM- CNT 0	2.0 ± 0.3	320 ± 40	1.01 ± 0.03	1.87 ± 0.08	43 ± 1	0.17
EM- CNT 2	1.9 ± 0.2	380 ± 50	0.98 ± 0.02	1.55 ± 0.05	44 ± 1	0.15
EM-CNT 3	2.6 ± 0.2	550 ± 20	0.99 ± 0.01	1.38 ± 0.02	45 ± 1	0.13
EM- CNT 6	2.8 ± 0.3	780 ± 20	0.98 ± 0.01	1.17 ± 0.03	46 ± 1	0.10
EM- CNT 9	2.6 ± 0.2	970 ± 20	1.07 ± 0.03	1.17 ± 0.03	48 ± 2	0.08
E-CNT 6-N	4.9 ± 0.6	540 ± 60	1.69 ± 0.08	3.14 ± 0.17	53 ± 0	0.10
E-N-CNT 6	3.6 ± 0.2	630 ± 80	1.61 ± 0.12	2.53 ± 0.26	51 ± 1	0.08

TABLE 3
Water contact angles on vulcanized rubber sheets

Compounds	Contact angle, °
EM-CNT 0	131 ± 2
EM-CNT 2	132 ± 7
EM-CNT 3	105 ± 7
EM-CNT 6	104 ± 6
EM-CNT 9	99 ± 4
E-CNT 6-N	108 ± 3
E-N-CNT 6	101 ± 5
N-CNT-6	104 ± 5

strength are found to be better than the masterbatch compounds at same loading of MWCNTs. Both the tensile strength and hardness observations can be explained by assuming that the MWCNTs are mainly located in the NBR phase of the masterbatch compounds. This conclusion was also made on the basis of the Payne effect values.

Based on the water contact angle values (Table 3), all the compounds had hydrophobic surfaces. The unfilled EPDM compound shows the highest water contact angle indicating the lowest surface energy. With increasing NBR (and simultaneously MWCNT) content, the contact angle decreasies, with a clear step between EM-CNT 2 and EM-CNT 3. With all compounds from the masterbatch series, the droplet shapes were observed to vary occasionally, taken as local variations in the surface composition, also seen in the standard deviations. Thus, the critical EPDM/NBR elastomer ratio for

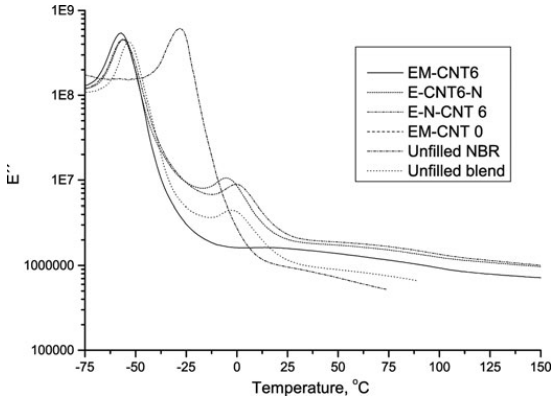

FIG. 4. DMTA curves of the EPDM/NBR compounds filled with MWCNTs.

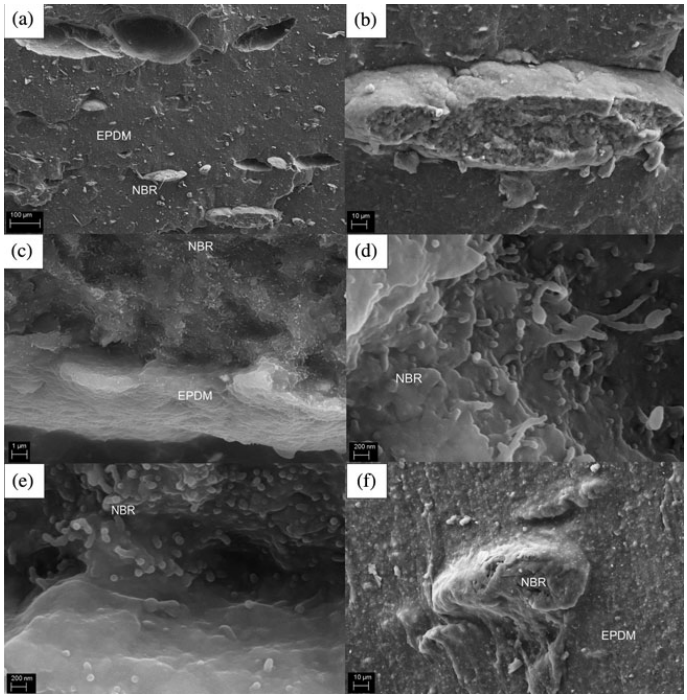

FIG. 5. FESEM images of a-e) EM-CNT 6 and f) E-N-CNT6.

surface properties to be dominated by NBR lies between the 96.7/3.3 and 93.4/6.6.

Based on the 1/Q values, the apparent cross-link densities are reduced by the addition of the NBR/MWCNT masterbatch (Table 2). This is in accordance with the torque values. Due to difference in cure rate of the two rubbers with same kind of curatives, the EPDM phases are remaining in a poor cure state as EPDM is a slow curing rubber. Migration of curatives can take place from the less polar rubber, EPDM, to the more polar rubber, NBR, resulting in overcured NBR and undercured EPDM, as discussed before. The three compounds with 6-phr MWCNTs do not show a significant difference in cross-link density, while the torque values, also an indication of the network density, did show differences. However, the methods of measurement in both cases was rather different: when swelling the material, other material properties such as weak interfaces between polymers and polymer and filler might also play a role and camouflage the differences in cross-link density.

Dynamic mechanical properties of the composites were studied and the glass transition temperature, Tg, of the polymers were evaluated from the loss modulus (E'')-temperature plots (Fig. 4). The pure EPDM (EM-CNT0) showed a glass transition temperature at nearly −50°C, whereas the glass transition temperature of pure NBR was measured at −25°C. The pure gum blend of EPDM and NBR showed two glass temperatures at −50°C and at 1°C: a considerable shift of the glass transition of NBR was observed. Based on the thermodynamic fact that these two elastomers are immiscible, all the elastomeric blend compounds should have shown two glass transition temperatures[15]: one corresponding to EPDM and the other one to NBR. However, after mixing the MWCNT-NBR masterbatch into EPDM (EM-CNT 6), only one glass transition temperature was found, which was very close to the glass transition temperature of EPDM.

This could be explained by highly filled NBR islands, which are no longer rubber-like and do not show glass transition

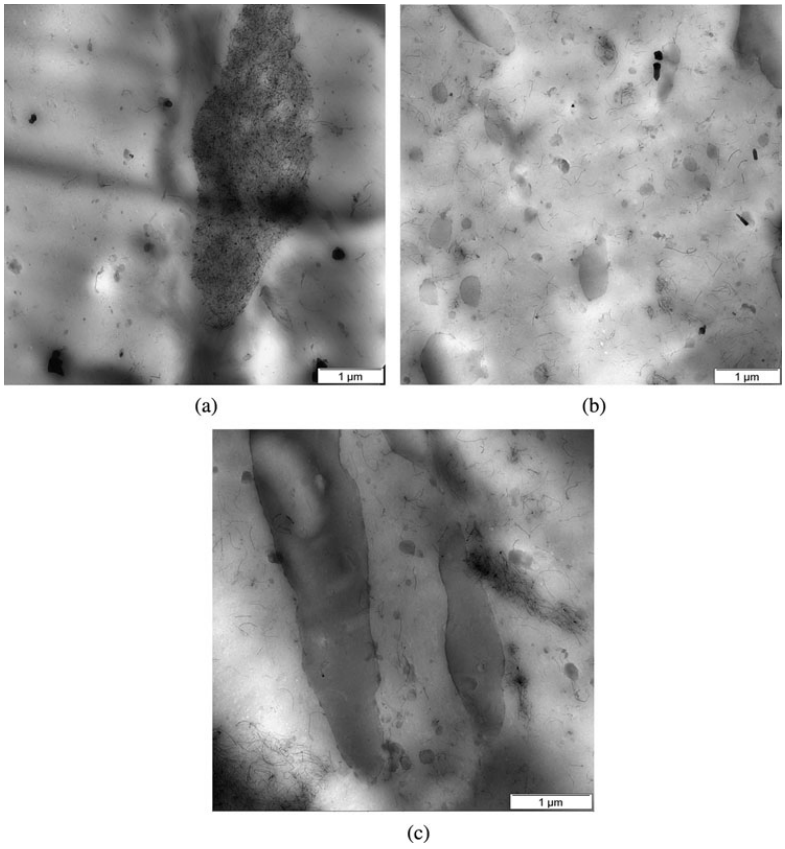

FIG. 6. TEM Images of a) EM-CNT 6 b) and c) E-CNT 6-N.

anymore. However, for directly mixed compounds, two different glass transition temperatures were found: one at nearly −50°C: EPDM, and another one at −3.2 or 0°C, depending on the mixing sequence. Assuming that this glass transition was caused by the NBR phase, a shift of nearly +25°C was measured. An explanation for this effect could be the filler-polymer interaction, which leads to an increase in Tg: The interaction results in a glassy phase around the filler particles, which needs a higher temperature to be relaxed into the rubbery state. Furthermore, a shift of the Tg can be expected if these two peaks are originating from the NBR phase. As also seen from the swelling experiments and other mechanical data, the EPDM phase is remaining in an undercured stage, but simultaneously the NBR phase is overcured, and due to a strongly cross-linked network, the Tg of NBR shifted considerably.

For imaging, the EM-CNT 6 and E-N-CNT 6 were selected, and they were studied in detail by FESEM and TEM. In the masterbatch mixed sample (EM-CNT 6), relatively large islands with clusters of MWCNTs can be found (Fig. 5a–b). Most probably, these are the NBR masterbatch fragments which were used in EPDM rubber and some of the compounds are not mixed or fragmented into smaller units. If these areas are enlarged, bundles of nanotubes can be seen (Fig. 5c–e).

Based on the relative volume fractions and failure surface ductility, the discontinuous phase was assigned as the NBR-MWCNT phase, and the continuous phase as EPDM. Presence of MWCNTs in the EPDM phase is not clearly observed. For the compound prepared in a direct way, the failure (Fig. 5f) did not take place within the NBR-MWCNT clusters, but rather in the surrounding EPDM phase; therefore, no MWCNTs were visible.

The TEM imaging supported the findings by FESEM, but gave more information. As shown in Fig. 6a, in the masterbatch mixed sample, the MWCNTs are concentrated in one phase, the NBR phase, as stated earlier. In the directly mixed compound (Fig. 6b–c), the NBR phase is more fragmented and is composed of both submicron and several microns-sized inclusions. There are both, high and low MWCNT concentration areas present, a signal of imperfect mixing. In the better dispersed areas in the EN-CNT 6 (Fig. 6b), the MWCNTs are uniformly distributed in the EPDM and NBR phase. However, there are also areas with high concentrations of MWCNT's: nondispersed nanotube clusters. There is also a fraction of MWCNTs organized along and to some extent, across the EPDM/NBR interface, as seen in Fig. 6c.

Based on the failure paths observed, it is suggested that in the masterbatch sample the interfaces between the different polymers is rather weak, while in the directly mixed blend samples, the interface between EPDM and NBR is stronger. The last conclusion is supported by the data from tensile tests, where direct mixed compounds have a higher strength at failure and also higher stresses at 100% and 300% elongation.

CONCLUSIONS

In this study, a series of MWCNT reinforced EPDM/NBR blends were prepared using a NBR/MWCNT masterbatch technique or direct mixing of the MWCNTs into a blend of NBR and EPDM. The mechanical properties of the composites were found to be largely depending on the mixing technique: direct gave a higher strength than the masterbatch mixed materials. In the masterbatch compounds, the NBR phase did not show a glass transition; only one Tg typical for EPDM was detected.

However, for directly mixed compounds, both rubber phases, EPDM and NBR, showed a Tg peak. In this case, the Tg of the NBR phase was shifted towards a higher temperature due to a higher cross-link density of the NBR phase. This is the result of overcuring of the NBR phase, as the curatives have a higher affinity to the more polar NBR. In transmission electron microscopic studies, a better dispersion of the nanotubes was found when the samples were prepared by direct mixing method. Overall it can be concluded that for this system, the direct mixing method gives better results than the masterbatch mixing method.

FUNDING

This work was supported by the Finnish Funding Agency for Technology and Innovation (TEKES) [Grant Number #40352/08].

REFERENCES

1. Das, A.; Jurk, R.; Stöckelhuber, K.W.; Engelhardt, T.; Fritzsche, J.; Klüppel, M.; Heinrich, G. Nanoalloy based on clays: Intercalated-exfoliated layered silicate in high performance elastomer. J. Macromol. Sci. A **2008**, *45*, 144–150.
2. Ghosh, S.; Sengupta, R.A.; Heinrich, G. High performance nanocomposite based on organoclay and blends of different types of SBR with BR, Kautsc. Gummi Kunstst. **2011**, *01–02*, 48–54.
3. Sperling, L.H. *Polymeric Multicomponent Materials*, John Wiley & Sons, Inc.: New York, 1997.
4. Nell, A.; Xia, T.; Mädler, L.; Ning, L. Toxic potential of materials at the nanolevel. Science **2006**, *311*, 622–627.
5. Monteiro-Riviere, N.A.; Inman, A.O.; Zhang, L.W. Limitations and relative utility of screening assays to assess engineered nanoparticle toxicity in a human cell line. Toxicol. Appl. Pharmacol. **2009**, *234*, 222–235.
6. Dubey, K.A.; Bhardwaj, Y.K.; Rajkumar, K.; Panicker, L.; Chaudhari, C.V.; Chakraborty, S.K.; Sabharwal, S. Polychloroprene rubber/ethylene-propylene diene monomer/multiple walled carbon nanotube nanocomposites: Synergistic effects of radiation crosslinking and MWNT addition. J. Polym. Res. **2012**, *19*, 9876–9884.
7. Jovanović, V.; Samaržija-Jovanović, S.; Budinski-Simendić, J.; Marković, G.; Marinović-Cincović, M. Composites based on carbon black reinforced NBR/EPDM rubber blends. Compos. Pt. B **2013**, *45*, 333–340.
8. Samaržija-Jovanović, S.; Jovanović, V.; Marković G., Konstantinović S., Marinović-Cincović M. Nanocomposites based on silica-reinforced ethylene–propylene–diene–monomer/acrylonitrile–butadiene rubber blends. Compos. Pt. B **2011**, *42*,1244–1250.
9. Das, A.; Mahaling, R.N.; Stöckelhuber, K.W.; Heinrich, G. Reinforcement and migration of nanoclay in polychloroprene/ethylene-propylene-diene-monomer rubber blends, Compos. Sci. Technol. **2011**, *71*, 276–281.

10. NANOCYL NC7000–10 March 2009 - V05, Product data sheet, Nanocyl S.A.
11. Das, A., Ghosh A.K., Pal S., Basu D.K. The role of thiophosphoryl disulfide on the co-cure of CR-EPDM blends, Polym. Adv. Technol. **2004**, *15*, 197–208.
12. Poikelispää, M.; Das, A.; Dierkes, W.; Vuorinen, J. The effect of partial replacement of carbon black by carbon nanotubes on the properties of natural rubber/butadiene rubber compound, J. Appl. Polym. Sci. **2013**, *5*, 3153–3160.
13. Subramaniam, K.; Das, A.; Heinrich, G. Development of conducting polychloroprene rubber using imidazolium based ionic liquid modified multiwalled carbon nanotubes, Comp. Sci. Technol. **2011**, *71*, 1441–1449.
14. Dierkes, W.; Tiwari, M.; Guo, R.; Datta, R.; Talma, A.; Noordermeer, J.; van Ooij, W. Overcoming incompatibility problems in elastomer blends by tailored surface properties of rubber additives. Rubber Chem. Technol. **2013**, *86*, 1–27.
15. Utracki, L.A. Polymer alloys and blends. Thermodynamics and Rheology, Hanser Publishers: Nördlingen, Germany, 1990.

Tampereen teknillinen yliopisto
PL 527
33101 Tampere

Tampere University of Technology
P.O.B. 527
FI-33101 Tampere, Finland

ISBN 978-952-15-3999-2
ISSN 1459-2045